

AMERICAN UNIVERSITY OF BEIRUT

ORTHODONTIC TRACTION OF PALATALLY IMPACTED
CANINES: A FINITE ELEMENT ANALYSIS STUDY

By

KINAN GHALEB ZENO

A thesis
submitted in partial fulfillment of the requirements
for the degree of Master of Science in Orthodontics
to the Department of Orthodontics and Dentofacial Orthopedics
of the Faculty of Medicine
at the American University of Beirut

Beirut, Lebanon
January, 2017

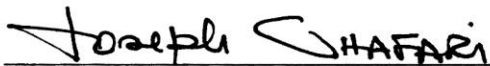
AMERICAN UNIVERSITY OF BEIRUT

ORTHODONTIC TRACTION OF PALATALLY IMPACTED
CANINES: A FINITE ELEMENT ANALYSIS STUDY

By

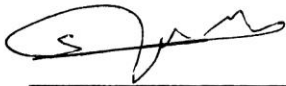
KINAN GHALEB ZENO

Approved by:



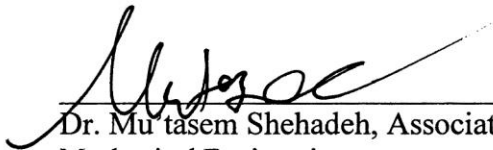
Dr. Joseph G. Ghafari, Professor and Head
Orthodontics and Dentofacial Orthopedics

Advisor



Dr. Samir G. Mustapha, Assistant Professor
Mechanical Engineering

Member of Committee



Dr. Mu'tasem Shehadeh, Associate Professor
Mechanical Engineering

Member of Committee



Dr. Ramzi V. Haddad, Assistant Professor
Orthodontics and Dentofacial Orthopedics

Member of Committee

Date of thesis defense: January 24th, 2017

AMERICAN UNIVERSITY OF BEIRUT

THESIS, DISSERTATION, PROJECT RELEASE FORM

Student Name:

Last	First	Middle
------	-------	--------

☐ Master's Thesis ☐ Master's Project ☐ Doctoral Dissertation

☐ I authorize the American University of Beirut to: (a) reproduce hard or electronic copies of my thesis, dissertation, or project; (b) include such copies in the archives and digital repositories of the University; and (c) make freely available such copies to third parties for research or educational purposes.

☐ I authorize the American University of Beirut, to: (a) reproduce hard or electronic copies of it; (b) include such copies in the archives and digital repositories of the University; and (c) make freely available such copies to third parties for research or educational purposes
after:

One ---- year from the date of submission of my thesis, dissertation, or project.

Two ---- years from the date of submission of my thesis, dissertation, or project.

Three ---- years from the date of submission of my thesis, dissertation, or project.

Signature

Date

This form is signed when submitting the thesis, dissertation, or project to the University Library

ACKNOWLEDGMENTS

I would like to give my sincere appreciation to my family who always supported and encouraged me and to the following whom if it was not for their contribution and devotion, this work would not have been possible,

Dr. Joseph Ghafari, for your supervision and for pushing us toward excellence and beyond our limits, and for the amount of time and work invested in our training;

Dr. Samir Mustapha and Dr. George Ayoub, for opening our eyes to this great field of finite element analysis and for allowing this opportunity of multidisciplinary work, and for all the constructive discussions;

Dr. Mu'tasem Shehadeh and Dr. Ramzi Haddad, for your great advice and supervision;

Dr. Maria Saadeh, for your remarkable work with our statistics and for being patient with our endless objectives,

Samah Mohtar, for his assistance and advice in the technical part of finite element analysis;

Rawad Hayek, Rakan Ammourey; for their different contributions in data organization, and graphics;

And to *Makram*, for literally always being there day and night, and for sharing this experience in every step of this trip and in its ups and downs making it both enjoyable and unforgettable.

AN ABSTRACT OF THE THESIS OF

Kinan Ghaleb Zeno for

Master of Science

Major: Orthodontics

Title: Orthodontic Traction of Palatally Impacted Canines: A Finite Element Analysis Study

Introduction:

The treatment of impacted canines is most challenging because of undesirable side effects, demanding anchorage control, and remarkable increase in treatment duration. Accurate localization of palatally impacted canines and careful application of forces are keys to successful treatment. Reaction forces on adjacent teeth vary with the mechanical design of the appliances used.

Aims:

1. Develop a scheme to determine the severity of palatally impacted canines (PIC) related to treatment objectives; 2. Determine the stresses on the impacted canine when subjected to initial force activation in various directions (buccal, vertical, and distal) and in relation to the severity of impaction; 3. Evaluate the stresses on adjacent teeth generated by different appliances.

Design:

The research comprised 2 major parts, a CBCT section in which the spatial position of PIC is evaluated along with the components contributing to its severity. The second section is the finite element analysis study in which stress on the impacted tooth is assessed in response to differently directed forces and different appliances.

Methods:

Part 1: 38 PIC were evaluated, derived from 28 CBCT scans of patients with a mean age of 16.06 years. Severity was based on an angle defined between the PIC axis and its projected virtual alignment within the arch virtual aligned canine (VAC). Measurements in axial, coronal, sagittal and panoramic CBCT sections were recorded and analyzed.

Part 2: 21 scans that included 30 PIC's were evaluated. A prototype 3D model was reconstructed and segmented into its anatomic components. The individual impacted canines were precisely positioned in the prototype model to portray their original position. Stresses in response to a distal, vertical and buccal force (1N) were evaluated at different levels of the root on the periodontal ligament of the PIC. Stress on adjacent teeth were also compared with different appliances. Statistics included analyses of variance for comparisons of variables, and regression analyses for associations among variables.

Results:

The highest correlations were observed between PIC angulation and the position of its cusp tip. Specifically, the canine angulation to midline was significantly correlated to both PIC/VAC ($r=0.85$), cusp-tip deviation ($r=0.67$), and cusp tip to midline ($r=-0.86$); ($p<0.001$). Based on multivariate analysis, the significant predictors of the PIC/VAC angle were the vertical position, angulation to midline in the coronal plane, and angulation to palatal plane in the sagittal plane. On the total PIC root, distal and buccal forces resulted in higher stress ($S=6.64$, 6.41 KPa respectively), compared to the vertical force ($S=5.97$ KPa). Buccal and distal forces were not statistically significantly different in stresses generated at the cervical level and over the whole root ($p>0.05$). In severity subgroups, only the vertical and distal force directions resulted in different stresses at the mid-root level ($P=0.001$, and $P=0.002$ respectively). Stresses on adjacent teeth were highest with appliances engaging all the teeth in the arch, particularly on the adjacent lateral incisor and first premolar.

Conclusion:

The inclination of the PIC to its simulated virtually aligned position reflects an effective measure of impaction severity. Medial cusp deviation on the axial view, angulation to midline and palatal plane on coronal and sagittal views were the major contributors to PIC/VAC thus, to impaction severity. A differential stress distribution was found with different force directions, the distal force yielding the highest stress values. The inclusion of individual variations in the study helped determine trends of responses to force application and ensuing clinical implications. Distal and vertical direction of forces may be preferable to buccal forces in the initial stages of canine traction, particularly with higher or more inclined canines. The application of a vertical force reduces the stresses at the apex of the canine and its inclusion with the other force directions (distal or buccal) would be recommended. Future research in dynamic time dependent FEA should elucidate many of the clinical implications.

CONTENTS

ACKNOWLEDGEMENTS.....	v
ABSTRACT.....	vi
LIST OF ILLUSTRATIONS.....	xi
LIST OF TABLES.....	xiii
LIST OF ABBREVIATIONS.....	xiv
Chapter	Page
1. INTRODUCTION	1
1.1. Definition.....	1
1.2. Prevalence.....	3
1.3. Type of Impaction.....	3
2. LITERATURE REVIEW.....	5
2.1. Etiology.....	5
2.2. Methods of Assessment.....	7
2.3. Management.....	12
2.4. Finite Element Analysis.....	19
2.4.1. Principles and Applications.....	19
2.4.2. FEA in Dentistry.....	20
2.4.3. FEA in Orthodontics.....	22
2.4.3.1. Mechanics of Tooth Movement.....	22
2.4.3.2. Craniofacial Growth Patterns.....	23
2.4.4. FEA of impacted canines.....	24
2.5. Significance.....	25
2.6. Specific Objectives.....	28
3. MATERIALS AND METHODS.....	29
3.1. Materials.....	29
3.2. CBCT Study.....	30
3.3. FEA Study.....	32
3.3.1. Model Reconstruction.....	34
3.3.1.1. Teeth Mask Reconstruction.....	34

3.3.1.2. Bone Mask Reconstruction.....	37
3.3.1.3. Canine Repositioning.....	40
3.3.2. Material Properties.....	44
3.3.3. Mesh Size.....	45
3.3.4. Boundary Conditions.....	46
3.3.5. Loading of the Impacted Canine.....	47
3.3.6. Loading of the Adjacent Teeth.....	49
3.3.7. Statistical Analysis.....	51
4. RESULTS.....	53
4.1. CBCT Study.....	53
4.1.1. Descriptive Data.....	53
4.1.2. Difference Between Severity Subgroups.....	53
4.1.3. Correlations Between PIC/VAC and Other Positional Parameters..	55
4.1.4. Associations Between PIC/VAC and Other Positional Parameters..	55
4.2. FEA Study.....	57
4.2.1. Stresses on Impacted Canine.....	57
4.2.1.1. Stress Distribution and Force Direction.....	57
4.2.1.2. Stress Distribution Among Severity Subgroups and Force Directions.....	58
4.2.1.3. Correlations Between Stress and Canine Positional Parameters.....	62
4.2.1.4. Associations Between Stress at Different Root Levels with Force Direction.....	66
4.2.2. Stresses on Adjacent Teeth.....	69
5. DISCUSSION.....	78
5.1. Introduction.....	78
5.2. CBCT Study.....	79
5.2.1. New Assessment of Palatally Impacted Canines.....	79
5.2.2. Comparison with Other Studies.....	83
5.2.3. Research Considerations.....	85
5.3. FEA Study.....	87
5.3.1. Canine Angulation Severity with Different Force Direction.....	87
5.3.2. Stress Distribution and Canine Positional Parameters.....	89
5.3.3. Stress on Adjacent Teeth with Different Appliances.....	91

5.4. Clinical Implications.....	94
5.5. Research Considerations.....	97
5.5.1. Strength.....	97
5.5.2. Limitations.....	98
5.5.3. Future Tracks and Recommendations.....	100
6. CONCLUSIONS.....	101
REFERENCES.....	103
Appendix	
1. Canine repositioning script.....	109
2. Box plots for different measurements distribution in the severity subgroups.....	112

ILLUSTRATIONS

Figure		Page
1.1	-Records of a 14 year old male with palatally impacted canine (PIC).	2
1.2	-Sagittal view of a CBCT showing the main impaction scenarios of maxillary canines.	4
2.1	-Diagrammatic representation of relationship of canine and incisors early in normal development and after canine eruption and final alignment.	6
2.2	-A combination of 2 periapical and axial intraoral radiographs used to locate the bucco-palatal crown position. After (Ericson & Kurol, 1988).	8
2.3	-Schematic illustration of projection of canine in the panoramic and axial vertex intraoral radiograph to assess the medial canine crown position. After (Ericson & Kurol, 1988).	8
2.4	-3D reconstruction of an impacted canine (red), based on a CBCT, shows accurately the position of the canine in its relationship to incisors, premolars and bone.	10
2.5	-KPG index components in X, Y, and Z planes. After (Kau et al, 2009).	11
2.6	-Palatally located crown positions of the canines on axial, sagittal, and coronal views of CBCT. After (Alqerban et al, 2015).	12
2.7	-Treatment progress photographs of maxillary arch of an 18.4 years old female with bilateral palatally impacted canines.	17
2.8	-Treatment progress photos of maxillary arch of a 14 years old male with unilateral palatally impacted canines.	18
2.9	-Maxillary arch of a 14 years old female with palatally impacted canine.	18
2.10	-Equivalent stress distribution to different force angulations on the PDL of the canine with different forces. After (Zhang et al, 2008).	25
3.1	-Movement in orange arrows from PIC: Palatally impacted canine to VAC: Virtually impacted canine.	31
3.2	-Panoramic view: PIC/VAC angle between palatally impacted canine and virtually aligned canine.	32
3.3	-Different views of CBCT scan and different positional parameters.	32
3.4	-Prototype model mesh from different views, composed of alveolar bone, periodontal ligament, and teeth.	33
3.5	-Segmentation and processing of teeth mask	35
3.6	-Removal of floating particles and excess in teeth mask	35
3.7	-Separation of contact points between teeth	36
3.8	-Alignment and adjustment of roots position in teeth mask	36
3.9	-Completed teeth mask	37
3.10	-Bone mask: Segmentation, removal of excess, and smoothening	38
3.11	-Completed bone and teeth masks	38
3.12	-Addition of periodontal ligament	39
3.13	-Addition of attachment and meshing of final model	40
3.14	-Canine repositioning: redefining global axes	41
3.15	-Meshing of canine mask and repositioning	42
3.16	-Viewing repositioned canine and final bilateral model	43
3.17	-Mesh size testing, comparison of two mesh sizes	46
3.18	-Boundary conditions: models constrained from translation and rotation posteriorly and superiorly	47

3.19	-Posterior and occlusal view of PIC with the 3 force directions, vertical, buccal, and distal	48
3.20	-Element sets in which stresses were evaluated at different levels (cervical, middle, and apical) of the PIC root.	48
3.21	-Meshed model of the maxilla and maxillary dentition attached with brackets and an arch wire	49
3.22	-Different views showing the transpalatal bar and the extending cantilever arm spring at rest and under tension	50
4.1	-Line chart showing the average stress on the canine root with different force directions.	58
4.2	-Line chart illustrating how stress is distributed along the root of the canine with different force direction.	58
4.3	-Line chart shows the interaction between severity subgroups and force directions (the lines cross) at the level of middle part root.	59
4.4	-Von Mises stress in periodontal ligament of right and left maxillary molar in case 1 (TP bar only).	71
4.5	-Von Mises stress in alveolar bone of right and left maxillary molar in case 1 (TP bar only).	72
4.6	-Von Mises stress in periodontal ligament of right and left maxillary molar in case 2 (TP bar and a SS AW wire).	73
4.7	-Von Mises stress in alveolar bone of right and left maxillary molar in case 2 (TP bar and a SS AW wire).	74
4.8	-Von Mises stress on PDL of adjacent teeth (Direct pull of canine to main SS AW).	75
4.9	-Maximum principal stress on PDL of adjacent teeth in direct pull against the wire showing areas of tension.	76
4.10	-Maximum principal stress on PDL of adjacent teeth in direct pull against the wire showing areas of compression.	76
4.11	-Transverse section across the maxilla at the level of second premolar showing maximum principal stress in PDL of adjacent teeth direct pull against the wire showing areas of compression.	77
5.1	-Graphic representation of palatally impacted canine (PIC) in severe, moderate, and milder configurations in axial, sagittal, and coronal planes	82
5.2	-Simulation of distal force and vertical forces and their associations with PIC inclination severity	91
5.3	-Maxillary arch photograph of a right maxillary canine being tracked against the AW with the resultant skewing corresponding to the differential stress distribution on the teeth adjacent to PIC and on the contralateral side.	93
5.4	-Graphic representation of stress distributions with TP bar alone (A, B), TPB with fixed appliances (C, D), and fixed appliances alone (E, F). Arrows indicate percentages of stress on the respective teeth.	94
5.5	-Intraoral photographs of maxillary arch displaying different approaches for PIC traction.	96

TABLES

Table	Page
1.1 -Prevalence of impacted canines from retrieved epidemiological studies	3
2.1 -Treatment options of palatally impacted canine	15
3.1 -Material properties of the FEA model	45
4.1 -Descriptive variables of positional components of palatally impacted canines	54
4.2 -Positional components of palatally impacted canines (PIC) in severity subgroups stratified on inclination between PIC and virtually aligned canine (VAC)	54
4.3 -Multivariate analysis of the relationship of PIC/VAC and remaining bivariate significant measures	56
4.4 -Correlations among positional parameters of palatally impacted canines (PIC) in various planes of space	55
4.5 -Distribution of stress (Von Mises KPa Mean + SD) according to direction of force at various levels of the canine root	57
4.6 -Stress distribution between severity subgroups (1/2) at various areas of the canine root when subjected to various force directions	59
4.7 -Comparison of stress distribution at various levels of the canine root between severity subgroups	59
4.8 -Comparison of stress distribution at various levels of the canine root in lower severity subgroup	60
4.9 -Comparison of stress distribution at various levels of the canine root in higher severity subgroup	61
4.10 -Correlations among Von Mises stresses and other parameters in various planes of space in the whole sample (N: 30)	63
4.11 -Correlations among Von Mises stresses and other parameters in various planes of space in the lower severity subgroup	64
4.12 -Correlations among Von Mises stresses and other parameters in various planes of space in the higher severity subgroup	65
4.13 -Multivariate regressions for prediction of stress at the middle level of the root while applying a vertical force.	66
4.14 -Multivariate regressions for prediction of stress at the cervical level of the root while applying a vertical force.	67
4.15 -Multivariate regressions for prediction of stress at the apical level of the root while applying a buccal force	67
4.16 -Multivariate regressions for prediction of stress at the middle level of the root while applying a buccal force	68
4.17 -Multivariate regressions for prediction of stress at the cervical level of the root while applying a buccal force	68
4.18 -Multivariate regressions for prediction of stress at the whole root of PIC while applying a buccal force	69
4.19 -Multivariate regressions for prediction of stress at the middle level of the root while applying a distal force	69
4.20 -Percentages of Von Mises stress (KPa) on adjacent teeth in different appliances while retrieving a maxillary left palatally impacted canine	70
5.1 -Working guidelines for canine traction	96

ABBREVIATIONS

PIC	Palatally Impacted Canine
VAC	Virtually Aligned Canine
CBCT	Cone-Beam Computed Tomography
PDL	Periodontal Ligament
FEA	Finite Element Analysis
FEM	Finite Element Method
CAD	Computer Aided Design
SIP	ScanIP Project
TPB	Transpalatal Bar
SS	Stainless Steel
AW	Arch Wire
RPE	Rapid Palatal Expander
PM	Premolar
PP	Palatal Plane
STL	Standard Triangle Language
N	Newton
KPa	Kilo Pascal
MPa	Mega Pascal
mm	Milli-Meter
2D	Two Dimensional
3D	Three Dimensional
USA	United States of America

CHAPTER 1

INTRODUCTION

1.1. Definition

Several definitions converge to describe the phenomenon of tooth impaction:

- “An 'impacted tooth' by definition is a tooth so positioned against another tooth, bone, or soft tissue that its complete and normal eruption is impossible or unlikely” (Mosby, 2009).
- Tooth impaction is defined as the infraosseous position of the tooth after the expected time of eruption.
- Tooth displacement is defined as the abnormal infraosseous position before the expected time of eruption (Litsas & Acar, 2011; Power & Short, 1993).
- Ectopic eruption is the deviation of the tooth from its normal eruptive path which in most cases leads to impaction. Inability to palpate the canine after the age of 10 years old strongly indicated a disturbance of eruption (Sune Ericson & Jüri Kurol, 1986b).
- Ectopic eruption of the permanent canine can cause impaction of the permanent canine which may be result in resorption of roots of permanent lateral and central incisors (Proffit, Fields Jr, & Sarver, 2014).

These definitions situate an impaction relative to (**Fig. 1.1**):

- location: an impacted tooth is necessarily in ectopic position relative to its normal place in the dental arch. In this perspective, the inclination of the tooth is a determining factor in the management of the condition.

- biologic environment: the definitions mostly refer to an “infraosseous” position, referring to the complete embedding of the tooth within the bone. However, in general terms, a tooth may be partially impacted in soft-tissue (gingival and mucosa).
- timing of eruption: eruption is abnormally delayed. This aspect relates to the early recognition of the condition, thus the suggestions for diagnosis through radiographs and clinical examination, such as palpation of the expected site of emergence.

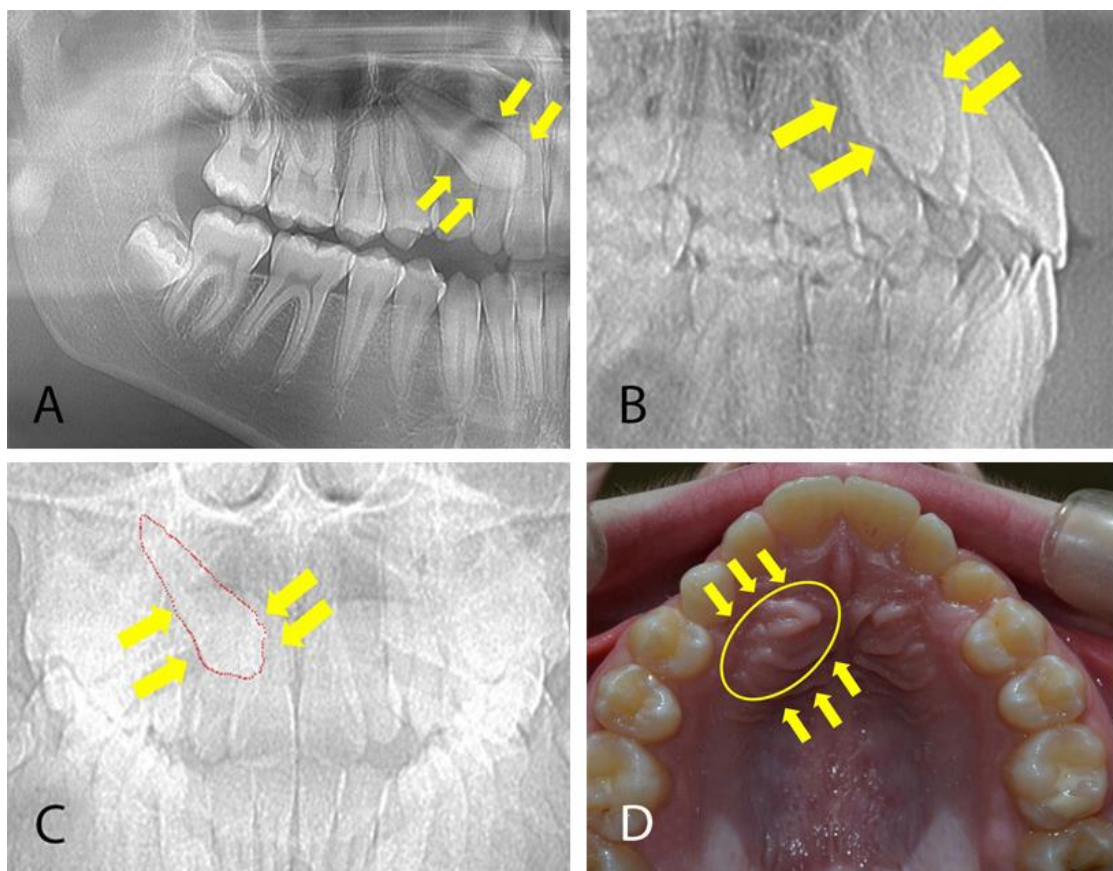


Fig. 1.1: Records of a 14 year old male with palatally impacted canine (PIC): A. Panoramic xray, PIC overlapping the lateral and half of the central incisor. B. Lateral cephalograph confirming the palatal position. C. PIC on postero-anterior cephalogram. D. Palatal bulge corresponds to the radiologic findings.

1.2. Prevalence

The most frequently impacted teeth after the third molars are the maxillary canines (P. S. Grover & L. Lorton, 1985). The frequency of impacted canines was dependent on the population studied (**Table 1.1**). The likelihood of their impaction ranges from 0.8 to 8.4% (Dachi & Howell, 1961; Fardi, Kondylidou-Sidira, Bachour, Parisi, & Tsirlis, 2011; Thilander & Myrberg, 1973), with reported averages of nearly 4% (Aydin, Yilmaz, & Yildirim, 2014; Zahrani, 1993). Impactions are twice as common in females than in males (Sune Ericson & Jüri Kurol, 1986a); 8% are estimated to be bilateral (Dachi & Howell, 1961).

Table 1.1: Prevalence of impacted canines from retrieved epidemiological studies

Author (Publication Year)	Country/ Population	N	Age	Prevalence
Takahama et al. (1982)	Japan	2,959	>18	0.3%
Dachi (1961)	USA	1,685	>20	0.92%
Thailander et al. (1972)	Sweden	939	10-13	1.37%
Kramer & Williams (1970)	USA	3745	-	1.64%
Erikson & Kurol (1986)	Sweden	505	>11	1.7%
Aktan et al. (2010)	Turkey	5000	15-80	1.74%
Groover & Lorton (1985)	USA	5000	18-26	1.2-2.3%
Sacerdoti & Baccetti (2004)	Italy	1,000	7-17	2.4%
Aydin et al. (2014)	Turkey	4,500	16-80	3.29%
Zahrani AA (1993)	Saudia Arabia	4,898	>13	3.6%
Fardi (2010)	Greece	1.239	7-92	8.4%

1.3. Type of Impaction

Impacted maxillary canines vary in their location bucco-palatally, vertically, and antero-posteriorly. Depending on the position of both the apex and the cusp tip, the

canines may have a nearly infinite variety of impaction positions. Impacted maxillary canines have been reported to be mostly palatally displaced (70-85%) while only 15-30% of them were displaced buccally or within the arch (Yadav & Shrestha, 2013); (**Fig. 1.2**). The incidence of palatal impaction was estimated to exceed labial impaction by a ratio of nearly 3:1 (Stellzig, Basdra, & Komposch, 1994) and up to approximately 6:1 (Jacoby, 1983). Differences may be related to populations studied or methodologies employed.

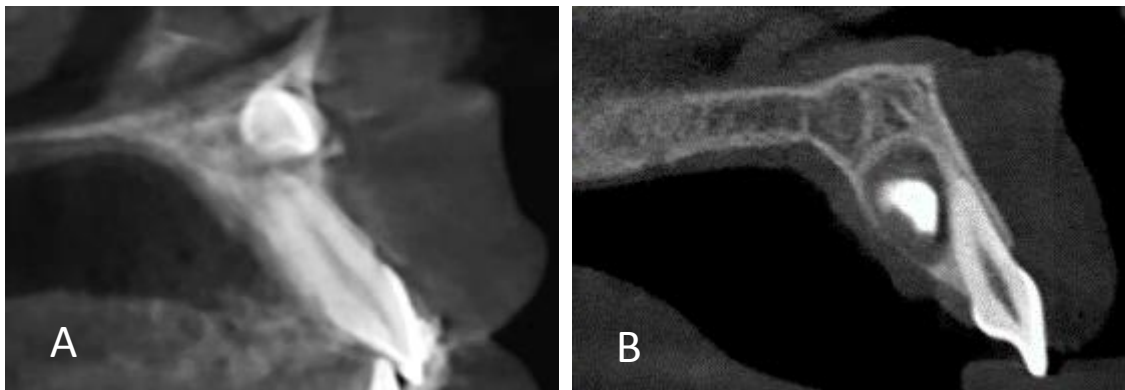


Fig. 1.2: Sagittal view of a CBCT showing the main impaction scenarios of maxillary canines: a. buccal impaction, b. palatal impaction

CHAPTER 2

LITERATURE REVIEW

2.1. Etiology

The etiology of canine impaction is multifactorial, and somehow controversial. While some researchers favor exclusively genetic etiology, others have advanced a variety of causes. Becker and Chaushu (2015) classified the causes into the following 4 main categories:

-1. Local hard tissue obstruction

Over retained deciduous canine, supernumerary teeth, odontomas, dilacerations or trauma can provide local hard tissue obstruction whether affecting the canine directly, or the incisors, causing them (particularly the lateral incisor) to be displaced, thus impeding on the normal eruptive pathway of the canine.

-2. Local pathology

Local pathology represents any lesion caused by the loss of vitality of the deciduous canine because of overretention beyond 12 years or carious lesions. Moreover, a granuloma that may lead to a dentigerous cyst can cause displacement of adjacent teeth including the canine.

-3. Disturbances in the eruption of incisors

The disturbances include congenitally missing, deformed, or peg shaped lateral incisors. Maxillary lateral incisors are the most frequently missing teeth that are genetically inherited. Besides, not only can they be absent but also late in

development, peg shaped, or small with only the earliest degree of root development. This disposition will deny the canine the guidance in its eruptive pathway leading it to erupt more palatally, whereby its branding as the *guidance theory* of canine impaction (Al-Nimri & Bsoul, 2011; Bass, 1967; Becker, 2012; Miller, 1963). Accordingly, the canine erupts along the root of the lateral incisor (**Fig. 2.1**), which serves as a guide, and if the root of the lateral incisor is absent or malformed, the canine will not erupt.

The previous factors (absence, malformation, delayed development of the lateral incisor) create a “genetically determined environment” resulting in the derivation of the forming canine of its guidance, thus influencing it to adopt an abnormal eruption path (Becker & Chaushu, 2015).

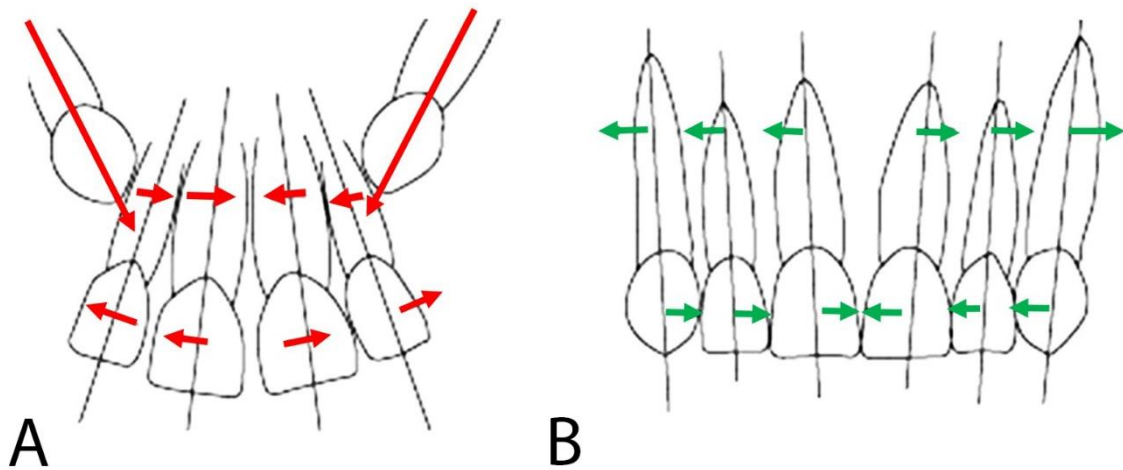


Fig. 2.1: Diagrammatic representation of relationship of canine and incisors. a. Unerupted canines in normal development at age 9-10 years. Canines restrict the roots into a narrowed apical area causing the flaring of the incisors crowns, b. In final alignment after eruption of canines. (Adapted from Becker A. The orthodontic treatment of impacted teeth. 2nd ed. Abingdon, United Kingdom, 2007).

-4. Heredity

This etiologic factor exclusively refers to a direct consequence of “primary displacement of the tooth bud” (Ericson & Kurol, 1988). Such instances are reported to be bilateral because the patient's left and right sides are genetically identical and the impaction is not related to or caused by lack of guidance.

Hence the *genetic theory*, which states that palatally impacted canines are among a complex of genetically determined tooth anomalies resulting from a developmental disturbance of the dental lamina, with reported familial recurrence of canine impaction. Associations between canine impactions and other dental anomalies as congenitally missing teeth have also been reported (Baccetti, 1998; Peck, Peck, & Kataja, 1994; Pirinen, Arte, & Apajalahti, 1996).

2.2. Methods of Assessment

The severity of palatally impacted canines has been classified according to their position and angulation, which affect treatment modality, complexity, and duration (Stewart et al., 2001; Zuccati, Ghobadlu, Nieri, & Clauser, 2006). Many authors have advocated schemes of evaluation that help assess the location of impacted canines. Using a combination of periapical and occlusal radiographs, (S. Ericson & J. Kurol, 1986) defined the position of the impacted canine relative to the dental arch as either palatal, tendency palatal, central, or buccal (**Fig. 2.2**). Later (Ericson & Kurol, 1988), they determined the difficulty of eruption on the panoramic radiograph: when the permanent canine crown overlapped less than half of the root of the lateral incisor, an excellent chance of 91% existed for normalization of the eruption path.

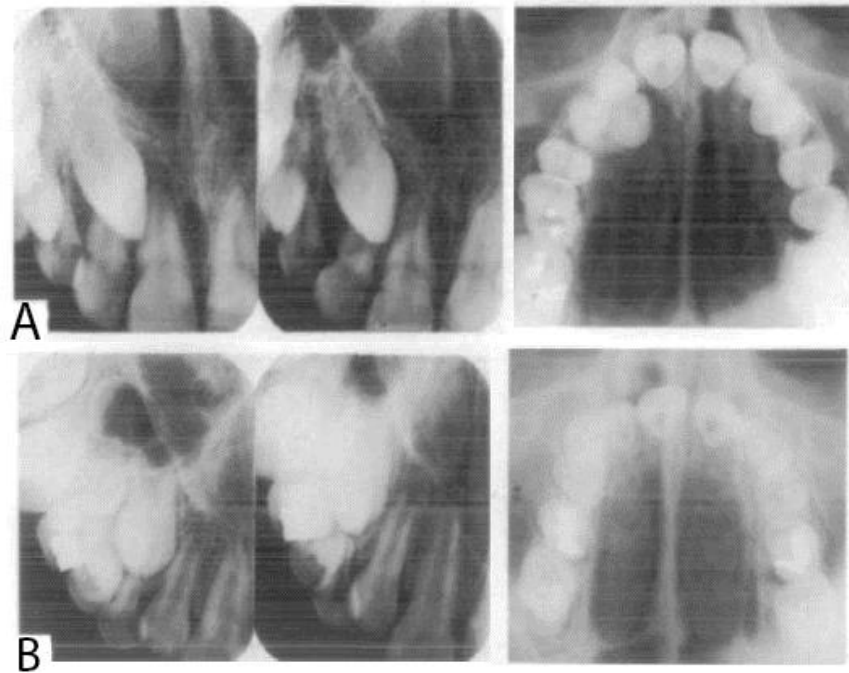


Fig. 2.2: A combination of 2 periapical and axial intraoral radiographs used to locate the bucco-palatal crown position of the impacted canine in 2 patients. a. Girl, age 12 years 4 months. The right canine is not clinically palpable and is positioned with the crown lingual to the dental arch. The left canine is clinically palpable with a central position in the dental arch. b. Girl, 10 years 3 months old. Both canines are palpable in a slightly buccal position relative to the dental arch. (Sune Ericson & Jüri Kurol, 1986b).

However, when the overlap was beyond half of the lateral incisor root, early extraction of the primary canine resulted in a 64% chance for normal eruption (**Fig. 2.3**).

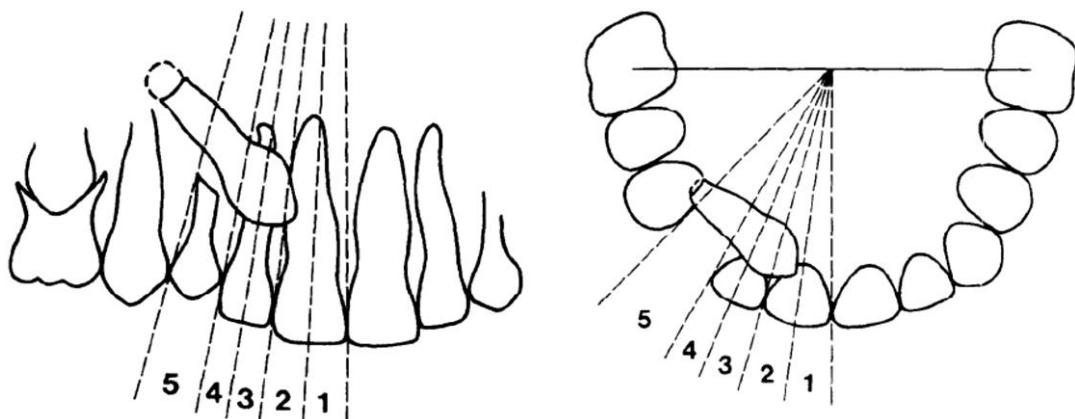


Fig. 2.3: Schematic illustration of projection of canine in the panoramic image (left) and axial vertex intraoral radiograph (right) in sectors (1-5), with 5 being the most medial canine crown position. After (Ericson & Kurol, 1988)

Stewart et al. (2001) used the vertical distance from cusp tip of the impacted canine to the occlusal plane measured on the panoramic radiograph: treatment time was shorter when the distance was less than 14 mm; at 14mm or more treatment was longer.

Pitt, Hamdan, and Rock (2006) established a more elaborate treatment difficulty index based on several contributing factors measured on the panoramic radiograph: the horizontal position of the impacted canine, age of the patient, vertical height, and bucco-palatal position. Crescini, Nieri, Buti, Baccetti, and Pini Prato (2007) related the angle between the long axis of the canine and the midline measured on the panoramic radiograph to treatment time: every 5 degrees of increase of this angle resulted in 1 more week of active treatment time.

The development of radiography ushered more accurate assessments of the impacted maxillary canines. Having developed from the periapical to the panoramic radiographs, the advent of cone beam computed tomography (CBCT) provided a simultaneous overall 3D view from various planes of space (**Fig. 2.4**). The nature of the problem being the same, the 3D images at a minimum facilitated a diagnosis that in the past might have needed multiple periapical and/or panoramic radiographs, and at best disclosed details on spatial position of adjacent teeth that in the past were only discovered during surgery.

Indeed, it is difficult to determine if the impacted canine is buccal or palatal to the incisors on the panoramic radiograph alone, requiring a more accurate location through a combination of a periapical and an occlusal radiographs or 2 periapical radiographs using the cone shift method (Jacobs, 1999). Likewise, an accurate evaluation of root resorption of the lateral and central incisors from the panoramic

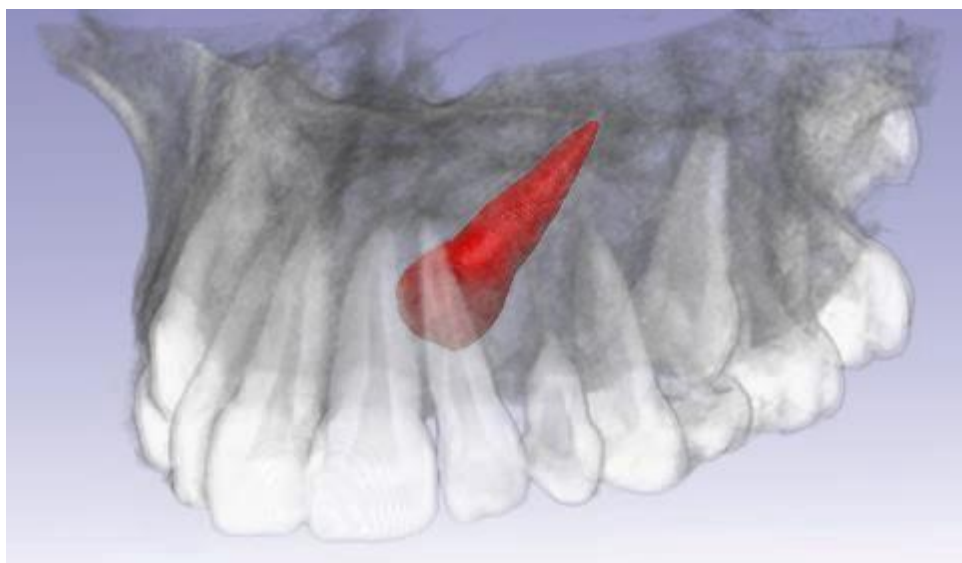


Fig. 2.4: 3D reconstruction of an impacted canine (red), based on a CBCT, shows accurately the position of the canine in its relationship to incisors, premolars and bone.

radiograph alone was near impossible, necessitating the use of one or more periapical x-rays.

Proper diagnosis based on better visualization impacts treatment planning, which ranges from no treatment to various approaches to exposure and traction to the dental arch. In this context, the previous 2D methods are deficient particularly because they did not reveal the accurate relationship of the canine to adjacent teeth and bone. Accordingly, two main advantages of CBCT scans over 2D radiographs in relation to treatment may be enlisted: the potential definition of the most efficient path of traction, and the extent of damage to the roots of adjacent permanent teeth.

Kau, Pan, Gallerano, and English (2009) developed the KPG index, which involved the calculation of a total score for “canine difficulty”, in relation to impaction severity and related treatment. The total was derived from CBCT images by adding the scores assigned to cusp tip (0-5) and root tip (0-5) antero-posteriorly, vertically on panoramic view of the CBCT and transversely relative to the arch on axial view of the

CBCT. The total score was projected into treatment difficulty: 0-9 is considered easy, 10-14 moderate, 15-19 difficult, and 20-30 extremely difficult (**Fig. 2.5**).

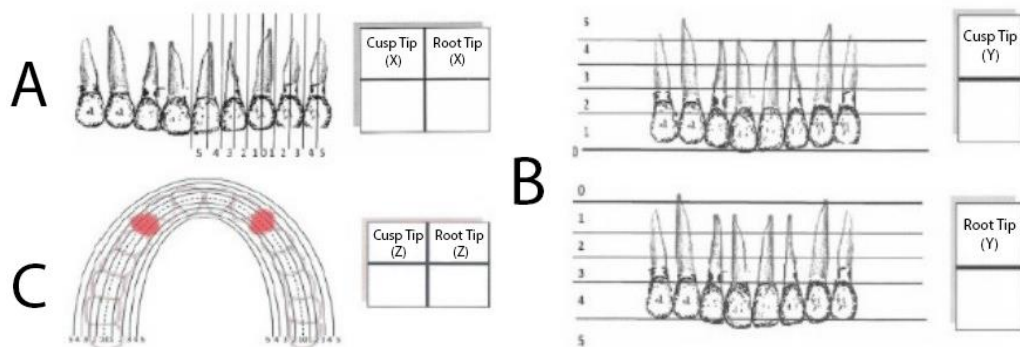


Fig. 2.5: KPG index: A. Anterior-posterior position, considered the X axis, was measured for both cusp tip and root tip. B. Vertical dimension, considered the Y axis, was also measured for cusp and root tips. C. Deviation from the occlusal arch transversally, considered the Z axis, was measured relative to the arch. Image adapted from Kau et al. (2009).

Alqerban, Jacobs, Fieuws, and Willems (2015) assessed different factors on CBCT scans to predict the possibility of impaction. The strongest predictors were: canine angulation to the lateral incisor on the coronal view, the canine cusp tip to the occlusal plane on the sagittal view, and the canine crown position relative to the arch and adjacent teeth (**Fig. 2.6**).

Despite the improvement in image quality and more accurate description of position of the impacted canine in its immediate environment, the following conclusions that are common to 2D and 3D evaluations emerge in reference to the factors associated with the severity of impaction, thus difficulty of treatment:

- a- The vertical distance between the impacted canine cusp tip and the occlusal plane
- b- The inclination of the canine relative to the incisors, a proxy measurement of other variables such as the inclination to the midline or the horizontal.

One factor distinctly better assessed in the 3D record seems to be the more accurate identification of the apex and its spatial position.

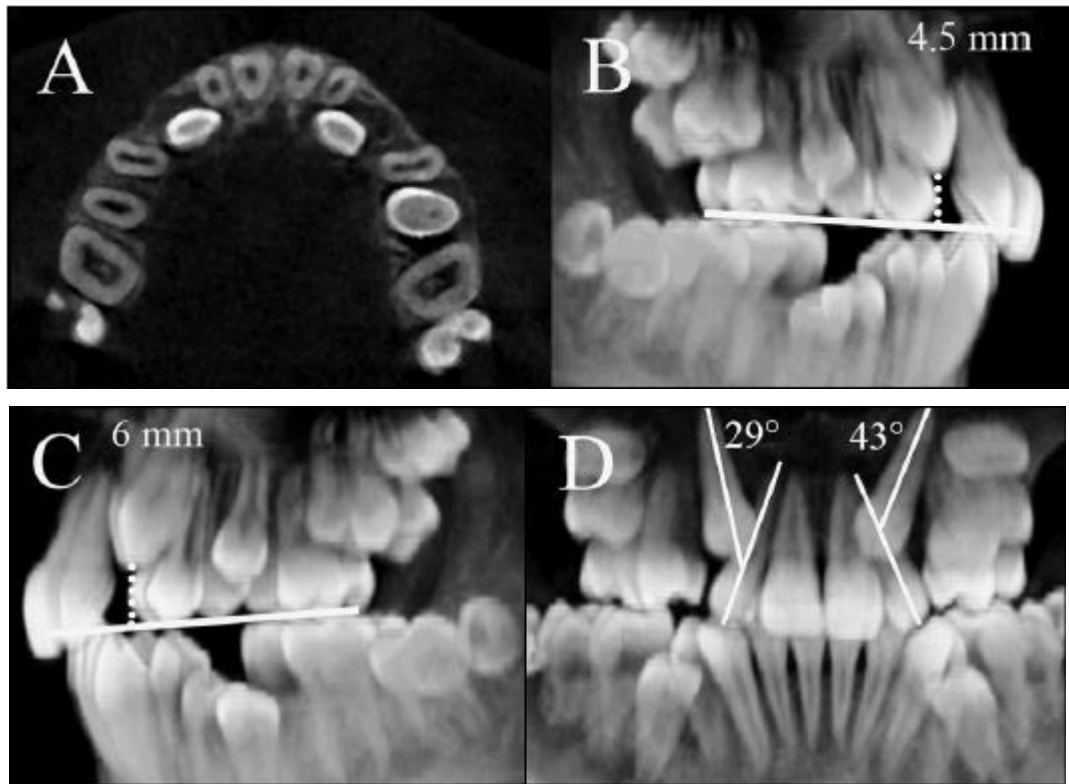


Fig. 2.6. A. Palatally located crown positions of the canines. B, C. Cusp tips of the right (B) and left (C) canines measured to the occlusal plane (4.5mm, 6mm, respectively) in the sagittal view. D. Angles of the right and left canines (29° and 43°, respectively) to the lateral incisor in the coronal view. From Algerban et al (2015).

2.3. Management

Impacted maxillary canines represent one of the most challenging clinical situations that orthodontists face, particularly regarding the decision to expose them and align them in the arch, or to extract them. This decision relies on the position of the canine, age of the patient, and motivation for treatment. Modalities of treatment include:

1. Surgical procedure (mainly extraction) indicated in specific circumstances

2. Depending on the patient age, prevention/early intervention/interceptive treatment
3. A clinical intervention of combined periodontal exposure and orthodontic traction when self-correction is ruled out, when the apex of the canine is closed, or when the tooth is deviated too far from its eruption path.

-1. Surgical approaches

Very high vertical position and nearly horizontal angulation can be either left under monitoring without treatment or may be extracted without exposing the tooth and orthodontic alignment. Sometimes, a failed exposure and traction lead to extraction. Inherent in the decision to extract the impacted canine is the potential damage to surrounding bone and teeth, whereby the tooth is best left alone. Noteworthy is the fact that the risk of ankylosis increases with the age of the patient. Therefore, surgical extraction of the canine could be the best viable option. Another option has been reported, consisting of corticotomy and surgical repositioning, or even transplantation. In either of these instances, the position of the tooth and condition of the surrounding bone must be favorable.

-2. Preventive/interceptive approach

Early diagnosis and intervention usually lead to space gaining, thus an opportunity for the eruption of the impacted canine and by extension, avoidance or limitation of root resorption of the adjacent (mostly lateral) incisors. At approximately age 10, if the primary canine is not mobile and there is no observable or palpable canine bulge, ectopic eruption of the permanent canine should be suspected. Early extraction of the deciduous canine may lead 78% of potentially impacted canines to revert to their

normal path of eruption (Ericson & Kurol, 1988). The use of headgear has been advocated with this approach. Other interceptive treatment modalities generally aim to creating more space in the arch for the canines to move down, either by rapid palatal expansion that relies on opening of the palatal suture and moving the incisors medially to target the created space for canine alignment, or by using cervical pull headgear in Class II malocclusions to help provide more space for the canine by distalization of posterior maxillary teeth.

-3. Exposure and alignment

Alignment of impacted canines during orthodontic treatment follows surgical exposure of the canine crown and often removal of overlying bone to clear the path of eruption. The flap can be either left open (open window) to allow for spontaneous open eruption (**Figs 2.7, 2.8**) or closed (**Fig. 2.9**) according to the position and height of the canine (Kokich, 2004).

Traction by means of orthodontic forces can be applied directly (**Fig. 2.7**) or after a period of time to allow for any spontaneous eruption (**Fig. 2.8 B, C**) and minimize the duration of active force application. Spontaneous eruption mainly contributes to reduction of total active traction time by reducing the vertical height but in almost all impactions, canines will need to be moved further buccally or distally as well later root torque correction (**Fig. 2.7 G, H**). The chosen strategy is related to the bucco-palatal position of the canine, its relationship to adjacent teeth, vertical height, and degree of root formation. Roots with open apices have more potential for spontaneous eruption.

A wide variety of appliances are available for the orthodontic retrieval of impacted canines. Different mechanical designs allow force application in several

directions according to the initial position of the canine, and taking into account the effect on the anchoring teeth that counteract the reactions to the forces exerted by the canine traction. Some mechanical assemblies anchor mainly on the adjacent teeth (lateral incisor and first premolar) such as pulling directly against the main AW or through a “ballista” spring (**Fig. 2.7 D-F**). Other appliances anchor on the posterior teeth (first molars only or along with premolars) such as a cantilever wire extending from the first molars buccally or palatally from a transpalatal bar (**Fig. 2.7 B, C**).

The options for management of the impacted canines are summarized in the following (**Table 2.1**).

Table 2.1: Treatment options of palatally impacted canine

	Option	Procedure / Mechanism
1	No active treatment	Leave and observe
2	Interceptive treatment	Early extraction of primary canine and/or providing space by means of arch expansion or posterior teeth distalization.
3	Open exposure	Spontaneous eruption followed by orthodontic traction.
4	Surgical exposure/traction	Orthodontic traction (Figures 2.7-9).
5	Surgical removal	
6	Surgical repositioning	Alignment or transplantation.

The treatment plan might change when diagnosing with a CBCT from the combination of periapical and panoramic radiograph because they allow locating the canine but do not reveal its relationship to adjacent teeth as it would be necessary to orthodontically move the canine away -distally, for example- from the roots of the incisors before bringing it down vertically. Therefore, the CBCT almost always provides added advantage in the cases of impacted canines. It was reported that in 27% of the situations, the CBCT can make a difference in the treatment plan compared to the panoramic and periapical (Haney et al., 2010).



A. Surgical exposure of bilateral palatally impacted canines (open window technique).



B. After only one month, first activation through distal pull using a 0.019*0.025 betaTi cantilever retraction loop anchored on transpalatal bar supported by the second molars.



C. Five months after exposure, cantilevers are activated vertically.



D. Direct pull in buccal direction against AW using elastic chain (11 months after exposure)



E. Direct pull with elastic chain on the right, and vertical-buccal pull with ballista spring (12 months after exposure)



F. Underlay NiTi wire used to align canines into the arch (13 months after exposure)



G. Engaging canines with the main AW (16 months post exposure)



H. Final alignment of canines after torque correction in finishing stage of treatment

Fig. 2.7: Treatment progress photographs of maxillary arch of an 18.4 years old female with bilateral palatally impacted canines



A. Pretreatment maxillary arch photograph. The retained right primary canine along with the submucosal palatal bulge indicated the corresponding permanent canine impaction.



B. PIC was exposed and left with an open window to allow for spontaneous eruption (one month after exposure)



C. After 5 months, the canine erupted more occlusally.



D. 7 months after exposure and only 5 weeks of active traction of canine against the arch wire.



E. After 6 months of initial canine traction, the canine was engaged in the wire and torque correction started.

Fig. 2.8: Treatment progress photos of maxillary arch of a 13 years old male with unilateral palatally impacted canines



Fig. 2.9: Maxillary arch of a 14 years old female with palatally impacted canine. A button attachment was bonded on the canine crown after surgical exposure and a distal traction mechanism activated through a closed eruption technique.

2.4. Finite Element Analysis (FEA)

2.4.1. Principles and Applications of FEA

Biomechanics is a fundamental aspect to in all dental specialties. This interaction includes dental restorations, movement of malaligned teeth, implant design, dental trauma, surgical removal of impacted teeth, and orthopedic growth modification. Following any functional load, stresses and strains are created within the biological structures. The amount of stress and how it is distributed over a tooth or prosthesis is critical and could lead to failure of the prosthesis, remodeling of bone, or dictate the type of tooth movement. However, in vivo methods that directly measure internal stresses without altering or damaging the tissues do not currently exist. The advances in computer modeling techniques offer another option to realistically estimate stress distribution.

Finite element analysis (FEA), a computer simulation technique, was introduced in the 1950s using the mathematical matrix analysis of structures to finite continuum bodies (Zienkiewicz & Kelly, 1982). Over the past 30 years, FEA has become widely used to predict the biomechanical performance of various medical devices and biological tissues due to the ease of assessing irregular-shaped objects composed of several different materials with mixed boundary conditions. Unlike other methods (e.g., dynamometer, strain gauge), which are limited to points on the surface of evaluated structures, the finite element method (FEM) can quantify stresses and displacement throughout the anatomy of a three dimensional configuration.

2.4.2. FEA in Dentistry

Earlier application of FEA in dentistry consisted mainly of 2D analysis and often required a high number of calculations to provide useful analysis (Farah, Craig, & Sikarskie, 1973; Peters, Poort, Farah, & Craig, 1983). The earlier 3D jaw models and tooth models were based on CT scans with coarse meshes that were analyzed to study chewing forces (Jones, Hickman, Middleton, Knox, & Volp, 2001; T. Koriath & Versluis, 1997; T. W. P. Koriath, 1993). With advancements in computers and modern medical imaging, more accurate modeling for complex 3D structures was possible using μ CT images. Moreover, the introduction of 3D computer-aided-design (CAD) have allowed accurate rendition of dental anatomy and prosthetic components such as implant configuration and veneer crowns. It was also recognized that the inclusion of the complete dentition is necessary to accurately predict stress-strain fields for functional treatment and jaw function (Field et al., 2009). Comparatively, in simple models that are comprised of a single tooth, the effect of tooth-tooth contacts that is important in critical biomechanical problems, such as anchorage control during orthodontic tooth movement, is ignored.

Current 3D models are first reconstructed from 3D images such as CBCT, μ CT, MRI or other imaging methods. Reconstruction of a model from the image is done by segmentation of the image into its structures using a 3D reconstruction software followed by discretization of the solid model. Among many 3D reconstruction softwares are ScanIP© (Simpleware, Exeter, UK), Mimics© (Materialise, Leuven, Belgium), and Amira© (FEI, Berlin, Germany).

Additionally, any specific appliances or gadgets such as dentures, prosthesis, orthodontics appliances, dental restorative materials, surgical plates and dental implants

can be added to the model using a CAD software like Solidworks© (Waltham, MA, USA), Pro Engineering© (Needham, MA). These models are then imported into solvers (e.g., Abaqus or Ansys) for the FEA analysis to be run.

FEA has been widely applied in dentistry. Cervical restorations were evaluated for the mechanical failure of biomaterials in clinical loading conditions. Further studies tested elastic modulus of restorative materials used and concluded that more flexible materials with elastic modulus of 1 GPa should be used for cervical restorations for the better results (Ichim, Schmidlin, Li, Kieser, & Swain, 2007).

Some biologists put into question the validity of results from FEA studies, emphasizing the need for a judicious justification for each model. However, the critics may be overlooking the valuable contributions of FEA to biomechanical principles. Indeed, the model is reasonably well validated if three of the construction steps are controlled:

1. Adequate representation of the anatomy, usually through a 3D image, which may be verified in many effective ways. In this context, FEA model construction on the basis of a typodont may not be as accurate.
2. The quality of FEA model division into its finite components (discretization or meshing), specifically by evaluating the results of different mesh sizes (mesh size testing), commonly referred to as numerical convergence (see Methods section).
3. Adherence to best anatomical fit of the material properties of the biologic components under study namely, bone, teeth, and periodontal ligaments. In this respect, assumptions are made about these tissues based on extensive studies available in the literature and validated with enough scientific support.

The overriding premise in this field of research is that such experiments on mechanical testing cannot be carried out in the living body because of their invasiveness to the tissues, and that outcome can only provide guidelines that may be further tested when applied clinically.

2.4.3. FEA in Orthodontics

Finite element analysis has not only been used in orthodontics since early 1990's and has been applied mainly in studying the mechanics of tooth movement, but also in testing the properties of craniofacial components and associated development.

2.4.3.1. Mechanics of tooth movement

Among the different applications of FEA in orthodontics is the determining some basic biomechanics principles such as center of rotation and center of resistance of certain teeth or structures to testing specific movements such as investigation of stress and displacement of maxillary teeth during en mass retraction by use of interdental miniscrews (E.-H. Sung et al., 2015).

Various appliances have been tested using FEA to determine how they function and test modifications in their design. For example, RPE arm shape and length, the vertical position of the expander, and the effect of the screw anchored expander on maxillary bone and teeth were investigated (Matsuyama, Motoyoshi, Tsurumachi, & Shimizu, 2014). Another FEA study gauged torque control of maxillary incisors during retraction (Liang, Rong, Lin, & Xu, 2009). Moreover, Sung SJ assessed the anti-tip and anti-rotation effects of reverse curve of spee in labial and lingual orthodontics (S. J. Sung, Baik, Moon, Yu, & Cho, 2003). K Tanne, Matsubara, and Sakuda (1995), used

finite element analysis to determine the location of the centre of resistance (CRe) for the nasomaxillary complex. They suggested that CRe of the nasomaxillary complex is located on the posterosuperior ridge of the pterygomaxillary fissure, registered on the median sagittal plane.

2.4.3.2. Craniofacial growth patterns

Finite element method or morphometry (FEM) is one of the descriptive applications to illustrate growth of craniofacial structures (Moss et al., 1985) or to describe how certain landmarks behave in specific anomalies such as Apert Syndrome (Bookstein, 1987). Other authors applied finite element morphometry in trying to explore the class III malocclusions and evaluate different structures contributing to it (Singh, McNamara Jr, & Lozanoff, 1998).

This application of FEM requires longitudinal data of specific landmarks that represent anatomical growth centers. Discretization of the studied maxillofacial components into smaller elements and nodes allows depicting the changes at each of those points and the amount of growth at the surface and within the structures. The major advantage of the FEM over routine cephalometric studies is that it can provide an estimate of the growth behavior of any point in the concerned body and also in all directions.

The application of FEM in studying growth of a complex structure over time is best summarized by Moss et al. (1985) as the analysis of a transformation by the FEM that necessitates before and after the transformation both the location of individual nodes and their accurate three-dimensional coordinates. Technically, the procedure

involves the ability to “map homologous points from one-time frame to another”, and “identify end points of the path of a particular point in space-time.”

While not employing the full spectrum and power of FEA in generating technically usable applications for tooth movement, the FEM usage in craniofacial growth remains mostly a research tool and has not found common use in daily orthodontic practice, probably because main conclusions inferred from the method do not contradict findings obtained from traditional 2D or more recently 3D imaging techniques.

2.4.4 FEA of Impacted Canines

Unlike other orthodontic tooth movement models, FEA studies of orthodontic retrieval of the impacted canine are scarce. The only available investigation was based on a single simplified model not including the adjacent teeth whereby the canine was subjected to several scenarios of force angulation (Zhang, Wang, Ma, Ru, & Ren, 2008). The authors found that the distribution of the equivalent stress was relatively even with the vertical force, while concentrated more on the load pointing side when the force was perpendicular to the long axis of the tooth (**Fig. 2.10**). With a 45° force angulation, the equivalent stress distributed between the previous two conditions.

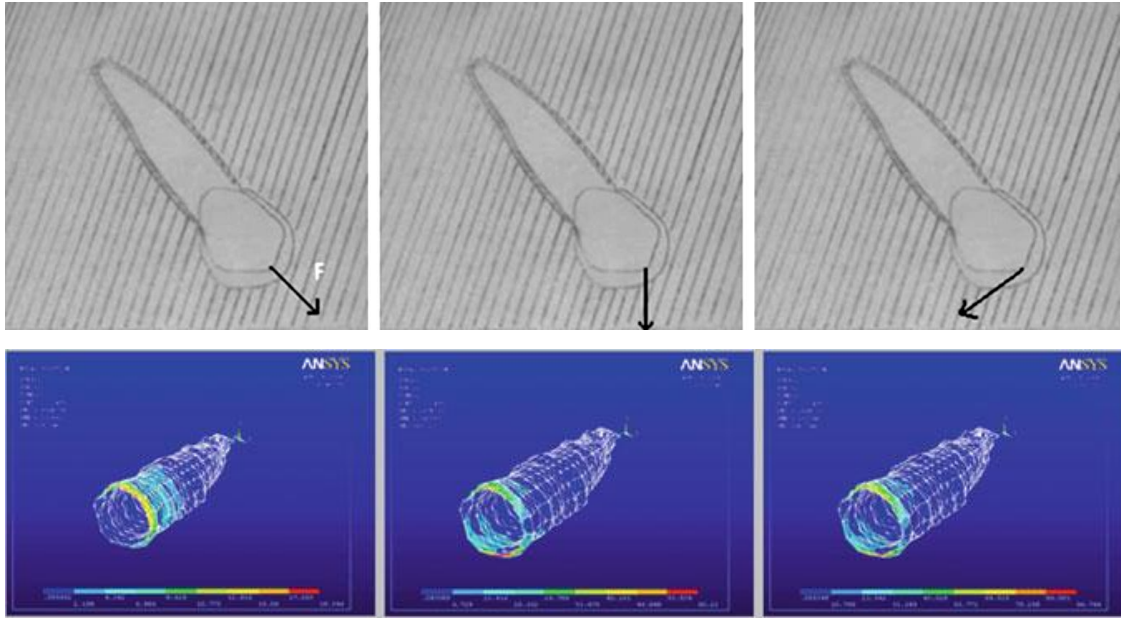


Fig. 2.10: Equivalent stress distribution to different force angulations on the PDL of the canine. 1: Vertical force (left), 2: force is 45° to long axis of canine, and 3: force is perpendicular to long axis of canine (right). Figures after (Zhang et al., 2008).

Zhang et al. (2008) did not consider the anatomy of the palate, adjacent teeth, and initial canine position. Therefore, the simulated conditions were of lesser direct clinical application. Also missing was the simulation of reactions to tooth movement across various individual impaction morphologies. The study provided information on the variation of stress with different loads. A more detailed analysis of stress distribution is needed to evaluate the variation in response and explore clinical implications.

2.5. Significance

Significance of the present study is based on the following determinations:

1. Total treatment time to bring the impacted canine to its optimal position in the dental arch after its exposure is usually related to the position and angulation of the tooth. Because of the time needed to align the root within the bone,

treatment time of an impacted canine ends up being longer (Becker & Chaushu, 2013; Mavreas & Athanasiou, 2008), with an added “tax” on the regular treatment of the existing malocclusion. Moreover, significant forces are usually needed for traction of the impacted canines, potentially causing significant reaction forces or stresses against adjacent anchoring teeth predisposing them to root resorption, the loss of root substance through the effect of odontoclasts (Blake, Woodside, & Pharoah, 1995; Woloshyn, Årtun, Kennedy, & Joondeph, 1994). The risk of occurrence of root resorption is higher in longer treatments and when using heavier forces, both of which are difficult to avoid during impacted teeth traction (Levander & Malmgren, 1988, 2000).

2. Extrusion is considered a tooth movement with least resistance compared to intrusion, bodily movement, torque, and other types of tooth movements (Smith & Burstone, 1984). The force direction is usually parallel to the long axis of the tooth in pure extrusion. This usually amenable movement becomes difficult to achieve because of the variable angulations, heights, and crown deviation of palatally impacted canines, and the potential interference with the adjacent teeth. Barring the predictability of this pure vertical force direction to move the impacted canines, additional forces are required, at times in undefined directions in order to align those impacted canines into the arch. Those forces and their resultant stresses are hard to be determined clinically solely especially with the infinite variety of impaction scenarios.

3. Different mechanical assemblies (appliances) are used to support the anchorage during retraction of impacted canines. The nature of the thicker cortical bone covering the palatal bone (Kang, Lee, Ahn, Heo, & Kim, 2007) and the relatively long root of the maxillary canine result in higher resistance to tooth movement, which in turns require applying relatively higher forces. Thus, orthodontic treatment of palatally impacted canines is more challenging and dictates well anchorage control.
4. The reaction to the traction of impacted canines is stress over the anchoring teeth, which is distributed differentially over the whole arch, albeit mainly over the neighboring teeth, thus the common root resorption of the lateral incisors (Ericson & Kurol, 2000). The stress may also cause tipping or could even result in the intrusion of anchoring teeth if the reaction forces are not well controlled. This complex relationship between canine traction and its effects on the adjacent teeth has not been studied in a way that allows predicting the required force direction relative to the initial impacted canine position/angulation, in order to prevent or at least minimize the adverse reactions to anchoring teeth.

According to the above realities, the significance of a comprehensive FEA study of palatally impacted canines is multifaceted:

1. It should allow the determination of stresses on the canine and adjacent teeth in a model that reconstitutes real maxillary anatomy rather than virtual situations taken out of the context of their immediate environment
2. Differential stress will be investigated in clinical settings that are not fully understood, when the initial activation is compared in clinically applied

directions (buccal, vertical and distal) without existing guidelines relating the movement to canine inclination and impaction severity.

3. The inclusion of various positions of the canine drawn from real clinical situations shall provide the closest application of FEA that would detect individual variation and average responses, compared to hypothetical problems that have heretofore dominated FEA orthodontic investigations.
4. The comparison of stresses on adjacent teeth is lacking when common orthodontic appliances are used.

The basic premise in such a study is the inability to conduct the research on living structures, thus resorting to the FEA enables the closest reproduction of the various anatomical components (teeth, bone, periodontal ligament) involved in the biologic response to forces applied to move the impacted tooth.

2.6. Specific Objectives

1. Develop on the basis of 3D imaging technology (CBCT scans) a scheme to determine the severity of palatal impaction of the maxillary canines that would be related to treatment objectives, not only diagnostic features.
2. Determine the level of stresses on the impacted canine when subjected to initial force activation in various directions: buccal, vertical, and distal.
3. Determine the association between the stresses thus generated with the severity of inclination of the impacted canines.
4. Evaluate the stresses on adjacent teeth generated by different appliances used for the traction of the impacted canines.

CHAPTER 3

MATERIALS AND METHODS

3.1. Materials

The material comprised cone beam computed tomography (CBCT) scans of 28 patients (mean age: 16.06 years) who had 38 palatally impacted canines (18 unilateral and 10 bilateral) and sought orthodontic treatment at the department of Orthodontics and Dentofacial orthopedics at the American University of Beirut Medical Center. The scans were prescribed specifically for accurate localization of the impacted canines after clinical examination and initial diagnostic panoramic or periapical radiograph. This study was approved by the Institutional Review Board (IRB) of the American University of Beirut on October 16th, 2015.

CBCT scans were selected according to the following criteria:

-Inclusion criteria:

- Presence of unilateral or bilateral palatally impacted canine. Canines had been considered at higher potential for impaction when
 - a. at the recorded clinical examination they were not palpable in the vestibule, prompting further radiographic confirmation.
 - b. when they had not erupted in the oral cavity beyond the age of 13 years (1 year after the normal maxillary permanent canine eruption age range of 11-12 years).

Within this scheme, 2 girls whose initial regional CBCT scans were taken at ages 10 and 11 were included in the study, and who were treated nearly one year later

with exposure of the canine then orthodontic traction into the arch. A subsequent CBCT was not taken to minimize radiation; the tooth was followed up with a periapical x-ray.

- CBCT scans of good quality and sufficient field of view covering at least half of the maxilla.

- Exclusion criteria:

- Presence of any craniofacial anomalies or syndromes.

- X-ray of limited field of view or of low resolution that does not allow accurate measurements.

The research includes two studies: **CBCT study** and **FEA study**. In the first investigation, all 38 canines from the 28 patients were included. In the latter, 30 canines from 21 of the 28 patients were processed in the FEA model.

3.2. CBCT Study

Linear and angular measurements were recorded on various sections of the scans, using Ez3D Plus 3D CDViewer Ver. 1.2.6.6 software (Vatech Global, Korea).

The measurements included:

- a. On the panoramic section (Fig. 3.2), PIC/VAC angle, formed between the long axes of the palatally impacted canine PIC and virtually aligned canine VAC (**Fig. 3.1**). The latter was determined by drawing a vertical line parallel to the adjacent teeth or along the long axis of the primary canine if present (**Fig. 3.2**).

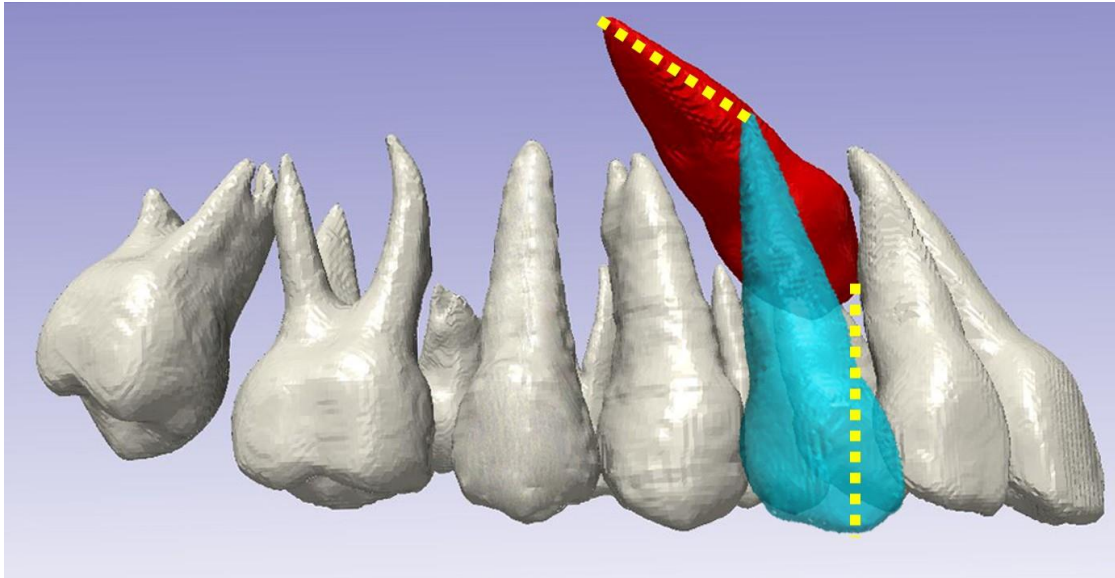


Fig. 3.1: Virtual alignment of impacted canine. Movement of apex and cusp tip in yellow dotted lines from palatally impacted canine (PIC in red) to virtually impacted canine (VAC in turquoise).

- b. On the coronal section, PIC angulation to the midline (**Fig. 3.3A**);
- c. On the axial section, cusp-tip and apex deviations, the respective distances between the cusp tips and apices of PIC and VAC (**Fig. 3-3B**).
- d. On the sagittal section, PIC angulation to palatal plane (PP), cusp-tip to occlusal plane (vertical projection), and the anterior projection of the cusp-tip to prosthion (Phulari, 2013) at the inter-incisal alveolar crest (**Fig. 3-3C**).

Two subgroups were categorized on the basis of severity of the angle PIC/VAC, the cutoff set at 30°, at nearly one third the maximum hypothetical range from vertical to totally horizontal inclination for the canine.

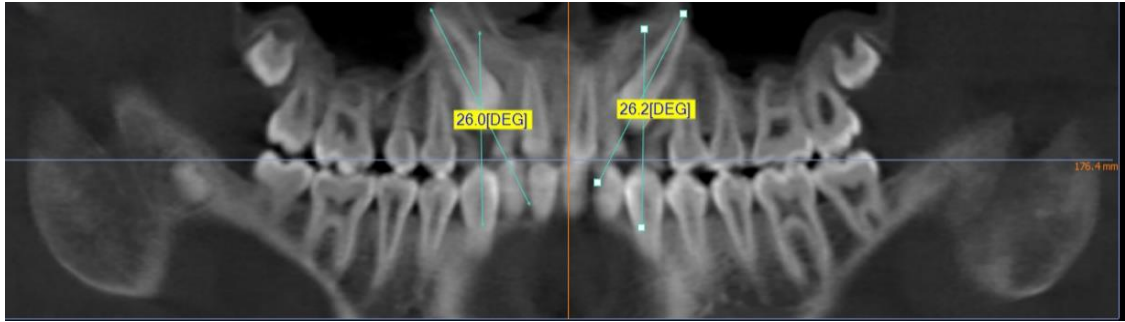


Fig. 3.2: Panoramic view: PIC/VAC angle between palatally impacted canine and virtually aligned canine.

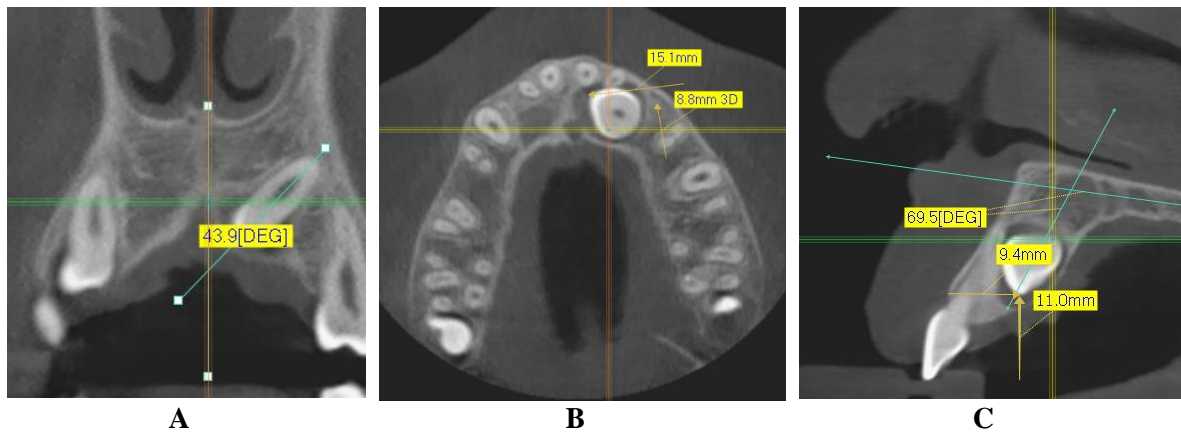


Fig. 3.3: Different views of CBCT scan. A. coronal view (PIC to midline angle); B, axial view (cusp and apex deviation, cusp and apex distance to midline); C, lateral view (PIC to PP angle, vertical height and anterior position of cusp).

3.3. FEA Study

CBCT scans were obtained of 21 patients (mean age 16.23 years) who had 30 palatally impacted canines (12 unilateral and 9 bilateral). The 21 scans were part of the 28 scans included in the CBCT study of the research.

A 3D model was initially reconstructed from a CBCT 3D scan representative of the PIC condition, with appropriate space for the alignment of the canine and minor alignment required for the rest of the teeth in the dental arch. The reconstruction consisted of performing 296 transversal sections with a pixel dimensions of 0.200X0.200X0.200 and a resolution of 400x400x296, using Scan IP 7.0 3D image processing software (Simpleware, Exeter, UK).

The model was initially segmented into alveolar bone, and the full maxillary dentition according to the grayscale value thresholds. The periodontal ligament PDL was fashioned as a separate layer of 0.25 mm. This 'FEA model' was used as a prototype model (**Fig. 3.4**), in which the remaining 29 impacted canines were repositioned according to their original location and inclination in the respective individual CBCT scans. To obtain this positional translation, the individual scans were aligned on the FEA model registered on prosthion anteriorly and the palatal raphe midline.

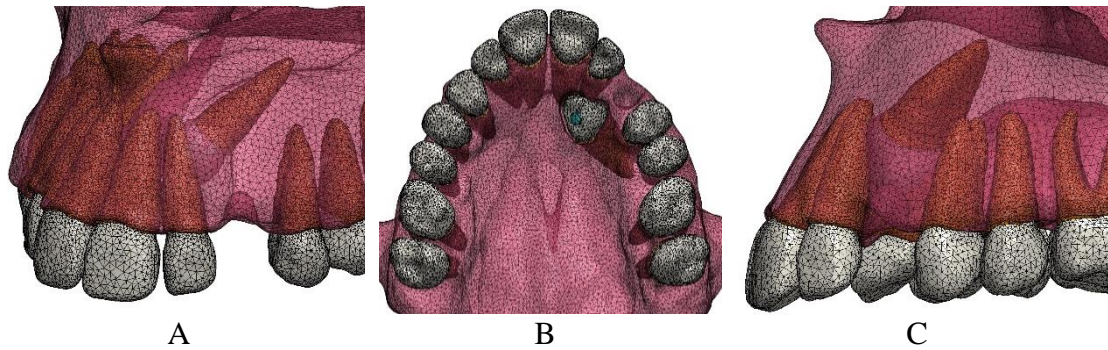


Fig. 3.4: Prototype model mesh from different views, composed of alveolar bone (red), PDL (orange), teeth (white)

FEA was used to simulate the effect of a force applied to displace the canine in various force directions (buccal, distal, vertical) and determine:

- 1 The resultant stresses on the PDL of the 30 different impacted canines
- 2 The reactive stresses on the adjacent teeth, tested only on the prototype FEA model and compared in the following loading scenarios, reflecting commonly used clinical strategies to move the PIC into the dental arch:
 - a. Direct pull against a rectangular stainless steel arch wire.

- b. Vertical extrusion using a transpalatal bar (TPB) anchored on the maxillary permanent first molars without any other fixed (braces) appliances.
- c. Vertical extrusion using a TPB anchored on the maxillary first molars combined with a stainless steel arch wire inserted in brackets attached to the entire maxillary dentition.

The 3D models were exported to the FEM analysis program, Abaqus V6.13-1 (Dassault Systemes Simulia Corp., Providence RI, USA).

3.3.1. Model Reconstruction:

Model reconstruction comprised 3 steps: **a. Teeth Mask Reconstruction**, **b. Bone Mask Reconstruction**, and **c. Canine Repositioning**.

3.3.1.1. Teeth Mask Reconstruction

Step 1. Segmentation and processing

- a. The initial CBCT scan was imported to the 3D editing software ScanIP and segmented into teeth mask by means of grayscale values (**Fig. 3.5A**). Noteworthy is the fact that the teeth and parts of the cortical bone have similar grayscale value.
- b. Processing of the teeth was initiated, along with cropping of the primary dentition, wisdom teeth, and mandibular teeth, by using the 3D editing tools ['Create area of interest', 'Delete'] (**Fig. 3.5B**).

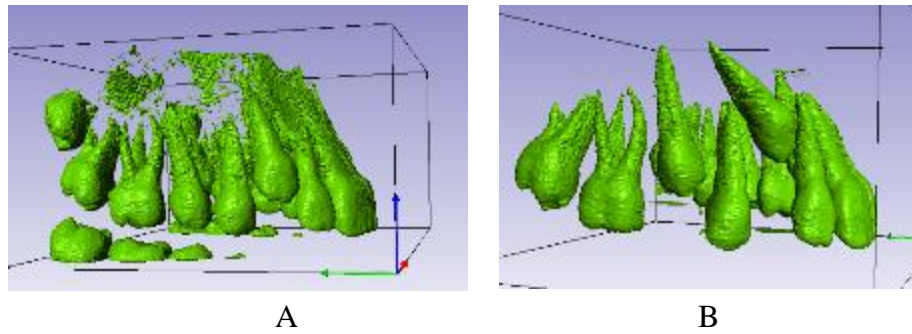


Fig. 3.5: Teeth mask reconstruction: segmentation (A), processing (B).

Step 2. Clean up

- a. All floating excess elements were removed with the ‘island removal’ tool followed by the ‘floodfill’ segmentation tool (**Fig. 3.6A**).
- b. The teeth were reconstructed using a combination of 3D editing tools and Manual 2D editing Paint/Unpaint, followed by median smoothening filter (**Fig. 3.6B**).

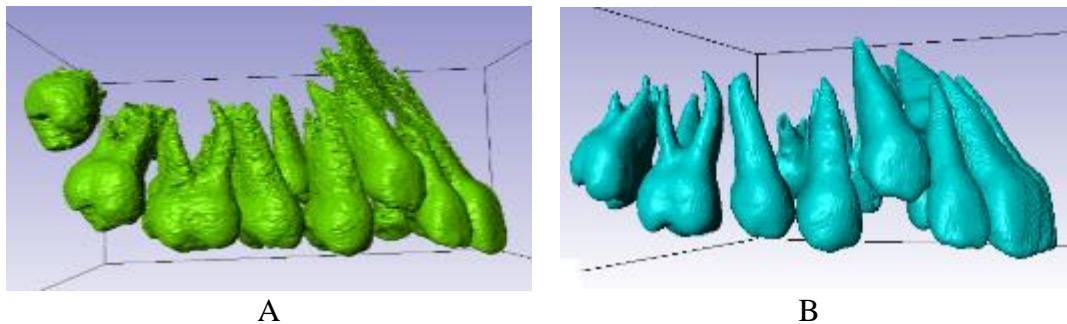


Fig. 3.6: Teeth mask reconstruction: removal of floating excess (A), smooth filtering (B)

Step 3. Separation of contact points

Any connected contact points were separated manually using a combination of 3D editing tools followed by local smoothening filter (**Fig. 3.7**).

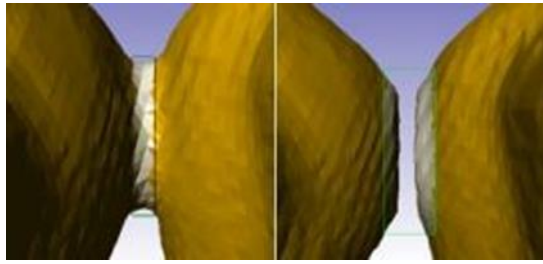
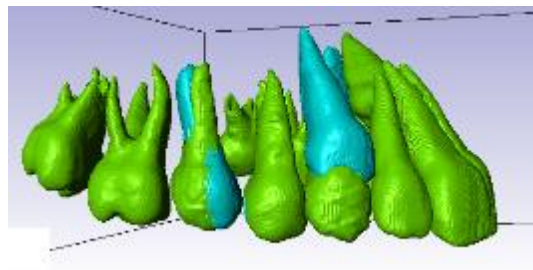


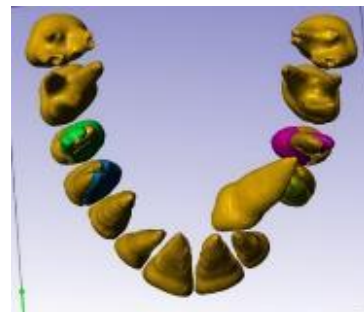
Fig. 3.7: Teeth mask reconstruction, separation of contact points

Step 4. Alignment of teeth

- a. Alignment of the maxillary canine (in its virtual corrected position in the arch) and of the second premolar (which was slightly tipped into a better position relative to the adjacent first molar and first premolar) was achieved using the selective area of interest on a copy of the teeth mask after deletion of the respective tooth on the original mask (**Fig. 3.8A**)
- b. Alignment of the teeth was completed with several steps superimposed (**Fig. 3.8B**).



A



B

Fig. 3.8: Teeth mask reconstruction: alignment of right canine and second premolar (A) and of other teeth (B)

Step 5. Completion of teeth mask

- a. The final teeth mask was completed without positioning the VAC, after applying a median smoothening filter (**Fig. 3.9A**).
- b. The VAC was inserted manually in the model along with all other original teeth, and the model was completed after applying a median smoothening filter (**Fig. 3.9B**).

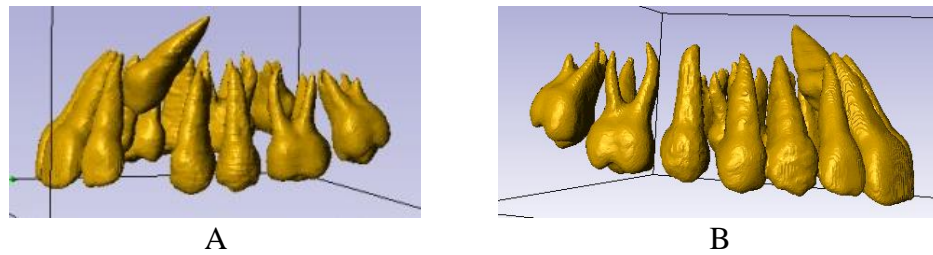


Fig. 3.9: Teeth mask reconstruction: completion (A) left view (B) right.

3.3.1.2. Bone Mask Reconstruction

To reduce the computational time of PIC traction simulation and because the main aim of the study is to investigate the effect of variation of canine position on the stresses generated within the PDL, the variation in the bone anatomy was disregarded and therefore, the created bone geometry from CBCT scan data was simplified into one material.

-Stage 1. Bone mask generation

- a. Initial segmentation of bone mask was carried out by means of grayscale values. Bone and parts of the teeth have similar grayscale value (**Fig. 3.10A**).
- b. Using the Paint with threshold tool, excess areas were separated from the bone for subsequent precise deletion, and large gaps were closed (**Fig. 3.10B**).
- c. A morphological “close” filter was applied, first general and then local, to close the remaining gaps in the bone (**Fig. 3.10C**).
- d. A floodfill segmentation filter was employed to remove any remaining floating elements, then a smoothing median filter of 2 pixels was applied (**Fig. 3.10D**).

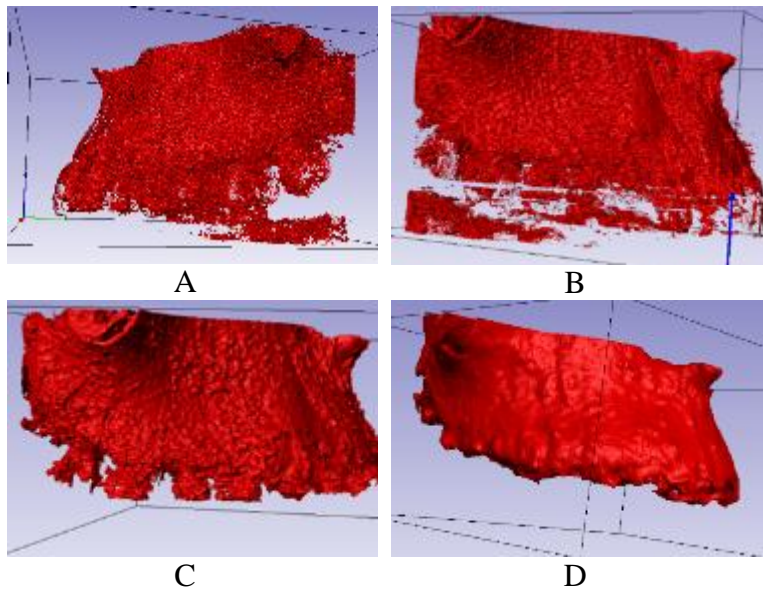


Fig. 3.10: Bone mask: initial steps of preparation. A. Initial segmentation. B. Excess areas separated. C. Morphological “filter” applied to close remaining gaps. D. Smoothing applied.

-Stage 2. Integration of bone and teeth

- a. Bone was regenerated after aligning the teeth using 2D paint. Then Boolean subtraction operation was used to remove any areas where bone and teeth masks overlap (**Fig. 3.11A**).
- b. The final bone mask was obtained after applying several smoothing filters and cavity fill tool to close any remaining gaps within the bone mask (**Fig. 3.11B**).
- c. Teeth and bone were joined to produce the final masks (**Fig. 3.11C**).

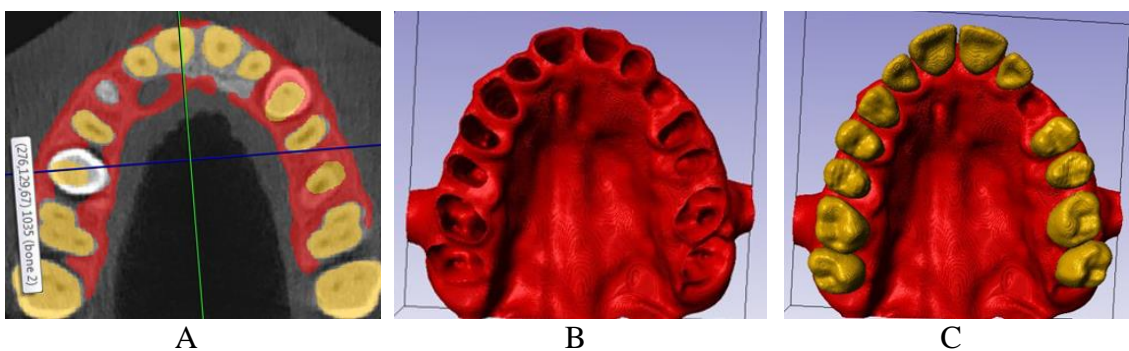


Fig. 3.11: Bone mask, integration of bone and teeth. A. teeth are aligned ad bone regenerated. B. smoothing of face mask. C. teeth and bone combined.

-Stage 3. Integration of periodontal ligament (PDL)

- a. The PDL was added by creating a dilated copy of the teeth mask, which is subtracted later from the original teeth mask by an average thickness of 0.25mm. This width is then subtracted from the bone using Boolean operations (**Fig. 3.12A**). The PDL was presumed as a layer with a constant thickness of 0.25mm, as widely adopted in existing literature (Field et al., 2009).
- b. A separate mask of 0.3 mm was added surrounding the crown of the canine to prevent the direct contact of canine-bone around the crown. This separation simulated the dental follicle canine crown space (**Fig. 3.12B**).
- c. Accordingly, the final 3D model was completed with 5 masks: teeth, canine, teeth PDL, canine PDL, and bone (**Fig. 3.12C**).

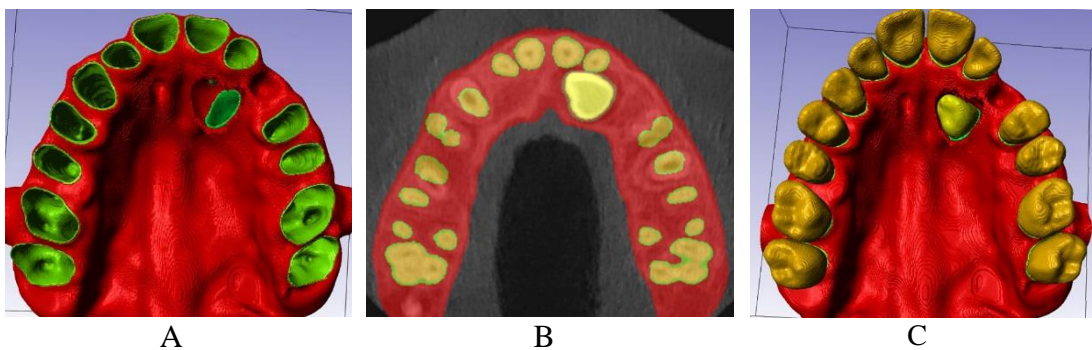


Fig. 3.12: Addition of PDL: A. Creation of PDL space (in green). B. Creation of canine crown space. C. Complete model with all 5 masks.

-Stage 4: Auxiliary attachment and mesh creation

- a. A separate attachment was added to the crown of the canine, representing a button to be used for applying the loads to the canine, as in the clinical situation (**Fig 3.13A**).
- b. A mesh of the model was created and included a total of [Nodes: 123,760. Elements: 627,250] (**Fig. 3.13B**).

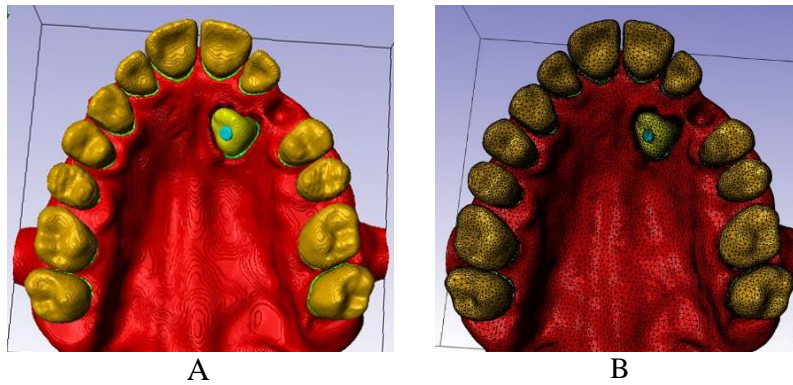


Fig. 3.13: Bone mask: A. addition of a lingual button on the canine. B. mesh of the model created.

3.3.1.3. Canine Repositioning

A new method was developed for the canine repositioning. The global axes were redefined in all 21 scans including the prototype model to the unified fixed reference point prosthion (Phulari, 2013). (**Fig. 3.14**). The below general steps were then followed:

1. Starting with the ScanIP project, 4 points were measured, the start (Original cusp and apex in prototype model) and end positions (Target cusp and apex of the other scan).
2. The previous measurements were exported and simple arithmetic computations in Microsoft Windows Excel were then performed as addition, subtraction, and normalization of vectors.
3. The canine meshed stl. file was exported along with the prototype FE model to the +CAD module of ScanIP.
4. Using a customized script in +CAD (See Appendix I), the canine was repositioned and exported along with the prototype model.

The detailed canine repositioning process involved the following sequences:

-Phase 1. Determination of position

- a. The origin (or registration) point (0,0,0) in (x,y,z) is redefined to point prosthion by

redefining the global axes of all scans to create a unified fixed reference to which the canine is accurately repositioned (**Fig. 3.14A-D**).

b. The positions of the impacted canine apex and cusp tip were measured relative to prosthion (**Fig. 3.14C**).

c. Final position of the global axes after redefining them at prosthion (most anterior point on the alveolar- **Fig. 3.14E**).

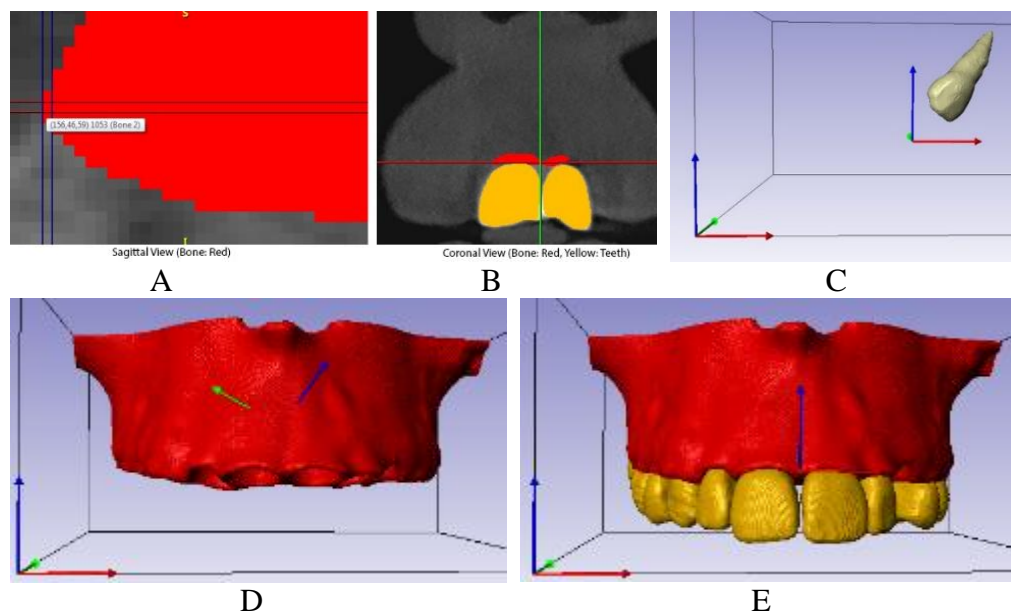


Fig. 3.14: Canine repositioning. Sagittal (A- in red) and coronal (B) views illustrating the determination of the individual canine positions relative to prosthion and midline. C. Cusp and apex positions established relative to prosthion. D. Initial position identified on CBCT global axes. E. Final position of the global axes on the complete model

-Phase 2: Creation of prototype canine mesh

- a. A mesh of the canine in the prototype model was created before exporting it to the CAD+ module along with the masks of prototype model (**Fig. 3.15A**). Twenty-one different models were then created with similar dentition, accurately reproducing the impacted canine position according to the different CBCT scans.

The positions of cusp tip and apex of canines in the prototype model and the other 20 scans were measured relative to the same reference point (prosthion). Prosthion was chosen because it represents a fixed reference that is readily reproducible and is easy to measure to.

- b. A copy to the prototype canine mesh was created (**Fig. 3.15B**).
- c. This copy mesh was repositioned to match the measured apex and cusp tip position according to each patient's CBCT scan using a customized script prepared specifically for this task (See Appendix I), (**Fig. 3.15C**).
- d. The repositioned canine mesh after the prototype canine mesh was removed (**Fig. 3.15D**).
- e. The repositioned canine mesh was fixed into the new position (**Fig. 3.15E**).

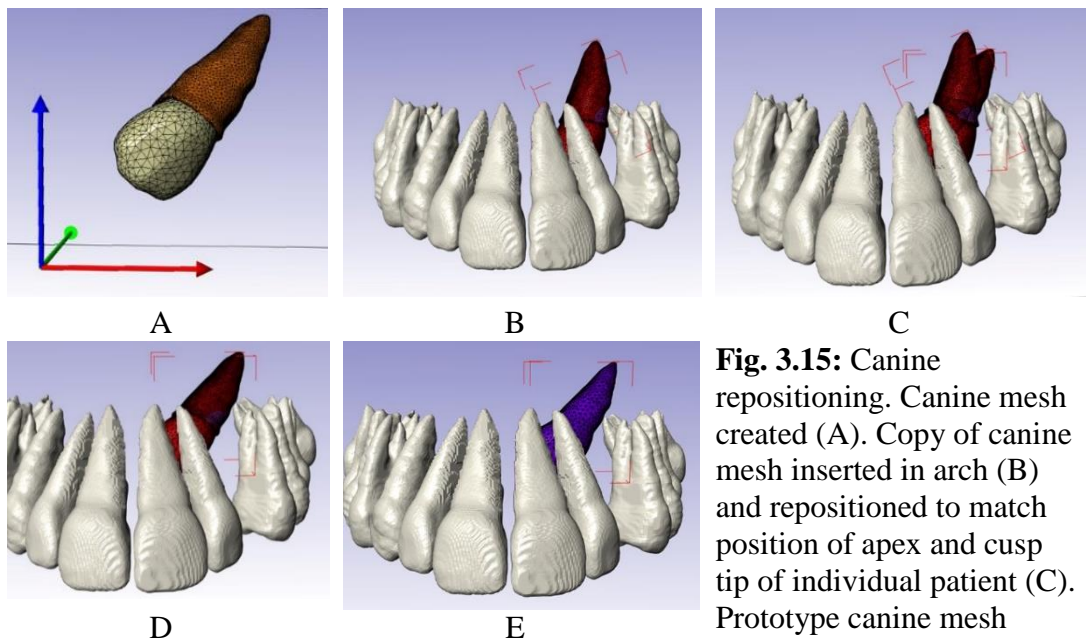


Fig. 3.15: Canine repositioning. Canine mesh created (A). Copy of canine mesh inserted in arch (B) and repositioned to match position of apex and cusp tip of individual patient (C). Prototype canine mesh removed (D) and individual canine mesh fixed (E).

-Phase 3. Correspondence in individual dentition

- a. The repositioned canine was saved and viewed in accordance with the remaining dentition and bone (**Fig. 3.16A**). When repositioning the impacted canine in a bilateral impacted canine scan, two copies of the prototype canine were generated and the canines repositioned according to their initial position in the individual CBCT scan (**Fig. 3.16B**).
- b. Three-dimensional coordinates were verified for the copy of the impacted canine mask, which was viewed and verified with its local axes before repositioning it according to the individual script (**Fig. 3.16C**).
- c. The resulting final mesh of the model after completion of the PIC repositioning was ready further FEA processing (**Fig. 3.16D**).

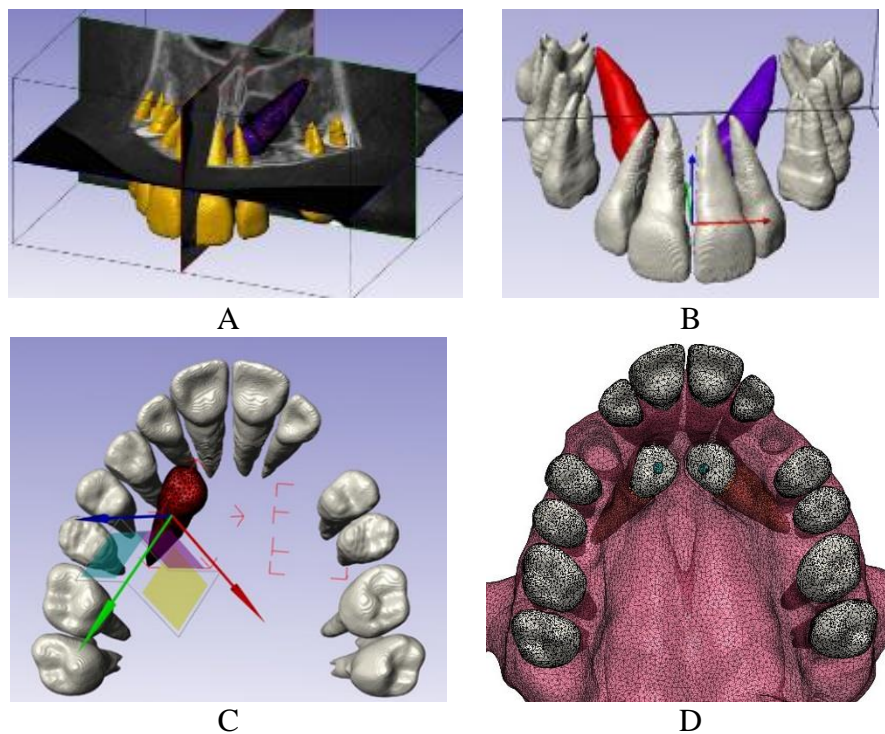


Fig. 3.16: Canine repositioning. A. Canine viewed with and in relation to rest of dentition. B. View of bilateral impacted canines in position within the FEA model. C. Canine mask viewed in its spatial position. D. Final mesh of model in bilateral impaction scenario.

-Creation of new PDL layer:

After canine repositioning and using Boolean operations, a new PDL layer was created for the repositioned canine following the same steps of creating the PDL of the other teeth. Bone was adjusted to fill any resulting gaps after the canine repositioning step, thus, eliminate any source of variation that is not related to position. The crown of the impacted canine was also cleared from any bony contact to allow for an accurate detection of stresses on the PDL of the canine. A complete model was created, meshed, and then exported for each canine.

3.3.2. Material Properties

In our model, all materials were linear and isotropic as summarized in (**Table 3.1**). The elements representing the teeth were assigned a Young's modulus of 20,000 MPa and a Poisson's ratio of 0.2 (Bourauel et al., 1999; NLY & ORM, 2001; Kazuo Tanne, Sakuda, & Burstone, 1987).

The periodontal ligament was assumed to have linear elastic properties sufficient to investigate initial responses under static loading and was assigned a Young's modulus of 0.68 MPa and a Poisson's ratio of 0.45 (Field et al., 2009; Qian, Fan, Liu, & Zhang, 2008).

Given the following facts:

- a. Our aim was to investigate the variation of the impacted canine position
- b. The bone at the palatal side of the maxilla is a relatively thicker cortical layer overlaying trabecular bone (Kang et al., 2007)
- c. Linear elastic material properties were applied to the PDL
- d. The elasticity material parameters of cortical and cancellous bone are at least

a factor of 10^4 greater than of the PDL tissue (Field et al., 2009); accordingly, their less significant effect on the outcome of the finite element analysis

e. To enhance the computational efficiency of the simulation, the alveolar bone was not differentiated into cortical and cancellous bone and was assigned a Young's modulus of 15,7500 MPa and a Poisson's ratio of 0.33 (Tanne et al, 1987).

Table 3.1 Material properties of the FEA model

Material	Young's Modulus (N/mm ² = MPa)	Poisson's Ratio
Stainless Steel	200.000	0.3
Tooth	20.000	0.2
Bone	15.750	0.33
PDL	0.68	0.45

3.3.3. Mesh size

The accuracy of the FEA results and required computing time are determined by the finite element size (mesh density). According to FEA theory, the FE models with fine mesh (small element size) yield highly accurate results but may take longer computing time. On the other hand, those FE models with coarse mesh (large element size) may lead to less accurate results but much shorter computing time. Smaller element size will increase the FE model's complexity, which is only used when high accuracy is required (More & Bindu, 2015).

In our finite element analysis model, we conducted only static analysis. The testing for ideal mesh size at which the model converges determined that the model should be discretized into elements of a minimum edge of 0.58 mm in order to obtain valid results.

The shape of the elements was tetrahedral. Convergence of the finite element solution was studied using 7 mesh sizes ranging from an average mesh size

minimum edge of 0.8 mm to 0.38 mm. The 7 models were tested by applying a vertical concentrated force of (1N) applied along the z axis. The solution was considered converged for a mesh size with minimum edge of 0.58 mm (**Fig. 3.17**).

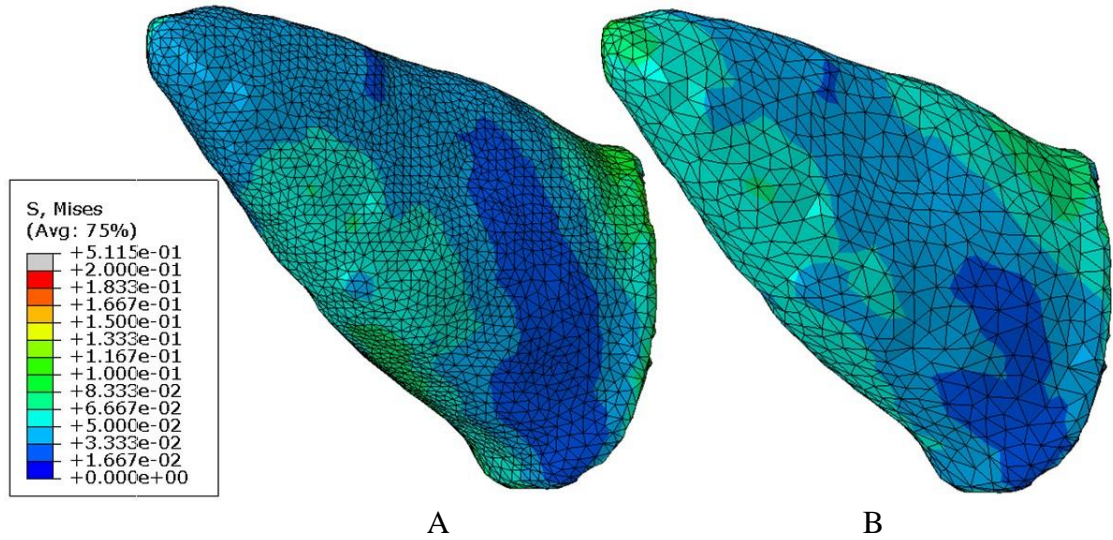


Fig. 3.17: Von Mises stress on PDL of canine with similar load (1N vertical force) but two different mesh sizes to check for convergence. A. Mesh size of -20 (minimum edge 0.38mm). B. Mesh size of -50 (minimum edge 0.8mm).

We concluded that the FE model which is meshed with -35 (minimum edge 0.58 mm) mesh size can give an optimal combination of accuracy and efficiency. The final FE mesh generated for each model contained approximately 91,500 elements, which was sufficient to obtain solution convergence.

3.3.4. Boundary Conditions

The following boundary conditions were applied in all parts of the study: models were fully constrained in translation and rotation at 2 surfaces of the maxilla superiorly and posteriorly, representing the attachments of the maxilla to its neighboring structures, the zygomatic, palatal and sphenoid bones (**Fig. 3.18**).

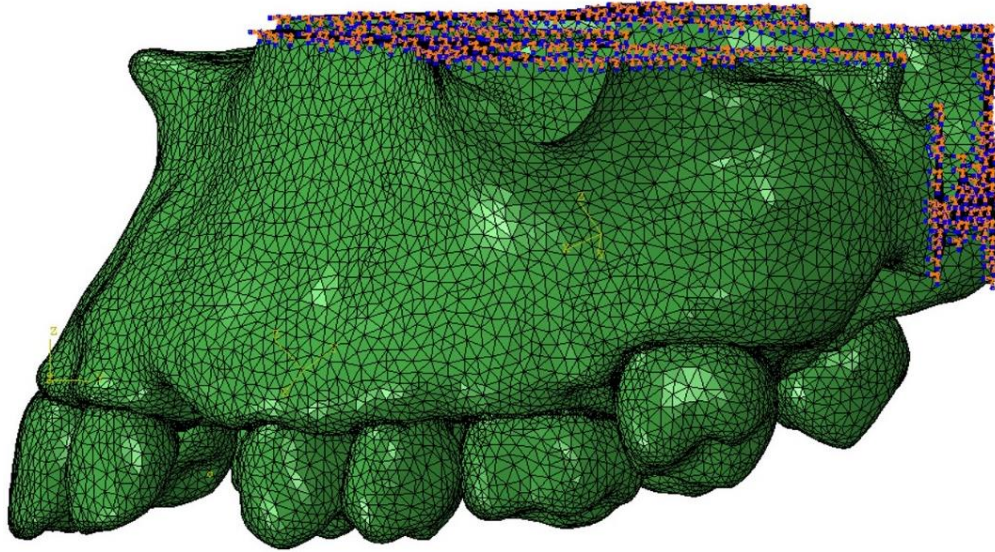


Fig. 3.18: Boundary conditions: models constrained from translation and rotation at areas of attachments of the maxilla to adjacent bones: zygomatic, palatal and sphenoid.

3.3.5. Loading of the impacted canine

Equal forces of a magnitude of 1N were applied on the button attachment placed on the palatal surface of the crown of impacted canine, simulating the clinical situation.

Forces were applied in 3 different directions, mirroring their delivery by specific orthodontic appliances (**Fig. 3.19**):

1. Buccal direction: reflecting the direct pull towards the maxillary arch wire AW (**Fig 2.7D**).
2. Distal direction: reproducing the pull towards a transpalatal bar (TPB) either directly or via a cantilever (**Fig. 2.7B, 2.9**).
3. Vertical direction: representing the extrusive force applied through a ballista or by a cantilever anchored over a TPB (**Fig 3.21, 2.7C, E**).

Stresses were evaluated at 3 levels of the PIC root, and for the whole root with each of the forces (**Fig 3.20**).

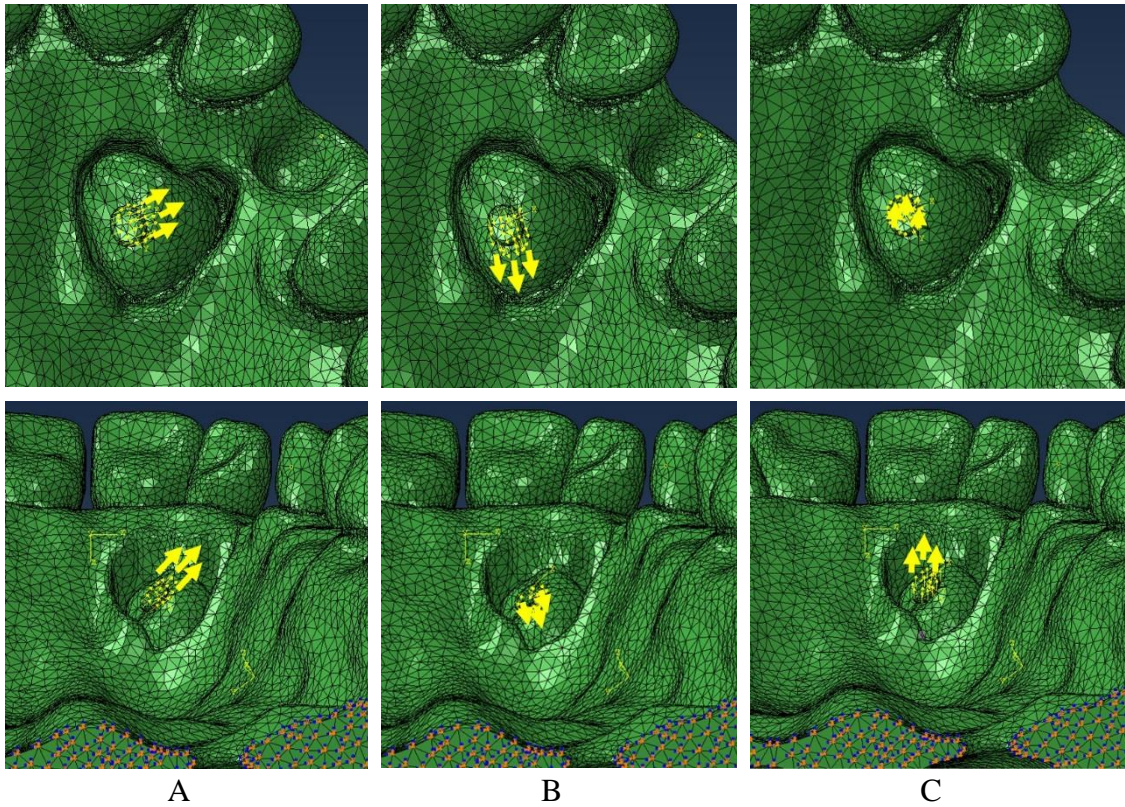


Fig. 3.19: Forces (yellow arrows) applied on canines shown in buccal (A), distal (B), and vertical (C) directions. Teeth are shown in occlusal (upper row) and posterior (lower row) views.

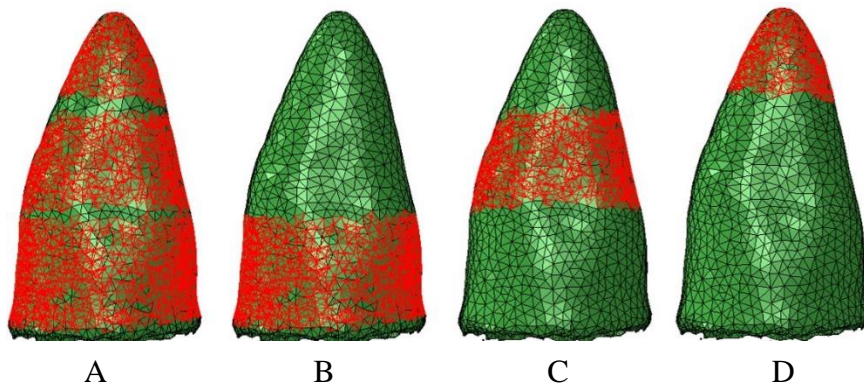


Fig 3.20: Element sets in which stresses were evaluated at different levels of the PIC root for each force (buccal, distal, and vertical). Stress was averaged on the entire PIC root (A), and its cervical level (B), middle level (C), and apical level (D).

3.3.6. Loading of The Adjacent Teeth

Three methods commonly used to move impacted canines into the dental arch were simulated for FEA study for the purpose of determining the reactions of the teeth adjacent to the canine to the applied forces.

- Appliance 1 consisted of a cantilever arm extending from a transpalatal bar (TPB) that was anchored on the permanent maxillary first molars and exerted vertical extrusion (**Fig 3.22**).
- Appliance 2: consisted of Appliance 1 in combination with a stainless steel arch wire engaged in brackets attached to the maxillary teeth except the permanent maxillary second molars (**Fig. 3.21, 3.22**).
- Appliance 3 comprised a rectangular stainless steel (SS) arch wire (AW) with the dimensions (0.018*0.025 inches) to which a direct pull against the canine resulted in a buccal force direction (**Fig. 3.21**).

Von Mises stresses generated in the PDL of right and left maxillary teeth were compared among the above-described 3 assemblies using the same force magnitude of 1N.

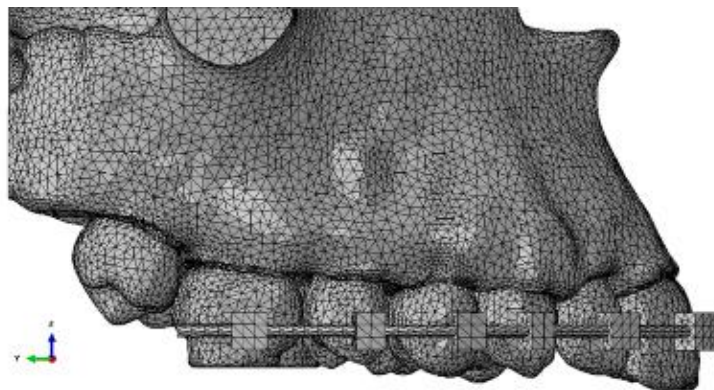


Fig 3.21: Meshed model of the maxilla and maxillary dentition attached with brackets, simplified to a size of 2x3mm on the premolar and 3x3mm on the rest of the teeth. A passively adjusted main stainless steel archwire was engaged in the maxillary brackets. Note that the second molars were not included in the assembly because they had not fully erupted.

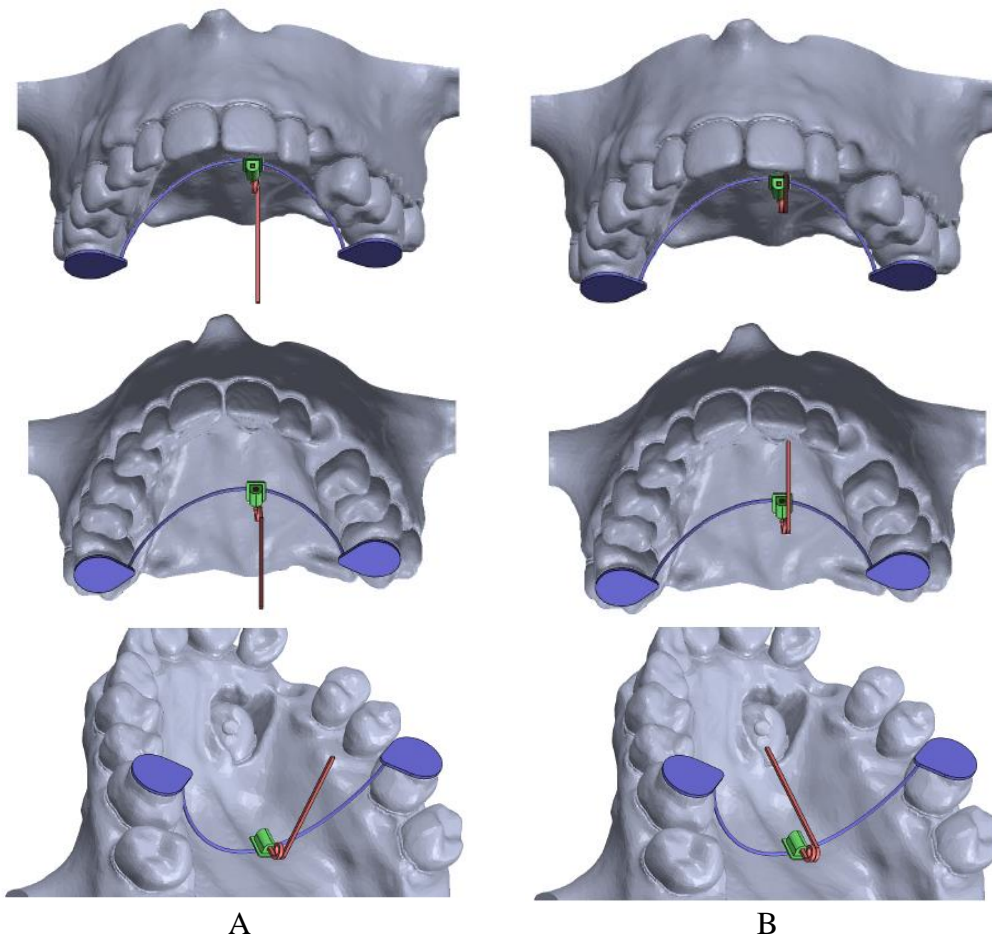


Fig. 3.22: Transpalatal bar (blue) shown in different views with the extending cantilever arm spring -red- at rest (A), and under tension (B).

3.3.7. Statistical Analysis

Three main levels of analysis-descriptive, bivariate and multivariate, were conducted on both, the main sample (N=38) in the CBCT study and on the subsample (N=30) in the FEA study. Moreover, both samples were also further subdivided into 2 subgroups based on their PIC/VAC angle severity to lower and higher severity subgroups.

Descriptive univariate analyses were based on angulation severity subgroups. For correlations, Pearson's correlation coefficient between PIC/VAC and other positional variables in the main sample and between stresses with positional variables in the subsamples. Furthermore, it was also used to correlate positional variables with stresses in different force directions in the higher and lower severity subgroups for the FEA study. Associations between the PIC/VAC and various positional variables were evaluated using multivariate regression analysis to test which variables would predict the severity of angulation.

Paired t-tests were used to test for differences in stress level comparing the two PIC/VAC severity groups under buccal, vertical and distal forces and at the varying root levels (cervical, mid-root, apical and average). To adjust for multiple statistical testing (12 tests), the critical value was adjusted to $p = 0.0042$ (Bonferroni correction). The repeated measures ANOVA was similarly used to detect differences in stresses generated between the difference force directions within each PIC/VAC severity group and for each level of root separately. When a significant difference was detected, the Bonferroni post-hoc multiple comparison test was used. When the variances were non-homogenous (Levene's test: $p\text{-value} < 0.05$), robust ANOVA (Welch) and the Games-Howell post-hoc test were reported. Again, to adjust for multiple testing (8 comparisons), the critical value was adjusted to $p = 0.0625$ (Bonferroni adjustment).

Mixed between-within subjects' two-way ANOVA tests were explored to test the effect of the between subjects' factor (severity) and the within subjects' factor (force direction) on the stress on the canine root (Cervical, mid-root, apical and average). The assumptions for homogeneity of variance and covariance were met only for stress at the mid-root level. The assumption of sphericity was met and therefore unadjusted *p* values were reported for the effect of severity and the interaction between severity and force direction.

In addition, bivariate and multivariate analyses were applied to explore the effects of potential covariates on stress in the periodontal ligament of PIC. All covariates associated with the outcomes at *p*-value<0.2 at the bivariate level were included in the multivariate analyses. For all variables included in the final multivariate models, adjusted odds ratio (OR), 95% confidence intervals (CI), adjusted coefficients of association (β) and *p*-values were reported. *P*-values less than 0.05 were considered statistically significant. The IBM® SPSS (V. 20.0) and STATA (V. 11.1) statistical softwares were used to perform all statistical analyses.

Intra examiner reliability was tested for Part I of the study (CBCT study), where measurements were repeated on 10 CBCT radiographs at least 14 days after initial assessment. The repeated measures were evaluated with the two-way mixed effects intra-class correlations for absolute agreement on single measures.

CHAPTER 4

RESULTS

4.1. CBCT Study

The intra-class correlation coefficients (ICC) gauging reliability of repeated measurements were high. The ICC values ranged from 0.942 to 0.997, except for the anterior ($r=0.79$) and vertical ($r=0.78$) distances in the sagittal plane.

4.1.1. Descriptive Data

The male to female ratio of patients with palatally impacted canines was 1:2.5. Their ages ranged from 10 to 32 years, with a mean age of 16.06 ± 4.9 years (16.9 years in males, 15.7 years in females). The range of the PIC/VAC angle was $9-59^\circ$ and its mean in the total sample was $32.47 \pm 15.46^\circ$ (**Table 4.1**). The average cusp deviation was 11.11 ± 3.15 mm, greater than the mean apex deviation of 8.20 ± 2.32 mm. The impacted canine angulation to midline was $27.44 \pm 15.18^\circ$, and to palatal plane $110.58 \pm 13.13^\circ$ (**Table 4.1**).

4.1.2. Difference Between Severity Subgroups

PIC/VAC angle was $19 \pm 6.6^\circ$ and $43 \pm 9.9^\circ$ in the lower and higher severity subgroups, respectively ($p<0.001$; **Table 4.2**). Differences between these subgroups were statistically significant: the inclination to palatal plane (sagittal; $p<0.001$), apex deviations and cusp to midline (axial plane; $p=0.003$ and 0.001 respectively), and inclination to midline (coronal; $p<0.001$) were all greater in the high severity group. The

distance between the antero-posterior position of first molar and the interincisal point in the axial view was smaller in the severe group compared to the less severe group (p=0.027; **Table 4.2**).

Table 4.1: Descriptive variables of positional components of palatally impacted canines (N=38)

	Male: 11 (28.9%) Female: 27 (71.1%)	Mean	SD	Min	Max
Age (years)		16.06	4.90	10	32
Panoramic view					
PIC/VAC* (degrees)		32.47	15.46	9	59
Sagittal view					
Anterior (mm)		9.11	1.98	4.6	15.22
Vertical (mm)		10.38	2.29	5	14.5
PIC to PP (degrees)		110.58	13.13	82.5	146.4
Axial view					
Cusp deviation (mm)		11.11	3.15	4.7	17.10
Apex deviation (mm)		8.20	2.32	4.4	12.30
Cusp to midline (mm)		4.89	3.01	0.9	60
Apex to midline (mm)		14.80	1.74	11	20.50
1 st molar to midpalatal plane (mm)		16.56	2.02	10.6	21.20
1 st molar to interincisal point (mm)		34.49	2.80	26.2	38.80
Coronal view					
PIC to midline (degrees)		27.44	15.18	4.7	57.3

VAC: virtually aligned canine; SD: Standard deviation; Min: minimum; Max: maximum

Table 4.2: Positional components of palatally impacted canines (PIC) in severity subgroups stratified on inclination between PIC and virtually aligned canine (VAC)

	PIC/VAC <30° n=18		PIC/VAC >30° n=20		p
	Mean	SD	Mean	SD	
Age of patient (years)	14.7	3	17.3	6	0.103
Panoramic view					
PIC/VAC (degrees)	19	6.6	43.6	9.9	<0.001*
Sagittal view					
Anterior (mm)	9.5	2.6	8.8	1.2	0.258
Vertical (mm)	9.7	2.2	11	2.3	0.098
PIC to PP (degrees)	103.6	8.97	116.9	13.26	0.001*
Axial view					
Cusp deviation (mm)	9.89	2.76	12.19	3.15	0.023*
Apex deviation (mm)	7.1	1.97	9.2	2.17	0.003*
Cusp to midline (mm)	6.5	2.64	3.5	2.65	0.001*
Apex to midline (mm)	14.5	1.4	15.1	2	0.333
1 st molar to midpalatal plane (mm)	16.5	1.8	16.6	2.3	0.900
1 st molar to interincisal point (mm)	35.5	2.26	33.5	2.65	0.027*
Coronal view					
PIC to midline (degrees)	17.2	11.9	36.7	11.53	<0.001*

*Statistically significant: p<0.05.

4.1.3. Correlations Between PIC/VAC and Other Positional Parameters

The highest correlations were observed between PIC/VAC angulation and the position of its cusp tip (**Table 4.3**). Specifically, the canine angulation to midline was significantly correlated to PIC/VAC ($r=0.85$), cusp-tip deviation ($r=0.67$), and cusp tip to midline ($r=-0.86$); ($p<0.001$). Moderate correlations ($0.46<r<0.62$) were noted between PIC/VAC and: cusp-tip, apex, and angulation to PP, and between apex position and angulation to PP ($r=0.62$); ($p\leq 0.002$).

4.1.4. Associations Between PIC/VAC and Other Positional Parameters

Based on the bivariate analyses, the significant predictors of the PIC/VAC value were the vertical position, angulation to midline in the coronal plane, and angulation to palatal plane in the sagittal plane, explaining 85% of the variation in PIC (**Table 4.4**). The addition of age to the multivariate regression model did not change the adjusted R^2 therefore, age was not a statistically significant variable in predicting PIC/VAC angle.

Table 4.4: Multivariate analysis of the relationship of PIC/VAC and remaining bivariate significant measures

Associated Variables	PIC/VAC Angle			
	Coef.	Std. Err.	95% CI	p value
Vertical Position	1.385	0.459	0.45 - 2.32	0.005*
PIC/midline	0.696	0.075	0.54 - 0.85	<0.001*
PIC/PP	0.398	0.085	0.23 - 0.57	<0.001*
Constant	-45.043	10.142	-65.654 - -24.43	<0.001
F (3,34)	63.24			
Prob > F	<0.001			
R2	0.848			
Adjusted R2	0.835			

*Statistically significant: $p<0.05$

Multivariate equation to predict PIC/VAC angle:

$X = 1.39*(\text{Vertical Position}) + 0.7*(\text{PIC/midline}) + 0.4*(\text{PIC/PP}) - 45.04$

X: PIC/VAC

Table 4.3: Correlations among positional parameters of palatally impacted canines (PIC) in various planes of space

Section	Measurement	Sagittal Plane†		Axial Plane†				Coronal‡	Sagittal‡	Axial Plane†	
		Anterior	Vertical	Cusp deviation	Apex deviation	Cusp to midline	Apex to midline	PIC to midline	PIC/PP	6 to midline	6 to Prosthion
Panoramic‡	PIC/VAC	0.01	0.3* [0.04]	0.57** [<0.001]	0.48** [0.002]	-0.7** [<0.001]	0.16	0.85** [<0.001]	0.6** [<0.001]	-0.02	-0.29
Sagittal†	Anterior†		0.07	0.25	0.22	-0.2	0.11	0.18	-0.23	-0.09	0.18
	Vertical†			-0.14	0.22	-0.17	-0.02	0.18	0.02	-0.32	-0.37
Axial†	Cusp deviation				0.37* [0.02]	-0.7** [<0.001]	-0.06	0.67** [<0.001]	0.46** [0.004]	0.19	0.09
	Apex deviation					-0.3	0.1	0.3	0.62** [<0.001]	-0.05	-0.05
	Cusp to midline						0.01	-0.86** [<0.001]	-0.35* [0.03]	0.2	0.39* [0.017]
	Apex to midline							0.29	-0.09	0.05	-0.14
Coronal‡	PIC to midline								0.37* [0.02]	-0.07	-0.32* [0.05]
Sagittal‡	PIC/PP									0.2	0.08
Axial Plane†	6- midline										0.7** [<0.001]

Correlation is significant at the: *0.05 level (2-tailed); **0.01 level (2-tailed). P values are listed in brackets and only for significant correlations.

PP: palatal plane; 6: permanent first molar

†: mm; ‡: degrees

4.2. FEA Study

4.2.1. Stresses on Impacted Canine

4.2.1.1. Stress Distribution and Force Direction

When evaluating the stress level on the whole root of PIC, distal and buccal forces resulted in higher stress ($S=6.64$ and 6.41 KPa, respectively); the vertical force produced the least stress ($S=5.97$ KPa) among force directions (**Fig. 4.1, Table 4.5**).

Pairwise comparisons of the stresses generated by different force directions at the apical third of PIC root were statistically significantly different in all force directions ($p=0.008$, $p=0.023$, and $p<0.001$; **Table 4.5, Fig. 4.2**). The distal and vertical forces resulted in the highest ($S=7.73$ KPa) and least ($S=6.05$ KPa) stress. However, stress amounts did not differ significantly between force directions at the mid-root level. Stress levels between buccal and distal forces were not statistically significantly different at the cervical level and over the whole root ($p=0.75$ and 0.39 , respectively).

At the cervical level and over the whole root, the stress levels were statistically significantly different between the vertical and distal forces ($p=0.027$ and <0.001 , respectively), and between the vertical and buccal forces ($p=0.01$ and 0.02 , respectively). Cervically, the buccal force resulted in the highest stress ($S=7.21$ KPa) and the vertical force in the least stress ($S=6.47$ KPa).

Table 4.5: Distribution of stress (Von Mises KPa Mean + SD) according to direction of force at various levels of the canine root

	Buccal	Vertical	Distal	Pairwise comparisons (Post hoc) p		
				B vs. V	B. vs D	V vs. D
Apical	6.92 (1.4)	6.05 (0.54)	7.73 (0.86)	0.008*	0.023*	<0.001*
Middle	5.1 (0.76)	5.39 (0.54)	5.21 (0.81)	0.384 NS	0.99 NS	0.99
Cervical	7.21 (0.93)	6.47 (0.63)	6.98 (0.65)	0.01*	0.75 NS	0.027*
Av. Root	6.41 (0.78)	5.97 (0.35)	6.64 (0.57)	0.02*	0.39 NS	<0.001*

*Statistically significant: $p<0.05$

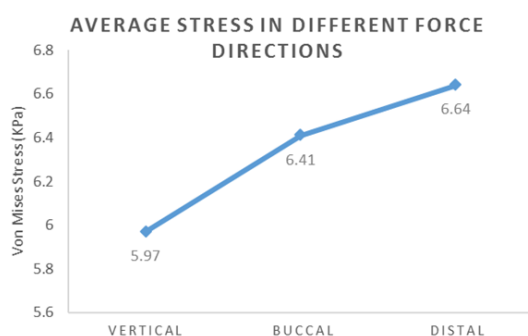


Fig. 4.1. Line chart showing the average stress on the canine root with different force directions.

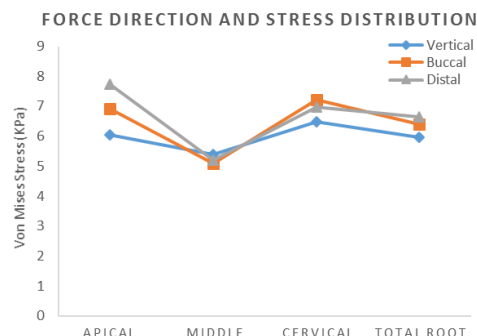


Fig. 4.2. Line chart illustrating how stress is distributed along the root of the canine with different force direction.

4.2.1.2. Stress Distribution Among Severity Subgroups and Force Directions

The mixed between-within subjects' two-way ANOVA, employed to test the effect of severity and force direction on stress at all levels of the PIC root, and for which the test assumptions (homogeneity of variance and sphericity) were only met for stress at the mid-root level, revealed that at this level, force direction had a significant effect on stress ($p = 0.036$; **Fig. 4.3**). A significant interaction was observed between force direction and severity subgroup; force direction affects stress differently depending on group, ($p < 0.001$). Severity subgroup was not significantly associated with stress ($p = 0.982$), thus as a separate entity, severity was only associated to stress as an interaction with force direction (**Fig. 4.3**).

Between the 2 subgroups, only the vertical and distal force directions resulted in different stresses at the middle third ($p=0.001$, and $p=0.002$ respectively). At the other levels of the root, the two groups were not statistically significantly different (**Table 4.6**).

In each subgroup, different force directions resulted in different stresses at each

level of the root (Apical $p < 0.001$, Middle $p = 0.001$, Cervical $p < 0.001$, Average root $p = 0.002$; **Table 4.7**).

Table 4.6: Stress distribution between severity subgroups (1/2) at various areas of the canine root when subjected to various force directions

	Buccal		p	Vertical		p Value	Distal		p
	PIC/VAC <30° n=13	PIC/VAC >30° n=17		PIC/VAC <30° n=13	PIC/VAC >30° n=17		PIC/VAC <30° n=13	PIC/VAC >30° n=17	
Apical	6.55 (0.78)	7.20 (1.67)	0.212	5.93 (0.23)	6.15 (0.68)	0.230	7.63 (0.94)	7.80 (0.81)	0.600
Middle	5.26 (0.78)	4.99 (0.75)	0.341	5.73 (0.46)	5.13 (0.45)	0.001*	4.71 (0.79)	5.59 (0.60)	0.002*
Cervical	6.81 (0.58)	7.51 (1.04)	0.036	6.16 (0.25)	6.71 (0.73)	0.009	7.16 (0.71)	6.85 (0.59)	0.205
Average	6.21 (0.52)	6.57 (0.92)	0.219	5.94 (0.23)	5.99 (0.42)	0.667	6.50 (0.71)	6.75 (0.42)	0.240

*P value significant below 0.0042

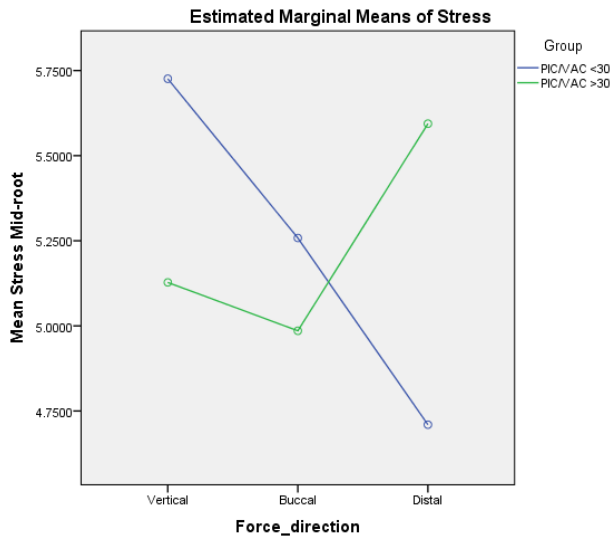


Fig. 4.3. Line chart shows the interaction between severity subgroups and force directions (the lines cross) at the level of middle part of the canine root. A statistically significant interaction exists between force direction and the severity group ($p < 0.001$). As separate entities, force direction was significantly associated with stress level ($p = 0.036$) whereas the severity group was not ($p = 0.982$).

Table 4.7: Comparison of stress distribution at various levels of the canine root between severity subgroups

	PIC/VAC <30° n=13			p value	PIC/VAC >30° n=17			p value
	Buccal	Vertical	Distal		Buccal	Vertical	Distal	
Apical	6.55 (0.78)	5.93 (0.23)	7.63 (0.94)	<0.001*	7.20 (1.67)	6.15 (0.68)	7.80 (0.81)	0.001*
Middle	5.26 (0.78)	5.73 (0.46)	4.71 (0.79)	0.001*	4.99 (0.75)	5.13 (0.45)	5.59 (0.60)	0.002*
Cervical	6.81 (0.58)	6.16 (0.25)	7.16 (0.71)	<0.001*	7.51 (1.04)	6.71 (0.73)	6.85 (0.59)	<0.001*
Average	6.21 (0.52)	5.94 (0.23)	6.50 (0.71)	0.002*	6.57 (0.92)	5.99 (0.42)	6.75 (0.42)	0.001*

*P value significant below 0.00625

-1. Lower PIC/VAC Severity Subgroup

At the apical level, stress from all forces (buccal, distal, vertical) was statistically significantly different.

At the middle level, response to the vertical force was statistically significantly different from the responses to the buccal ($p=0.001$) and distal ($p<0.001$) forces (**Table 4.8**), while the latter were not ($p=0.039$). The distal and vertical forces resulted in highest ($S=7.63\text{KPa}$) and least ($S=5.93\text{KPa}$) stress.

At the cervical level, stress from the vertical force was significantly different from that generated by the buccal and distal forces ($p<0.001$ in both cases); the latter were not different from each other ($p=0.096$; **Table 4.8**). The distal and vertical forces resulted in the highest ($S=7.16\text{KPa}$) and least ($S=6.16\text{KPa}$) stress.

On the whole root average, stress from the buccal force was not significantly different from either the vertical or distal forces ($p=0.014$, $p=0.093$, respectively). However, the responses to the vertical and distal forces differed significantly ($p=0.004$).

Table 4.8: Comparison of stress distribution at various levels of the canine root in lower severity subgroup

	PIC/VAC <30 n=13			Pairwise comparisons (Post hoc)		
	Buccal	Vertical	Distal	B vs. V	B. vs D	V vs. D
Apical	6.55 (0.78)	5.93 (0.23)	7.63 (0.94)	0.006*	0.002*	<0.001*
Middle	5.26 (0.78)	5.73 (0.46)	4.71 (0.79)	0.001*	0.039	<0.001*
Cervical	6.81 (0.58)	6.16 (0.25)	7.16 (0.71)	<0.001*	0.096	<0.001*
Average	6.21 (0.52)	5.94 (0.23)	6.50 (0.71)	0.014	0.093	0.004*

*P value significant below 0.00625

2.- Higher PIC/VAC Severity Subgroup

At the apical level, the vertical force generated stress that was statistically significantly different from the response to the buccal ($p=0.004$) and distal (<0.001) forces, the latter not differing with each other ($p=0.180$; **Table 4.9**). Stress with the vertical force ($S=6.15\text{KPa}$) was lower than that in response to the buccal ($S=7.2\text{KPa}$) and distal ($S=7.8\text{KPa}$) forces.

At the middle level, response to the vertical force was not significantly different from that to the buccal ($p=0.422$) and distal (0.013) forces. However, the buccal force engendered stress ($S=4.99\text{KPa}$) that was lower than that produced by the distal force ($S=5.59\text{KPa}$, $p=0.001$).

At the cervical level, stress from the buccal force ($S=7.51\text{KPa}$) was significantly different from the stress created by the vertical ($S=6.71\text{KPa}$) and distal ($S=6.85\text{KPa}$) forces ($0.001 > p \geq 0.004$); the responses to the latter were not different ($p=0.465$).

For the total root, the average stress resulting from the vertical force ($S=5.99\text{KPa}$) was lower than that from the buccal ($S=6.57\text{KPa}$) and distal ($S=6.75\text{KPa}$) forces ($0.001 > p \geq 0.004$). Nevertheless, stress from the buccal force did not differ significantly from that of the distal force ($p=0.401$; **Table 4.9**).

Table 4.9: Comparison of stress distribution at various levels of the canine root in higher severity subgroup

	PIC/VAC >30 N=17			Pairwise comparisons (Post hoc)		
	Buccal	Vertical	Distal	B vs. V	B. vs D	V vs. D
Apical	7.20 (1.67)	6.15 (0.68)	7.80 (0.81)	0.004*	0.180	<0.001*
Middle	4.99 (0.75)	5.13 (0.45)	5.59 (0.60)	0.422	0.001*	0.013
Cervical	7.51 (1.04)	6.71 (0.73)	6.85 (0.59)	0.001*	0.004*	0.465
Average	6.57 (0.92)	5.99 (0.42)	6.75 (0.42)	0.004*	0.401	<0.001*

*P value significant below 0.00625

4.2.1.3. Correlations Between Stress and Canine Positional Parameters

Higher correlations were noted between stresses with the vertical force at the mid-root level and various positional variables: PIC/VAC, cusp deviation, cusp to midline and angulation of PIC to midline ($0.66 < r < 0.73$; **Table 4.10**). Moreover, the stress at the cervical level in reaction to the vertical force correlated with PIC/VAC ($r=0.61$) and PIC to midline ($r=0.65$; **Table 4.10**). Various moderate correlations were also noted.

Table 4.10: Correlations among Von Mises stresses and other parameters in various planes of space in the whole sample (N: 30)

Section	Measurement	Von Mises Stress in Buccal (KPa)				Von Mises Stress in Vertical (KPa)				Von Mises Stress in Distal (KPa)			
		Apical	Middle	Cervical	Avg	Apical	Middle	Cervical	Avg	Apical	Middle	Cervical	Avg
Panoramic‡	PIC/VAC	0.21 NS	-0.27 NS	0.49* [0.007]	0.23 NS	0.29 NS	-0.73* [<0.001]	0.61* [<0.001]	0.14 NS	0.16 NS	0.42* [0.02]	-0.1 NS	0.24 NS
Sagittal†	Anterior†	-0.25 NS	-0.25 NS	-0.07 NS	-0.26 NS	-0.16 NS	-0.17 NS	0.00 NS	-0.17 NS	-0.13 NS	-0.52** [<0.001]	0.09 NS	-0.28 NS
	Vertical†	0.11 NS	0.19 NS	-0.04 NS	0.11 NS	0.00 NS	0.08 NS	0.16 NS	0.14 NS	0.01 NS	-0.09 NS	-0.16 NS	-0.10 NS
Axial†	Cusp deviation	0.16 NS	-0.39* [0.03]	0.47** [0.01]	0.15 NS	0.23 NS	-0.66** [<0.001]	0.40* [<0.03]	0.02 NS	-0.15 NS	0.07 NS	-0.07 NS	-0.07 NS
	Apex deviation	-0.13 NS	-0.42* [0.02]	0.28 NS	-0.10 NS	-0.04 NS	-0.52** [<0.001]	0.28 NS	-0.12 NS	-0.29 NS	-0.10 NS	-0.04 NS	-0.21 NS
	Cusp to midline	-0.25 NS	0.25 NS	-0.47** [0.01]	-0.25 NS	-0.28 NS	0.66** [<0.001]	-0.46* [0.01]	-0.08 NS	0.05 NS	-0.09 NS	0.06 NS	0.01 NS
	Apex to midline	-0.34 NS	-0.30 NS	-0.11 NS	-0.34 NS	0.00 NS	-0.36* [0.05]	0.22 NS	-0.05 NS	0.18 NS	0.08 NS	0.10 NS	0.17 NS
Coronal‡	PIC to midline	0.24 NS	-0.20 NS	0.51** [<0.001]	0.28 NS	0.39* [0.03]	-0.69** [<0.001]	0.65** [<0.001]	0.24 NS	0.18 NS	0.29 NS	-0.02 NS	0.22 NS
Sagittal‡	PIC/PP	0.12 NS	-0.32 NS	0.41* [0.02]	0.13 NS	0.14 NS	-0.53** [<0.001]	0.33 0.07	-0.01 NS	-0.08 NS	0.30 NS	-0.11 NS	0.06 NS

Correlation is significant at the: *0.05 level (2-tailed); **0.01 level (2-tailed). P values are listed in brackets and only for significant correlations.

PP: palatal plane; 6: permanent first molar

†: mm; ‡: degrees

Table 4.11: Correlations among Von Mises stresses and other parameters in various planes of space in the lower severity subgroup

Section	Measurement	Von Mises Stress in Buccal (KPa)				Von Mises Stress in Vertical (KPa)				Von Mises Stress in Distal (KPa)			
		Apical	Middle	Cervical	Avg	Apical	Middle	Cervical	Avg	Apical	Middle	Cervical	Avg
Panoramic‡	PIC/VAC	-0.42 NS	-0.53 NS	0.05 NS	-0.47 NS	-0.50 NS	-0.50 NS	-0.03 NS	-0.51 NS	0.001 NS	-0.40 NS	-0.07 NS	-0.17 NS
Sagittal†	Anterior†	-0.11 NS	-0.31 NS	0.05 NS	-0.19 NS	-0.27 NS	-0.34 NS	-0.01 NS	-0.32 NS	-0.26 NS	-0.69** [0.009]	-0.01 NS	-0.37 NS
	Vertical†	0.03 NS	0.15 NS	-0.11 NS	0.05 NS	-0.35 NS	0.19 NS	0.02 NS	0.02 NS	-0.24 NS	-0.45 NS	0.02 NS	-0.27 NS
Axial†	Cusp deviation	-0.35 NS	-0.68** [0.01]	0.16 NS	-0.46 NS	-0.17 NS	-0.74** [0.004]	0.1 NS	-0.51 NS	-0.09 NS	-0.33 NS	-0.18 NS	-0.22 NS
	Apex deviation	-0.47 NS	-0.45 NS	-0.26 NS	-0.56* [0.046]	-0.67* [0.013]	-0.60* [0.029]	-0.17 NS	-0.69** [0.01]	-0.59* [0.033]	-0.37 NS	-0.39 NS	-0.53 NS
	Cusp to midline	0.28 NS	0.48 NS	-0.13 NS	0.33 NS	-0.01 NS	0.49 NS	-0.22 NS	0.25 NS	0.05 NS	0.59* [0.031]	-0.01 NS	0.24 NS
	Apex to midline	-0.34 NS	-0.32 NS	0.07 NS	-0.31 NS	0.18 NS	-0.5 NS	0.36 NS	-0.15 NS	0.16 NS	-0.13 NS	0.11 NS	0.06 NS
Coronal‡	PIC to midline	-0.05 NS	-0.39 NS	0.41 NS	-0.07 NS	0.32 NS	-0.41 NS	0.53 NS	0.02 NS	0.15 NS	-0.40 NS	0.18 NS	-0.03 NS
Sagittal‡	PIC/PP	-0.21 NS	-0.57* [0.041]	0.02 NS	-0.39 NS	-0.38 NS	-0.55 NS	-0.13 NS	-0.54 NS	-0.03 NS	0.22 NS	-0.42 NS	-0.07 NS

Correlation is significant at the: *0.05 level (2-tailed); **0.01 level (2-tailed). P values are listed in brackets and only for significant correlations.

PP: palatal plane; 6: permanent first molar

†: mm; ‡: degrees

Table 4.12: Correlations among Von Mises stresses and other parameters in various planes of space in the higher severity subgroup

Section	Measurement	Von Mises Stress in Buccal (KPa)				Von Mises Stress in Vertical (KPa)				Von Mises Stress in Distal (KPa)			
		Apical	Middle	Cervical	Avg	Apical	Middle	Cervical	Avg	Apical	Middle	Cervical	Avg
Panoramic‡	PIC/VAC	0.11	-0.09	0.40	0.20	0.34	-0.65** [0.005]	0.60* [0.011]	0.30	0.23	0.05	0.37	0.34
Sagittal†	Anterior†	-0.57* [0.017]	-0.31	-0.14	-0.48	-0.21	-0.28	0.18	-0.11	0.20	-0.25	0.27	0.13
	Vertical†	0.08	0.31	-0.17	0.07	0.03	0.31	0.09	0.18	0.19	-0.06	-0.24	-0.02
Axial†	Cusp deviation	0.19	-0.12	0.44	0.25	0.24	-0.41	0.30	0.15	-0.33	-0.20	0.24	-0.19
	Apex deviation	-0.18	-0.34	0.32	-0.08	-0.01	-0.25	0.22	0.03	-0.16	-0.46	0.44	-0.12
	Cusp to midline	-0.29	-0.04	-0.42	-0.34	-0.26	0.49* [0.048]	-0.32	-0.15	0.20	0.14	-0.20	0.11
	Apex to midline	-0.41	-0.26	-0.24	-0.41	-0.06	-0.27	0.15	-0.05	0.18	0.09	0.17	0.24
Coronal‡	PIC to midline	0.19	0.14	0.38	0.30	0.42	-0.59* [0.013]	0.63** [0.007]	0.38	0.17	0.12	0.23	0.27
Sagittal‡	PIC/PP	0.08	-0.08	0.38	0.17	0.14	-0.25	0.22	0.11	-0.24	-0.08	0.32	-0.04

Correlation is significant at the: *0.05 level (2-tailed); **0.01 level (2-tailed). P values are listed in brackets and only for significant correlations.

PP: palatal plane; 6: permanent first molar

†: mm; ‡: degrees

4.2.1.4. Associations Between Stress at Different Root Levels with Force Direction

-1. Vertical Force

At the apical level and on the entire PIC root, no significant multivariate models were found to predict the amount of stress generated by the vertical force.

At the mid-root level, a significant regression equation was found ($p < 0.001$, $R^2 = 0.65$). The apex to midline distance was a significant predictor ($p = 0.014$). Stress decreased by 0.11 KPa with every 1 mm increase in this distance. Other positional parameters were included in the final model (cusp and apex deviations, cusp to midline distance and PIC/midline angulation), however, they were not significant predictors of stress at the mid-root level under the vertical force (**Table 4.13**).

Table 4.13: Multivariate regressions for prediction of stress at the middle level of the root while applying a vertical force

	Vertical Direction: Middle Third			
Associated Variables	Coef.	Std. Err.	95% CI	p value
PIC/VAC (°)	-0.146	0.0080	-0.031 - 0.002	0.083
Cusp-Deviation (mm)	-0.051	0.0317	-0.117 - 0.015	0.121
Apex-Deviation (mm)	-0.039	0.0305	-0.103 - 0.024	0.210
Cusp-Midline (mm)	0.055	0.0465	-0.041 - 0.151	0.249
Apex-Midline (mm)	-0.110	0.0411	-0.195 - 0.025	0.014*
PIC/Midline (°)	0.012	0.0120	-0.013 - 0.037	0.322
Constant	7.8136	0.6942	6.378 - 9.250	<0.001
F (6,23)	9.95			
Prob > F	<0.001			
R ²	0.7219			
Adjusted R ²	0.6494			

*P value significant below 0.05

A significant regression equation was also found at the cervical level ($p = 0.0005$, $R^2 = 0.46$). The cusp to midline distance ($p = 0.001$) and PIC/midline angle ($p = 0.03$) were significant predictors of stress, which increased when these parameters augmented. PIC/PP angulation and molar to prosthion (mm) were not significant predictors (**Table 4.14**).

Table 4.14: Multivariate regressions for prediction of stress at the cervical level of the root while applying a vertical force

	Vertical Direction: Cervical Third			
Associated Variables	Coef.	Std. Err.	95% CI	p value
PIC/PP (°)	0.010	0.0081	- 0.006 - 0.027	0.213
Cusp-Midline (mm)	0.139	0.0603	0.014 - 0.263	0.030*
Molar-Prosthion (mm)	- 0.043	0.0324	- 0.110 - 0.024	0.196
PIC/Midline (°)	0.043	0.0108	0.020 - 0.065	0.001*
Constant	4.9348	1.2976	2.262 - 7.607	0.001
F (4,25)	7.23			
Prob > F	0.0005			
R ²	0.5365			
Adjusted R ²	0.4624			

*P value significant below 0.05

-2. Buccal Force

At the apical level, and within a significant regression equation (($p=0.01$, $R^2=0.32$), the apex to midline distance and PIC angulation to midline were significant predictors of stress ($p=0.01$, 0.036) respectively (**Table 4.15**).

Table 4.15: Multivariate regressions for prediction of stress at the apical level of the root while applying a buccal force

	Buccal Direction: Apical Third			
Associated Variables	Coef.	Std. Err.	95% CI	p value
Anterior Deviation (mm)	- 0.176	0.1054	- 0.393 - 0.042	0.109
Cusp-Midline (mm)	0.216	0.1654	- 0.125 - 0.558	0.203
Apex-Midline (mm)	- 0.387	0.1383	- 0.673 - 0.102	0.010*
Molar-Midline (mm)	- 0.201	0.0991	- 0.406 - 0.003	0.054*
PIC/Midline (°)	0.073	0.0329	0.005 - 0.141	0.036*
Constant	14.505	2.4216	9.508 - 19.503	<0.001
F (5,24)	3.73			
Prob > F	0.0122			
R ²	0.4372			
Adjusted R ²	0.3200			

*P value significant below 0.05

No significant predictors of stress were found at the mid-root level (**Table 4.16**), nor were any of the parameters related to the position of the PIC at the cervical level (**Table 4.17**).

Table 4.16: Multivariate regressions for prediction of stress at the middle level of the root while applying a buccal force

Associated Variables	Buccal Direction: Middle Third			
	Coef.	Std. Err.	95% CI	p value
Cusp Deviation (mm)	- 0.051	0.0427	- 0.139 - 0.371	0.246
Apex Deviation (mm)	- 0.106	0.0593	- 0.228 - 0.016	0.096
Apex-Midline (mm)	- 0.104	0.0663	- 0.241 - 0.323	0.128
Molar-Midline (mm)	- 0.075	0.0589	- 0.196 - 0.046	0.213
Constant	9.3668	1.3792	6.526 - 12.207	<0.001
F (4,25)	3.44			
Prob > F	0.0226			
R ²	0.3552			
Adjusted R ²	0.2520			

*P value significant below 0.05

Table 4.17: Multivariate regressions for prediction of stress at the cervical level of the root while applying a buccal force

Associated Variables	Buccal Direction: Cervical Third			
	Coef.	Std. Err.	95% CI	p value
PIC/PP (°)	0.0168	0.0144	- 0.013 - 0.465	0.255
Cusp Deviation (mm)	0.1408	0.0903	- 0.046 - 0.327	0.132
Cusp-Midline (mm)	0.1669	0.1153	- 0.071 - 0.405	0.161
Molar-Midline (mm)	- 0.2038	0.0794	- 0.368 - - 0.040	0.017*
PIC/Midline (°)	0.0299	0.0179	- 0.007 - 0.668	0.108
Constant	5.4898	1.8195	1.734 - 9.245	0.006
F (5,24)	4.13			
Prob > F	0.0075			
R ²	0.4626			
Adjusted R ²	0.3507			

*P value significant below 0.05

Over the total root, the significant regression equation ($p < 0.001$, $R^2 = 0.46$) included the variables: cusp to midline, apex to midline, molar to midline, and angulation to midline as significant predictors of stress ($p = 0.04$, 0.002 , 0.009 , 0.004 , respectively; **Table 4.18**). With increases in the cusp-midline distance (by 1mm) and PIC/midline angulation (by 1 degree), stress augmented (by 0.18 KPa and 0.05 KPa, respectively); with increases in the apex-midline and molar-midline distances by 1mm each, stress decreased by 0.25 KPa and 0.14 KPa, respectively).

Table 4.18: Multivariate regressions for prediction of stress at the whole root of PIC while applying a buccal force

	Buccal Direction: Total Root			
Associated Variables	Coef.	Std. Err.	95% CI	p value
Anterior cusp position (mm)	- 0.100	0.0532	- 0.210 - 0.009	0.072
Cusp-Midline (mm)	0.180	0.0834	0.008 - 0.352	0.041*
Apex-Midline (mm)	- 0.245	0.0697	- 0.389 - - 0.101	0.002*
Molar-Midline (mm)	- 0.143	0.0499	- 0.246 - - 0.040	0.009*
PIC/Midline (°)	0.054	0.0166	0.019 - 0.088	0.004*
Constant	10.955	1.2215	8.434 - 13.476	<0.001
F (5,24)	5.96			
Prob > F	0.001			
R ²	0.5539			
Adjusted R ²	0.4610			

*P value significant below 0.05

-3. Distal Force

At all apical, cervical, and the total root levels, the stress could not be predicted from the variables that were studied. At mid-root level, the regression equation was significant ($p < 0.0001$, $R^2 = 0.46$), with PIC/VAC angulation predicting increased stress (0.024 KPa with every additional 1 degree of the angle, and the PIC anterior position predicting a reduction of 0.218 KPa in stress when it increased by 1mm (**Table 4.19**).

Table 4.19: Multivariate regressions for prediction of stress at the middle level of the root while applying a distal force

	Distal Direction: Middle Third			
Associated Variables	Coef.	Std. Err.	95% CI	p value
PIC/VAC (°)	0.024	0.007	0.010 - 0.038	0.002*
Anterior cusp position (mm)	- 0.218	0.053	- 0.327 - - 0.109	<0.001*
Constant	6.416	0.531	5.327 - 7.504	<0.001
F (2,27)	13.08			
Prob > F	0.0001			
R ²	0.4921			
Adjusted R ²	0.4545			

*P value significant below 0.05

4.2.2. Stresses on adjacent teeth

Stress on the adjacent teeth varied according to the appliance used to tract the canine. Stresses on adjacent teeth with the different appliances tested are summarized in (**Table 4.20**).

Table 4.20: Percentages of Von Mises stress (KPa) on adjacent teeth with different appliances used to move a maxillary left palatally impacted canine

Appliance Type: *	R						L						Total Stress
	16	15	14	13	12	11	21	22	23	24	25	26	
I	1.45 [51.7%]	0.00	0.00	0.00	0.00	0.00	0.00	0.00		0.00	0.00	1.35 [48.3]	2.80
II	1.28 [26.3%]	0.50 [10.3%]	0.32 [6.6%]	0.11 [2.4%]	0.09 [1.8%]	0.22 [4.6%]	0.21 [4.3%]	0.11 [2.2%]		0.27 [5.7%]	0.52 [10.7%]	1.22 [25.1%]	4.85
III	0.14 [2.6%]	0.18 [3.2%]	0.20 [3.6%]	0.24 [4.4%]	0.28 [5%]	0.50 [9.1%]	0.81 [14.7%]	1.28 [23%]		0.91 [16.5%]	0.58 [10.4%]	0.42 [7.5%]	5.54
IV	0.00	0.00	0.00	0.00	0.00	0.00	0.00	0.00		0.00	0.00	0.00	0.00

*Appliance I: Cantilever extending from a TP bar only, force direction is vertical force of 1N (100g)

*Appliance II: Cantilever extending from a TP bar and a SS AW engaged in teeth 6-6, force direction is vertical force of 1N (100g)

*Appliance III: Canine was pulled against the SS AW directly, force direction was buccal force of 1N (100g)

*Appliance IV: Cantilever extending from a palatally mini-implant in a vertical direction with a force magnitude of 1N (100g)

-Appliance 1

The vertical extrusive force from the cantilever arm (**Fig 3.21**) resulted in only the molar teeth withstanding the reactive forces. Von Mises stresses were evaluated in both the PDL and the bone of maxillary first molars. In the PDL, stresses were distributed along the bifurcation area, concentrated more on the distal and palatal roots. This distribution indicated the side effects illustrated by the intrusion and distal root tip of the molars (**Fig. 4.5**). The stresses in the bone coincided with the PDL, distributed along the bifurcation and distally in the intradental septal bone mesial to the second molar (**Fig 4.6**).

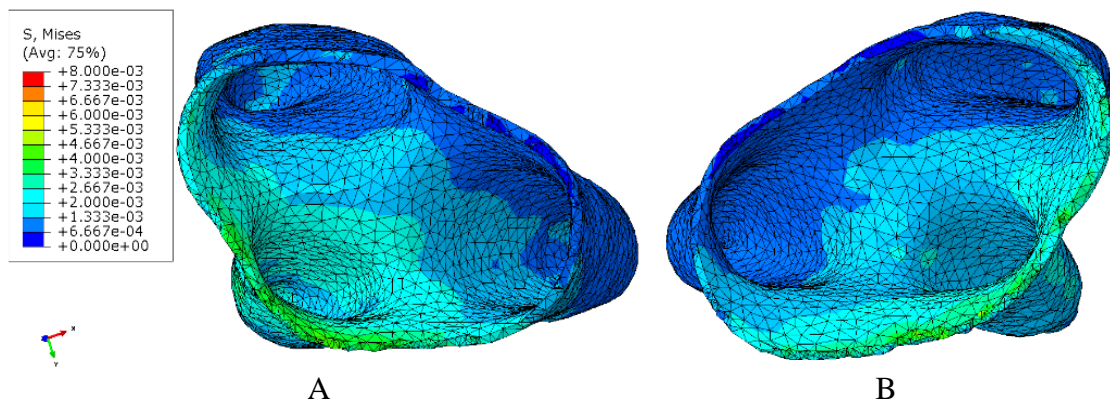


Fig. 4.4. Von Mises stress in periodontal ligament of right (A) and left (B) maxillary molars in treatment with simulated appliance 1 (TP bar only). Note the higher stresses (turquoise, green) at the bifurcation area and distal and palatal roots, indicating the side effects (Intrusion and distal root tip) on the molars.

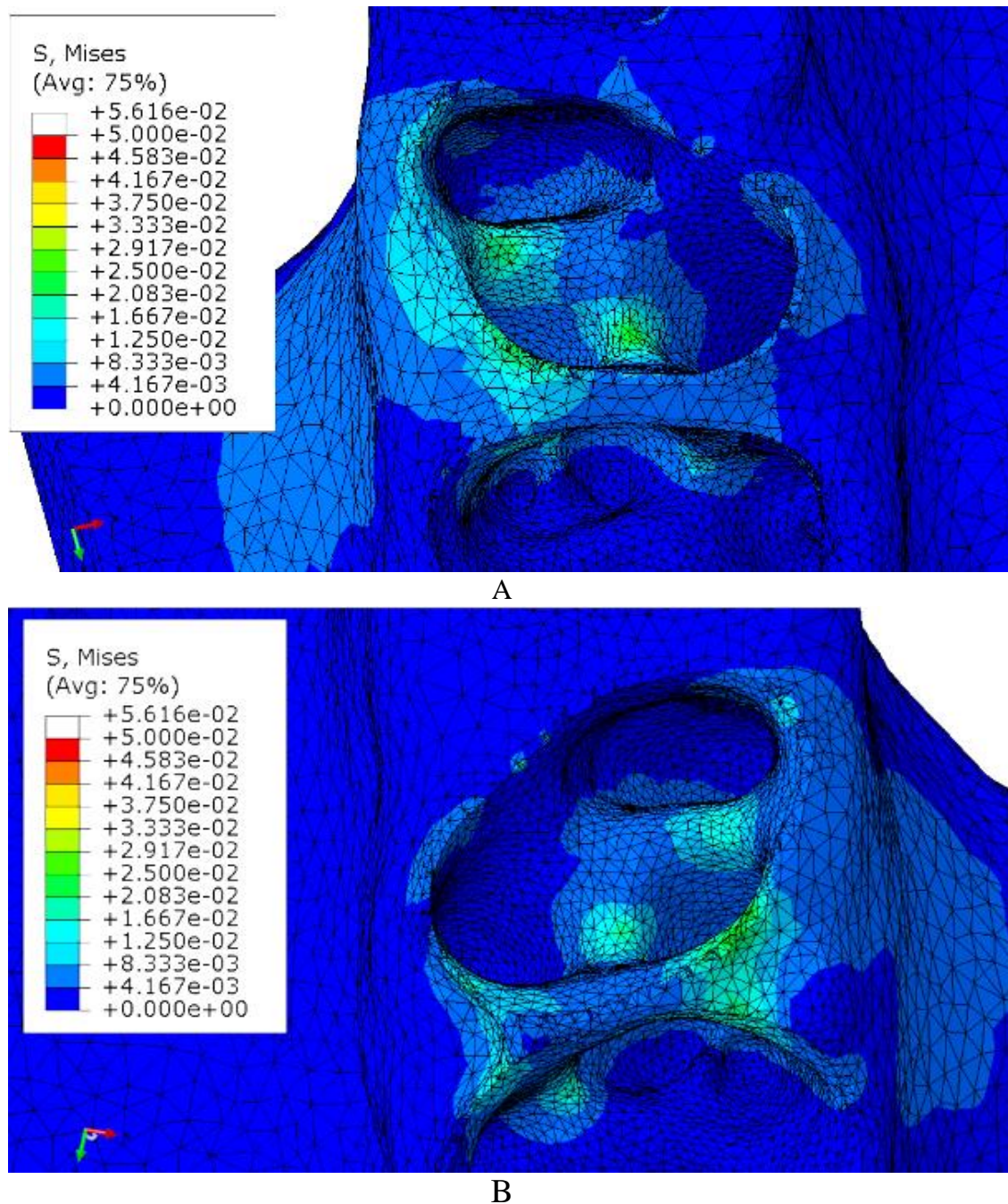


Fig. 4.5. Von Mises stress in alveolar bone of right (A) and left (B) maxillary molar in treatment with simulated appliance 1 (TP bar only). Note the higher stresses (turquoise, green) at the bifurcation area distally and at the septal alveolar bone distal to the first molars, indicating the side effects (intrusion and distal root tip) on the molars.

-Appliance 2

Vertical extrusion from the cantilever arm in combination with a stainless steel arch wire engaging all maxillary teeth except the maxillary second molars resulted in the maxillary molars withstanding the bulk of reactive forces. However, the stresses were also distributed through the arch wire to the whole maxillary dentition. The stresses in the PDL of the first molar depicts were lower in amount of stress in comparison to the molar reaction with appliance 1, more significantly on the buccal side (**Fig. 4.7**).

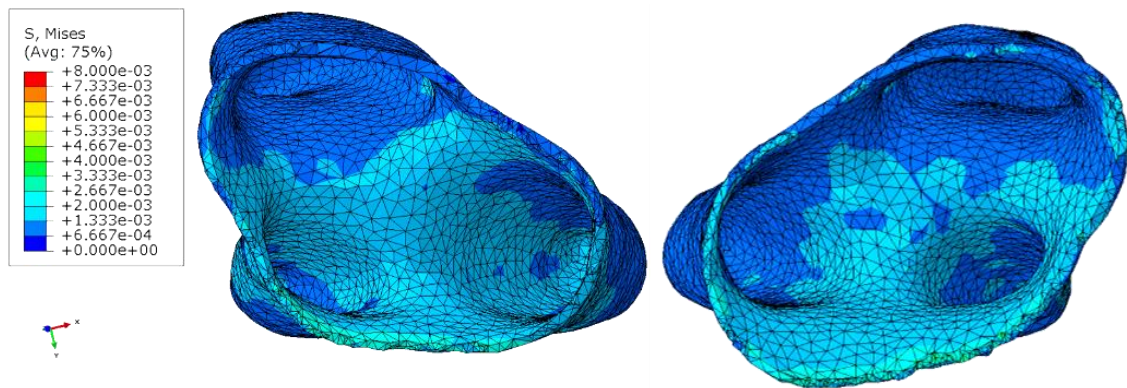
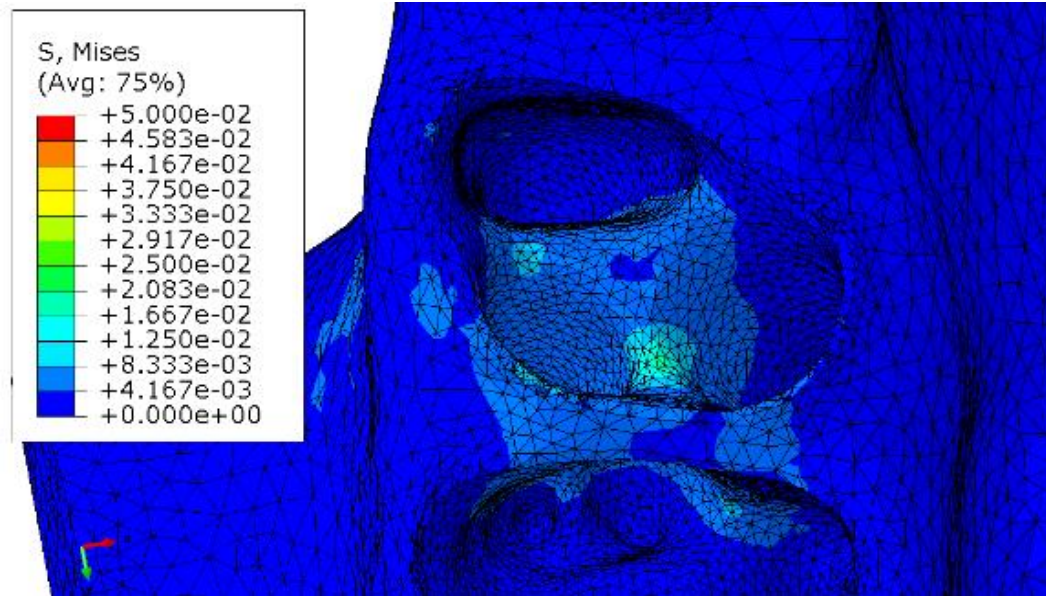
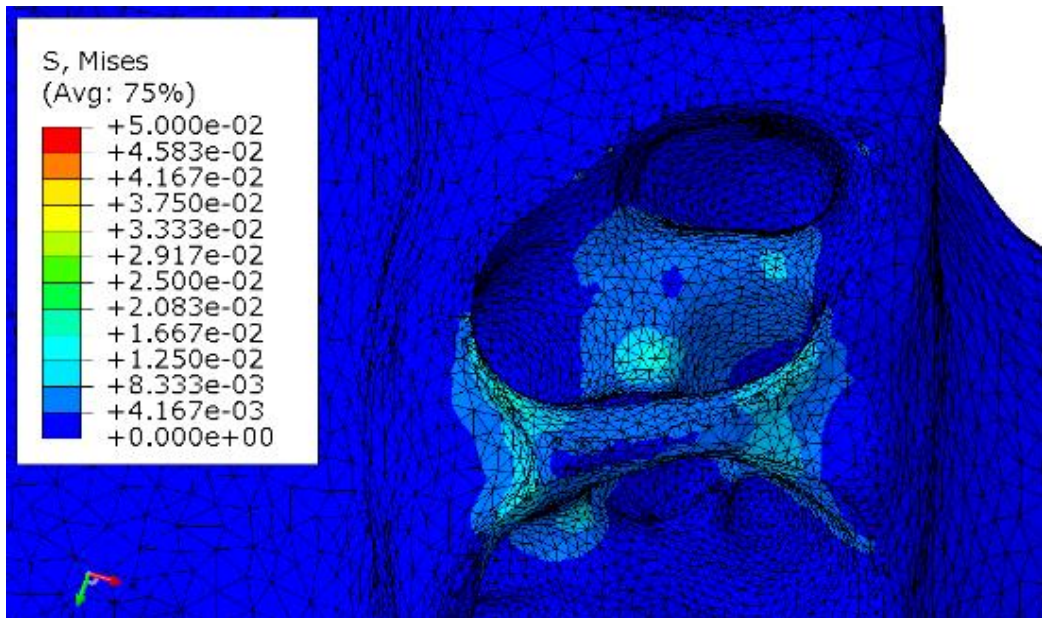


Fig 4.6: Von Mises stress in periodontal ligament of right (A) and left (B) maxillary molar in treatment with simulated appliance 2 (TP bar and a SS AW wire). Note the lower stresses (light blue) compared with appliance 1 (in Fig. 4.6, turquoise and green) distributed more evenly at the bifurcation area and distally and indicating the milder side effects (intrusion and distal root tip) on the molars with this appliance.

Stresses at the bone level also confirm the lower stresses in general and particularly on the buccal plate. However, the same distal concentration pattern persisted indicating the potential side effects (intrusion and distal root tip) similar to those with appliance 1 but to a lesser extent (**Fig. 4.8**).



A



B

Fig 4.7. Von Mises stress in alveolar bone of right (A) and left (B) maxillary molar in treatment with simulated appliance 2 (TP bar and a SS AW wire). Note the lower stresses compared with appliance 1 in Fig. 4.9 (green, light blue) distributed more evenly at the bifurcation area distally and at the septal alveolar bone distal to first molars, indicating the milder side effects (intrusion and distal root tip) on the molars with this appliance.

-Appliance 3

The direct pull of the PIC against a rectangular stainless steel arch wire in a buccal direction (**Fig. 3.20**) resulted in the adjacent teeth withstanding the reactive forces. The Von Mises stresses decreased progressively in distal direction from the first premolar and mesially from the lateral incisor toward the contralateral first molar distally (**Fig 4.9**).

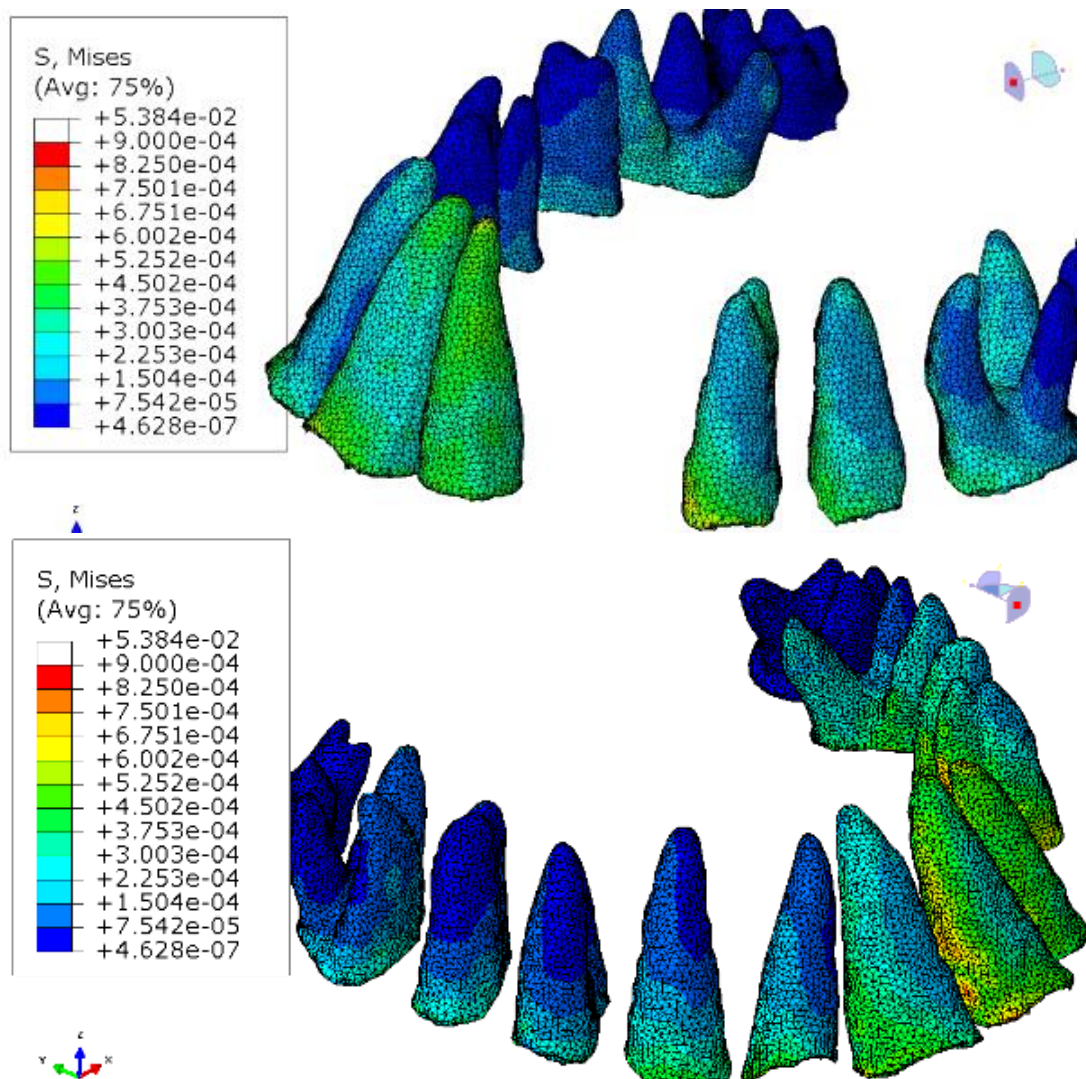


Fig 4.8. Von Mises stress on PDL of adjacent teeth with appliance 3 (direct pull of canine to main SS AW). Stresses are concentrated on the immediate adjacent teeth particularly (left lateral incisor and first premolar). Stresses are dissipated progressively further away from the impacted canine toward the posterior teeth.

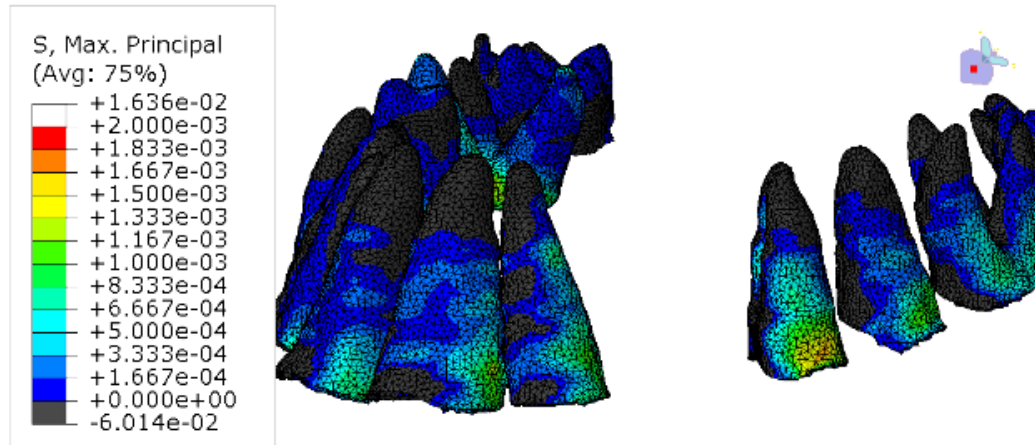


Fig 4.9. Maximum principal stress on PDL of adjacent teeth with appliance 3 (direct pull of canine to main SS AW) showing areas of tension. The higher tension areas, illustrated in green and yellow, are observed on the buccal surfaces of teeth adjacent to the PIC, and on the palatal surfaces of contralateral teeth.

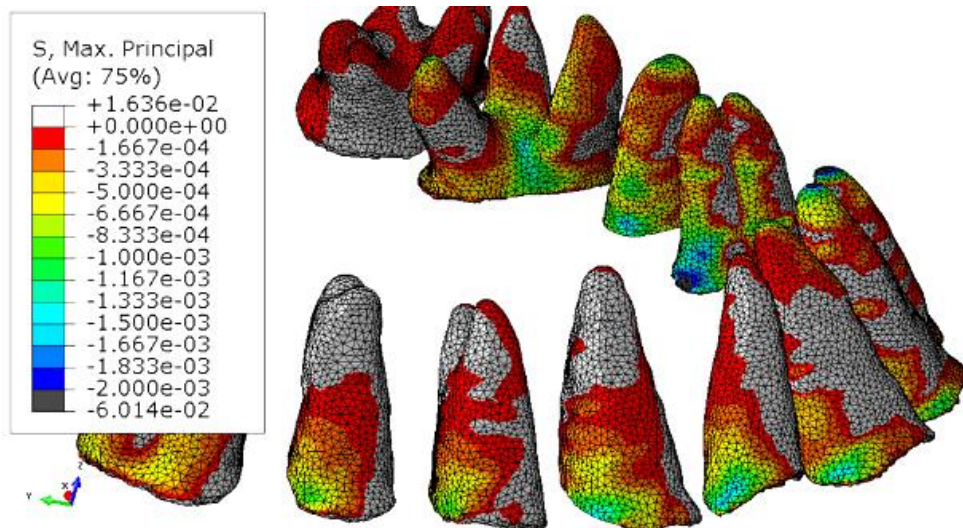


Fig 4.10. Maximum principal stress on PDL of adjacent teeth with appliance 3 (direct pull of canine to main SS AW) showing areas of compression in red. Note the distribution of stress on the palatal surfaces of the teeth adjacent to the PIC on the side of traction, and on the buccal surfaces on the contralateral side.

Evaluation of maximum principal stresses on the PDL of the adjacent teeth in the tension areas (**Fig 4.10**) disclosed higher tension on the buccal surfaces of teeth adjacent to the PIC and the palatal surfaces of contralateral teeth. The areas under compression were the palatal surfaces of the teeth adjacent to the PIC on the side of traction, the buccal

surfaces on the contralateral side, and over the apical region of the incisors and adjacent premolars (**Fig 4.11**).

A transverse section at the level of the second premolars in a left PIC scenario portrays the areas of compression, buccal surface of the right premolar and apical area, and palatal surface of left premolar (**Fig 4.12**).

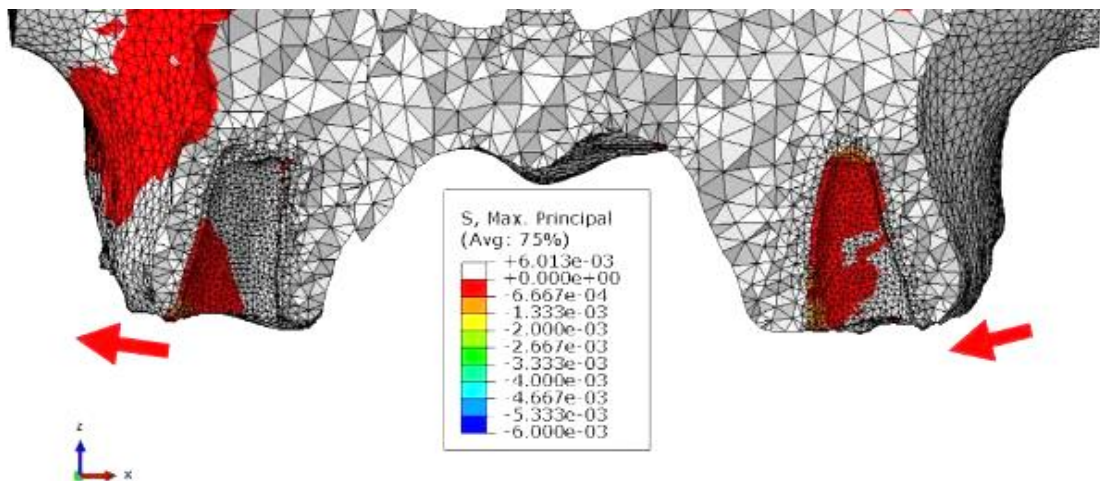


Fig 4.11: Transverse section across the maxilla at the level of the second premolar showing maximum principal stress in the PDL of adjacent teeth with appliance 3. Areas of compression are in red color. The red arrows indicate the direction of reactionary forces to canine traction (buccal force direction)

CHAPTER 5

DISCUSSION

5.1. Introduction

The contributions of this research are multifaceted:

1. A new scheme for assessment of severity was developed, based on projected treatment outcome rather than positional deviations from normative values, as previously reported in the literature.
2. A new approach to FEA analysis, whereby force systems were not applied in a simplified virtual array of various force applications, but simulated in different subjects taking into consideration the clinically-significant individual variations that reflect a scale of impaction severity.
3. The incorporation of a full maxillary arch and dentition was also a new addition to the literature, in which
 - a. Forces were applied in various directions simulating clinical force applications.
 - b. Stress was analyzed on adjacent teeth both on the side of the impacted canine and the contralateral side, following the simulation of specific commonly used orthodontic appliances.
4. The fact that 30 different individual clinical conditions of PIC were evaluated allowed the performance of statistical analyses that detected the scope of variations and a predictive model, computations heretofore not possible with only singular model analyses in the available literature.

5.2. CBCT Study:

Several methods have been applied to assess the severity of palatally impacted canines and associated difficulty of treatment. The original most commonly used scheme developed by Ericson and Kurol (1986) involved dividing the area between the canine and central incisor into sectors that delineate the severity of impaction based to the crown position. The system is easy to use and reflects initial assessment, but like all 2D-based methods relies on the panoramic radiograph, thus limited by the inherent magnification and distortion.

The new advances in radiographic techniques ushered the implementation of 3D based methods especially needed for the diagnosis of palatally impacted canines. CBCT images carry the advantage of accuracy and precision in both angular and linear measurements if scans are of a sufficient resolution since almost no distortion happens. However, CBCT studies that used only the panoramic view of the CBCT have not totally benefited from the offerings of 3D scans (Kau et al., 2009).

5.2.1. New assessment of PIC

Various schemes have been suggested to determine the severity of palatal impaction, stemming from the fact that orthodontic treatment is lengthened remarkably because of highly variable time to align the impacted tooth, and sometimes with less than optimal results, notwithstanding the potential side effects, most notably the resorption of adjacent teeth, particularly the lateral incisors. Treatment length is reported to increase by 6 to 12 months to move the PIC into the arch. Resorption of the incisors may reach 50% or more, and was related to unduly sustained forces in a protracted treatment.

For these reasons, we approached the evaluation of PIC in 2 perspectives: defining the components most responsible for impaction severity, thus alignment difficulties, and establishing a realistic threshold for alignment severity (30°), nearly one third of the most severe possibility of a totally horizontal impaction, presumably at 90° to the occlusal plane. Accurate determination dictated the reliance on 3D images.

Three important observations are extracted from the results, illustrated in (**Fig. 5.1**):

1. The inclination of PIC to the midline in the coronal plane, and the position of the apex in the axial plane were more significant: severe impaction is associated with a more distal apex and more coronal crown, thus a medial inclination of the tooth (**Table 4.2, 4.3**). These components would dictate a more taxing and a longer trajectory of correction. The crown of the less severely inclined PIC was nearly twice away from the axial midline (6.3mm), thus more buccal than the cusp tip of the PIC in the severe group. The cusp and apex deviations between PIC and VAC reflected the projected movement of crown tip and apex to align the canine into the arch. Average distances of nearly 2 mm greater in severe group were statistically significantly different for apex but not cusp deviation. Of particular importance is the finding that crown movement would amount to an average 1 cm in the least severe group, and apex movement to nearly the same amount (9.11 mm), some 30% greater than a similar displacement in the milder severity group.
2. Linear measurements in the sagittal section were not statistically significantly different between severity groups: cusp tip projections vertically to the occlusal plane and anteriorly to the interincisal alveolar crest were not primary contributors to severity. On the other hand, the angulation of PIC to palatal plane was statistically significantly

different between severity groups. A similar finding for the inclination of PIC to the midline reflects the fact that the angulation of the tooth in all planes of space indicates the albeit that PIC/VAC had a higher correlation to the medial angulation of PIC ($r=0.85$) than to the palatal plane ($r=0.6$; **Table 4.3**).

3. These observations are further delineated by the high correlation of cusp tip position farther away from the crest with the path of correction of the PIC (PIC/VAC to: cusp deviation $r=0.57$, and cusp to midline $r=0.70$; **Table 4.3**). These correlations with cusp deviations were higher than the corresponding correlations with apex deviation (PIC/VAC to: apex deviation $r=0.48$ and apex to midline $r=0.16$), probably indicating that the cusp tip variation affected more the final position of impaction. This finding is not surprising when one considers a wider margin of displacement within bone for the crown than for the apex.

Our findings support earlier conclusions drawn from 2D analyses that bucco-palatal position and inclination of PIC to the midline were indicators of severity (Crescini et al., 2007; Pitt et al., 2006). On the other hand, 3D studies support the concert of cusp tip and root tip position to impaction severity. However, our study delineates important nuances:

1. The findings demonstrate that the position of the apex at all levels of severity tends to be along a similar plane but more posterior in the more severe impactions (**Fig. 5.1**). Even if the apex is more coronal in the lower severity PIC/VAC subgroup, the correlation between PIC/PP and apex deviation in the sagittal plane ($r=0.62$; **Table 4.3**) indicates that the posterior position of the apex (more distal) is more defining of severity

than the transverse position of the apex, whereby no statistically significant differences were noted between severity groups (**Table 4.2**).

2. The vertical position, critical in the alignment of a palatally impacted canine, was as important in the less and more severe groups, since the vertical measure was not statistically significantly different between severity groups (**Table 4.2**), and all correlations between the vertical position and any of the measurements recorded in the coronal, sagittal and axial planes were low ($-0.37 < r < 0.22$; **Table 4.3**).

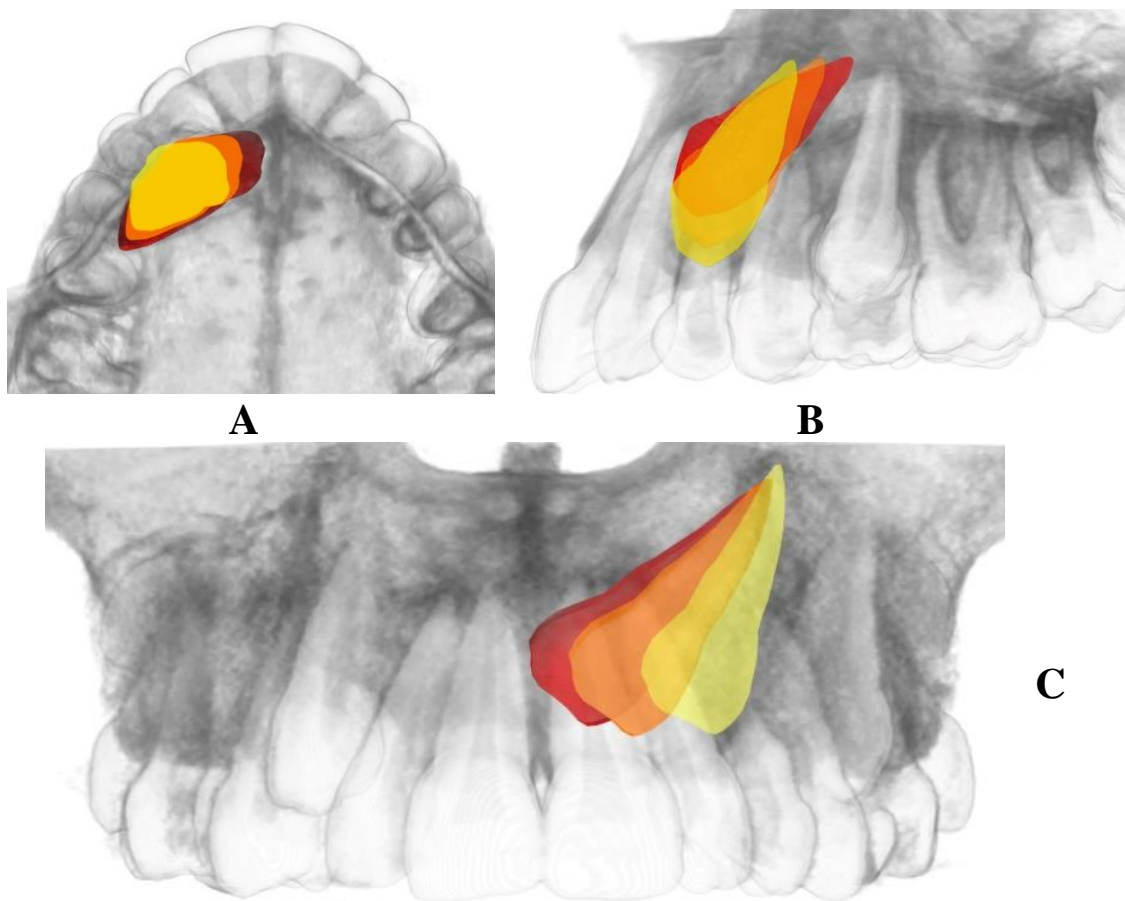


Fig. 5.1. Different impaction severity scenarios: graphic representation of palatally impacted canine (PIC) in severe (red), moderate (orange) and milder (yellow) configurations in the occlusal/axial (A), sagittal (B) and coronal (C) planes. Notable is the more distal apical and the more medial cuspal positions of the PIC in the more severe group.

5.2.2. Comparison with Other Studies

The male to female ratio of palatally impacted canines was 1:2.5, which coincides with the prevalence of 1:2 reported by (Sune Ericson & Jüri Kurol, 1986b). Our findings compare favorably with the most commonly used or quoted studies on palatally impacted canines, albeit with clear distinctions related to the new assessment (PIC/VAC).

For decades, the studies by (Sune Ericson & Jüri Kurol, 1986b; Ericson & Kurol, 1988) and his co-workers provided the optimal guidelines for diagnosis and treatment of palatally impacted canines, first on periapical and later on panoramic radiographs. Perhaps the trademark of their multifactorial analysis was the relationship between the impacted tooth and its adjacent lateral incisor, falling in predefined “sectors” of assigned severity projecting self-correction to treatment need. In our model, this relationship is reflected in the most severe PIC/VAC angulations. The position of the lateral may vary with its own inclination, thus possibly leading to error in locating the canine within the appropriate sector. Cusp deviation is indirectly inherent to the amount of overlap with the lateral incisor, yet our research indicates that cusp deviation undergoes more deviation than the apex deviation, thus its assessment in individual patients would improve predictability of outcome.

Stewart et al. (2001) gauged the severity of canine impaction from their height to the occlusal plane measured on panoramic radiographs. When PICs height was less than 14 mm from occlusal plane, treatment duration was only 6-8 months longer. Our data show averages less than the 14 mm cut-off by Stewart. The disparity in these numbers may be related to methodology. Our material was derived from more accurate CBCT images and measured on the sagittal view, thus absent the magnification in panoramic

radiographs and the errors derived from the position (tip) of the head in the x-ray machine.

Vertical height emerged as a component of a treatment difficulty index developed by Pitt et al. (2005), along with the horizontal and bucco-palatal position of the PIC. In our study, the vertical height was not statistically significantly different between severity groups. In a different index (KPG), Kau et al (2009) included cusp and root tips graded in sectors relative to their AP and vertical position on the CBCT frontal panoramic view, and the angulation to the lateral incisor on the coronal view. In a comparison among the works of Kurol (1986), Stewart (2001) and Kau et al (2009), Dalessandri et al. (2014) validated the latter group's KPG, though it did not contradict the previous indices.

The strongest predictors for PIC in a CBCT study by Algerban et al. (2015) included components close to ours, such as the PIC angulation to the lateral incisor on the coronal view, compared to the PIC angulation to the midline in our study, the vertical cusp tip to occlusal plane on the sagittal view as in our methods, and the crown position relative to arch and adjacent teeth, close in concept to our cusp tip position in various planes. However, our cornerstone measure of PIC inclination to the canine's virtual correction in the arch indexes the severity of inclination relative to its virtual correction, potentially yielding more severity than the previous methods. While most studies attempted to link severity of impaction with treatment guidelines, our definition of the severity embeds an indirect measurement of movement of both apex and crown from the location of the impacted tooth to its virtual alignment on the arch.

5.2.3. Research considerations

The research was restricted to palatal impaction. However, in the process of selection, we noted that buccally impacted teeth tended to assume more horizontal positions than the PIC. Additional research should be invested in this area, particularly that earlier 2D research indicated the contribution of horizontality to impaction severity (Crescini et al., 2007; Pitt et al., 2006).

The selection of the angle between PIC and its virtual alignment (VAC) has not been used in prior studies. An early choice employed by many investigators is the relationship between PIC and the neighboring lateral incisor, by assessing their angulation or relative positions (Stewart et al., 2001; Zuccati et al., 2006). A myriad of other measures to craniofacial references have been advocated (angulation to occlusal plane, axial, sagittal and coronal planes or midlines). All such variables relate to diagnosis, whereas PIC/VAC relates directly to treatment considerations. In evaluating the association between PIC/VAC and other “diagnostic” parameters, its highest association was with the PIC inclination to the midline in the coronal plane.

The accuracy of virtual position may be questioned, particularly regarding malocclusions where space was needed to align the canines, and the difference of set up in Class II malocclusion that requires distal movement of posterior teeth before canine displacement, or in case of anterior crowding that also required distalization of more posterior teeth. The provision in this project was to align the canine in its position with its axis parallel to both the adjacent lateral incisor and first premolar. Accordingly, any further distal movement of the canine to accommodate other malocclusion needs was not factored in. Such assumption would obviously prolong treatment time, a detail not clarified in most studies of duration of treatment of PIC.

In this context, the significance of scoring severity must be revisited, with the goal of keeping it simple. Most studies point to more severity with more deviation. Various schemes have been used based on multivariate analyses. Nevertheless, any index carries some level of arbitrary assessment, assigning weights according to seemingly justifiable cutoffs, such as the inclination of PIC to a reference. In reality, in the case of PIC, the score projects morbidity (necessarily longer treatment and potential root resorption of adjacent teeth, notwithstanding additional side effects in case of ankylosis of the tooth).

A better scheme to explore would include estimates of treatment duration and potential side effects (unless avoided by mechanotherapy), and should be of more practical value to patient and practitioner. Much work and review of treatment reports with various details are required, but the outcome of such research would indicate options for treatment planning, including considering leaving the canine in place or extracting it.

Dental measurements revealed a closer distance of the maxillary permanent first molars to the interincisal point in the more severe PIC/VAC group, possibly indicating more crowding (such as mesial drift into the impacted canine space) and/or class II relationship (**Table 4.3**). The distance between molars and midline in the axial plane denote similarity between groups. Focused research including space analysis on dental casts and corresponding radiographic measurements would be required to further elucidate dental relationships.

Finally, the importance of 3D assessment in disclosing accurate diagnosis must be balanced with careful use of radiation exposure, which was restricted to the pertinent maxillary segment in our population. Nevertheless, Haney et al. (2010) reported that the

majority of PIC assessed on 2D radiographs received the same diagnosis and treatment plan after they were gauged on corresponding CBCT images. One quarter (27%) ended up with a different treatment plan. Without underestimating the importance of this relatively low percentage, the findings indicate a potential disparity that may be critical in the individual patient. They also underline the need to further explore the variations in PIC position in 3D imaging, to improve the determination of potential success of treatment, and in associations between PIC position and treatment modalities.

5.3. FEA study

In addition to the introduction of the PIC/VAC angulation, the FEA application is also novel because of the inclusion of a variable sample and the use of different force systems that replicate the clinical situations. Accordingly, the resulting analyses yielded outcomes of initial response that are interpretable clinically, and form the basis for future elaborate studies that would ultimately incorporate the FEA model in actual treatment planning.

5.3.1. Canine Angulation Severity and Different Force Directions

The distal force resulted in the highest stress over the root in general ($S=6.64$ KPa), while it was lower ($S=5.97$ KPa) in the vertical load ($p<0.001$; **Table 4.5**). The buccal stresses were also significantly different from the vertical but not the distal stresses, suggesting one of the following scenarios:

- a. The distal force generates higher resistance to movement and the vertical force would encounter the least resistance. The stress distribution with the distal force suggests the generation of a moment because of higher stress at the apical and cervical level but not the middle area of the root. Accordingly, the greater moment created with

the distal force than the vertical force would account for the difference in resistance to movement by these forces. This interpretation seemingly contradicts the engineering tenet that greater stress is consistent with greater strain within the PDL (stress $[\sigma] = \text{strain } [\epsilon] \times \text{stiffness } [E]$). However, in the context of the prevalent aberrant inclinations of the impacted canine within its bony housing, the advanced interpretation is plausible (see next section 5.3.2 and **Fig. 5.2**). This finding would translate into higher forces needed for distal activation which in turn would lead to higher reaction stresses on adjacent teeth.

The clinical implication of this interpretation would be the need for a vertical force to be applied before or at least in conjunction with the distal force.

b. The distal force generates greater initial movement. This conclusion would be more compatible with clinical goals. The distal direction of PIC movement is usually contemplated to avoid contact with the roots to the incisors and prevent their root resorption. When planned as the first movement, it is usually followed by a vertical or buccal displacement or a combination of both, depending on the amount of medial deviation of the canine crown from the arch.

The clinical implication of this premise would be a faster correction of the anterior inclination of the PIC.

This discussion that includes the above interpretations pertaining to the PIC relates to the uniqueness of this impaction. In other orthodontic settings, such as the distalization of posterior teeth, or the retraction of canines into the first premolar extraction space, the teeth are usually upright over the occlusal plane and not nearly as variable in their inclination and other positional characteristics as the PIC. In addition, the teeth are moved along a generally well defined track, the dental arch.

Interestingly, the stresses related to this initial movement were not statistically significantly different for the average stress on the canine root (**Table 4.5**). This result was consistent when severity groups were compared (**Table 4.6**). Differences were observed at the various levels of the root.

Significantly higher stresses were concentrated at the apical level of the root with the highest stresses in the distal direction ($S=7.73$ KPa). At the mid-root level, the stress in general was not significantly different between force directions ($p>0.3$; **Table 4.5**). Moreover, stress at the mid-root level was lower than that of apical and cervical, a finding that can be attributed to the increased tipping movement of the canine with the buccal and distal forces relative to the vertical force (**Fig 4.2**).

In the subgroups, the same pattern was observed, except for the buccal force in the higher severity subgroup, which showed the middle and cervical stresses to be statistically significantly different from those generated by the distal force (**Table 4.9**). More specifically, with the buccal force, the middle root stresses were lower than those from the distal force, and the reverse true at the cervical level. This difference may be related to the more horizontal direction of the impacted tooth, leading to differential tipping with changing force directions. The inclusion of a vertical component to either the buccal or distal force could allow for more even distribution of stress over the canine root and would presumably alleviate the stress concentration at the apical level.

5.3.2. Stress Distribution and Canine Positional Parameters

The computed correlations were higher across the severity spectrum and not within the severity subgroups (**Tables 4.10-12**). The following interpretations may be advanced:

- a. The finding reflects the progressive relationship of the canine impaction condition, rather than the therapeutically-targeted subgroup separations, which arbitrarily shift weights of severity in these subgroups.
- b. The smaller sample size in the subgroups
- c. The correlation might not be present in a smaller range of variations.

PIC/VAC and all other PIC positional variables had low and non-significant correlations when the distal force was applied (**Table 4.10**). This finding may be explained by the fact that the more severe PIC/VAC, the more mesial the cusp tip and the more increased PIC/midline angle coronally. Accordingly, less variation would occur between the long axis of the canine and the distal force direction, which tends to be close to 90°. In other words, the variation is in a frontal/coronal plane, while the distal force is almost perpendicular to that plane (**Fig. 5.2**). In contrast, with the vertical force, an increased PIC/VAC translates into direct increase in the angle between the long axis of the canine and force direction (**Table 3.14**).

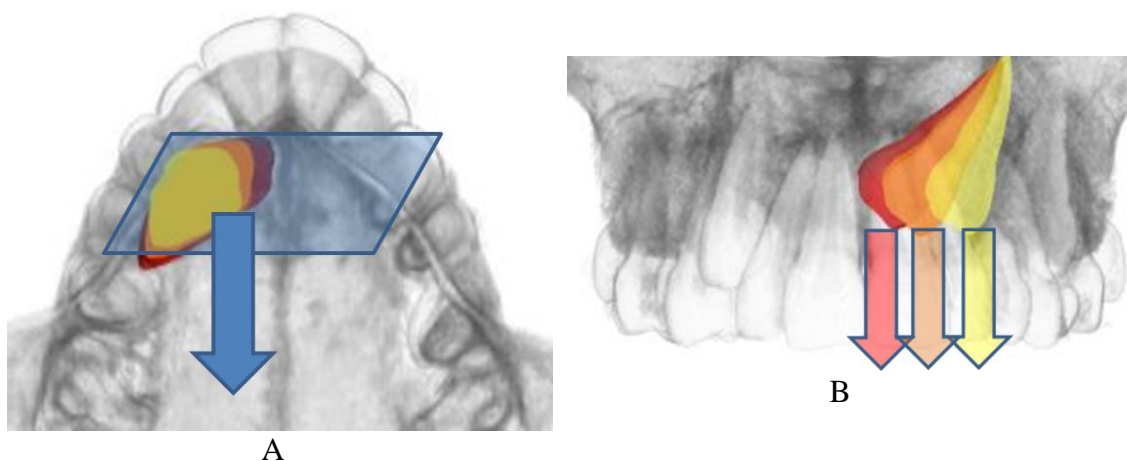


Fig. 5.2. Simulation of distal force (A) yielding lower association with the severity of inclination of PIC/VAC in the coronal plane, while a vertical force (B) would yield stresses more proportional to the severity of inclination of PIC/VAC (coronal plane).

Stresses at the mid-root level with the vertical force direction correlated with PIC/VAC ($r=-0.73$) and most positional measures, except the anterior and vertical distances measured on the sagittal view (**Table 4.10**). Stresses at the cervical level followed with nearly half of the correlations high and statistically significant. The greater number of associations between stresses and the mid-root probably reflects the basic resistance to movement in the vertical direction as severity of PIC angulation increases.

Upon buccal force application, stresses at the cervical level correlated the most with PIC position (PIC/VAC, PIC to midline and PP, cusp deviation and cusp to midline: $0.41 < r < 0.51$).

The multivariate regression analysis exposed several significant measures as predictors of stress at different levels of the PIC root: Cusp to midline, Apex to midline, PIC angulation to midline (coronal view) with the buccal and vertical forces; PIC/VAC and anterior deviation with the distal force. The predicting parameters mainly related to the position of the tooth either in distance or angulation to the midline, which we defined in part 1 (CBCT Study) as measures of severity of PIC impaction (Tables 4.13-19).

5.3.3. Stress on Adjacent teeth with Different Appliances

After sufficient space in the arch is opened for the PIC, the use of supplementary anchorage assemblies is always beneficial during the traction of the tooth. The first movement is usually distal, vertical, or a combination of both to clear the canine crown away from the roots of the incisors, or to bring down a high PIC.

These movements are best carried out by a cantilever anchored on a transpalatal bar (TPB) along with fixed orthodontic appliances that include a stiff stainless steel arch wire encompassing the most posterior permanent second molars. Additionally, or alternatively, the cantilever may be anchored on a bracket head palatal temporary anchorage device (TAD). These precautions help prevent the otherwise potential side effects on the anchoring molars such as intrusion and distal root tip (**Fig. 4.5-4.8**).

After the initial canine movement, the tooth can be pulled vertically. Such vertical movement or a combined vertical buccal or vertical distal movement - depending on initial impaction position- allows the canine to be closer to the arch for a direct activation toward the orthodontic arch wire through a buccal force direction. This movement has a direct stress that dissipates over the AW along the adjacent teeth (**Fig. 4.9**). The major load is in this situation withstood by the lateral incisor and first premolar, probably leading to adverse reactions and side effects over the dentition. Buccal crown torque is evident on the contralateral teeth (**Fig. 4.10**). Lingual tipping of adjacent premolar and lateral, and buccal root torque of anterior teeth could also result as potential side effects of such an activation (**Fig. 4.10-12**).

If were not well controlled and managed, these side effects combined could result in “skewing” of the arch that results from the “bowing” out of the arch wire on the contralateral side against the PIC side (**Fig. 5.3**), and/or root resorption.

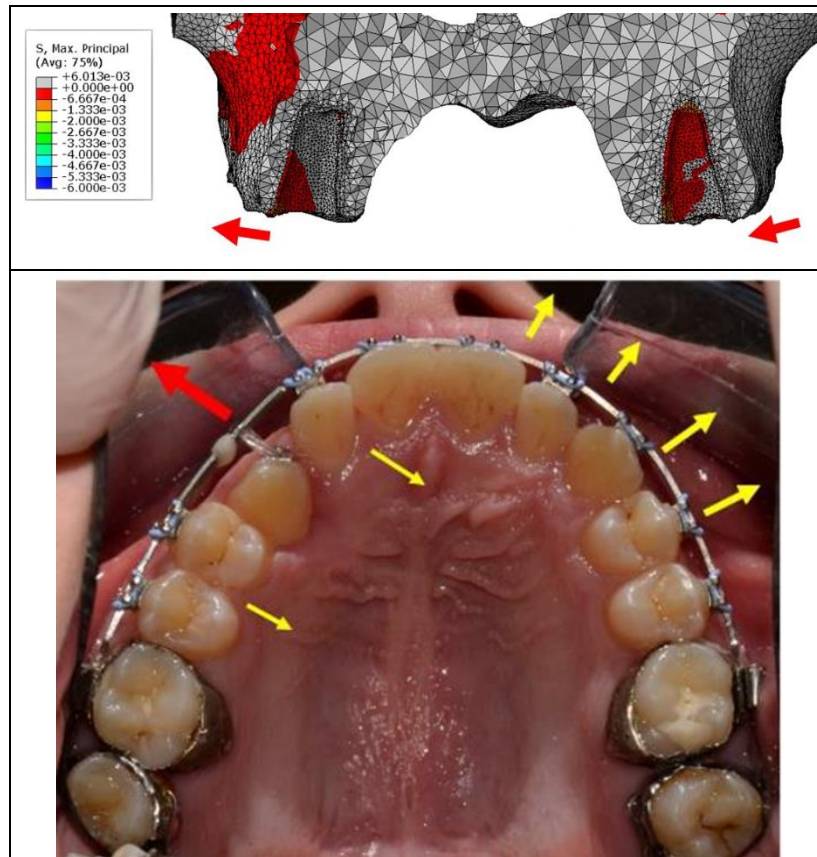


Fig. 5.3: Correspondence between maximum principal stress in PDL of adjacent teeth at the level of second premolar (A) following activation of force against PIC in an experimental FEA setting (Fig. 4.17) resembling the clinical situation (B) whereby a direct buccal force (red arrow) is applied on the canine toward the arch wire that connects the rest of maxillary teeth. Note the reactive forces (yellow arrows) on the adjacent teeth, leading to some “skewing” of the arch on the contralateral side.

Stresses on the adjacent teeth generated through the different appliances (**Table 4.20**) indicate that the direct buccal pull carries the most stress on adjacent teeth, greatest on the immediate neighboring lateral incisor and first premolar, decreasing thereafter to the most distal teeth. When fixed appliances were used along with the transpalatal bar (TPB), stresses were distributed along all teeth in gradual decrease toward the incisors, nearly 25% assumed by each of the right and left molars anchoring the TPB. The same molars shared alone the stresses when the TPB was used alone. The supposed usage of a force non-anchored on any teeth, hypothetically generated from a miniscrew implanted in the bone, expectedly did not result in stress on any teeth.

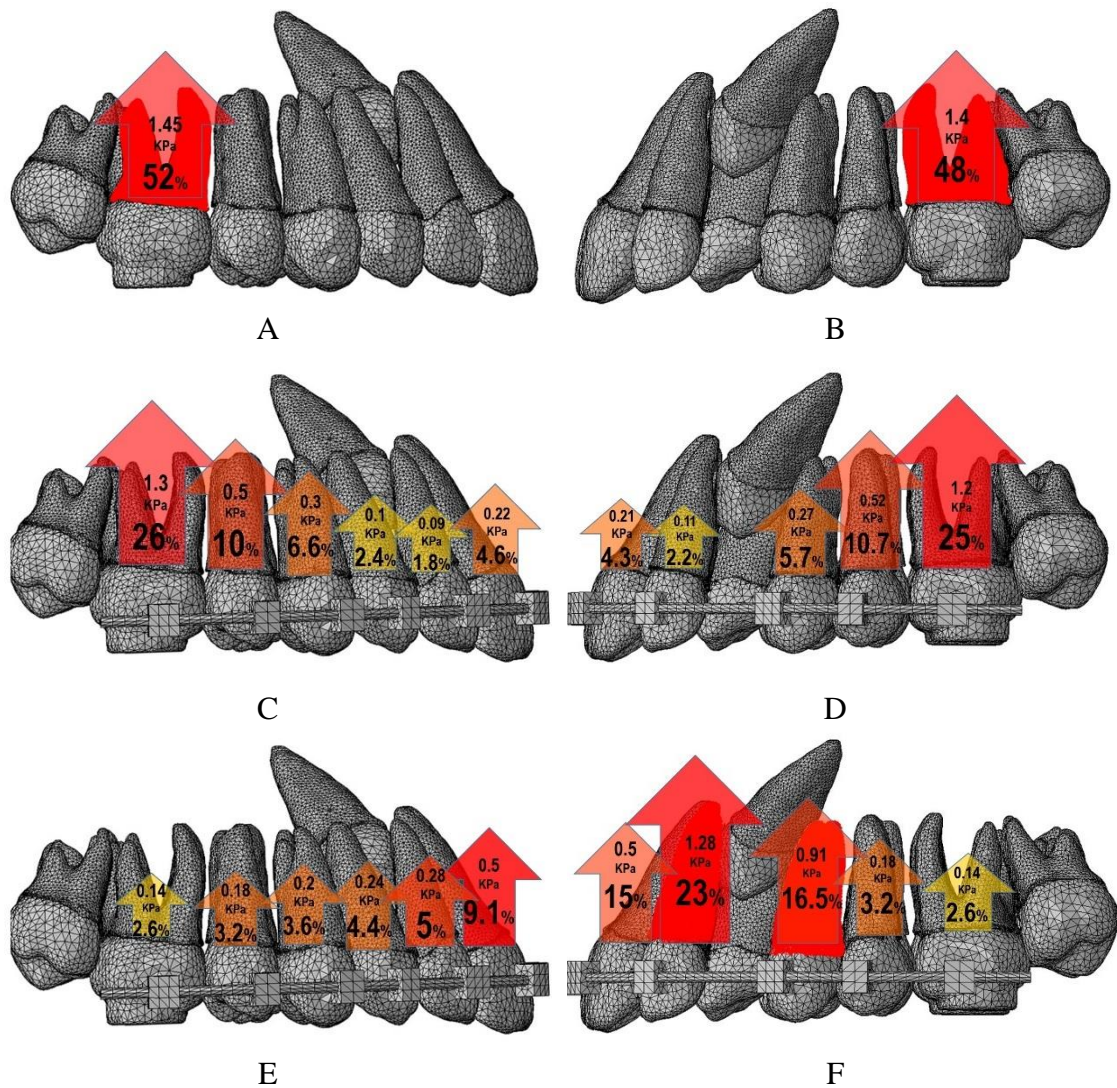


Fig. 5.4. Graphic representation of stress distributions with TP bar alone (A, B), TPB with fixed appliances (C, D), and fixed appliances alone (E, F). Arrows indicate percentages of stress on the respective teeth.

From these comparisons, the use of distal pull from a TPB, in conjunction with or without fixed appliances on the rest of the teeth, results in the least stress on the teeth adjacent to the canine, presumably avoiding the deleterious side effects, most notably root resorption of the lateral incisor (**Fig. 5.4**).

5.4. Clinical implications

Different preventive measures could be taken to minimize or prevent the side effects of reaction forces during PIC traction.

1. The use of forces that impact adjacent teeth (lateral incisor, premolar) with the least stress. In this context, distal and vertical direction of forces may be preferable to buccal forces at least in the initial stages of canine traction. The higher or more inclined the canine, the more this strategy should be applied.
2. The use of supplementary anchorage reduces the risks of side effects from heavy stresses. Such anchorage may be derived from transpalatal bars anchored on the more voluminous molars that would resist root resorption better than single-rooted (lateral incisor) or double-rooted (premolar), temporary auxiliary devices in the palate, and cantilevers (mainly palatal but also buccal) that help shoulder the anchoring forces over larger teeth or a group of teeth. The inclusion of the full dentition with rigid (rectangular) stainless steel arch wires falls within this category of buttressing anchorage (**Fig. 4.11-14**).
3. As differential stresses between the PIC side and contralateral sides observed in part 3 of the research indicate, arch “skewing” may result. The use of stopped rigid arch wires would help preserve arch perimeter and minimize arch deformation.
4. Use of slightly lighter force allows/ prevents the exacerbation of the side effects and allows management as soon as it is detected.
5. Inclusion of a vertical force component with the other needed force directions if needed will help reduce the stresses at the canine root generally and particularly at the apical level. This would also help minimize the active traction force (e.g. distal or buccal), which in turn would lessen their side effects by reducing the reaction forces.
6. Adding palatal root torque on incisors while pulling directly against arch wire.

Based on the compression/tension observed during the direct pull of the impacted canine buccally to the arch wire (**Fig. 4.11**), counteracting a potential resulting buccal root torque in the individual situation, an added palatal root torque in the wire might be indicated.

On the basis of the previous implications, some interim guidelines may be recommended (**Table 5.1**). In general terms, any appliance that may minimize the pressure on the adjacent lateral incisor (particularly prone to root resorption) and the first premolar would be preferred.

Table 5.1. Working guidelines for canine traction

PIC Position	Recommended Initial Movement (Force Direction)	Appliance Design
-Nearly all conditions	-Vertical alone or vertical component	Palatal cantilever from a TP bar or from a palatal miniscrew
-More anterior cusp tip (closer to prosthion)	-Distal, including a vertical direction -Distal only	-Palatal cantilever from a TP bar or from a palatal miniscrew -Chain tied distally to a TPB or TAD
-More medial crown	-Buccal	-Palatal cantilever from a TP bar or from a palatal miniscrew -Soldered buccal arm or a buccal cantilever from a double tube molar band -If loading against AW directly, rigid SS stopped AW are recommended. -Addition of palatal root torque on the incisors helps counteract side effects

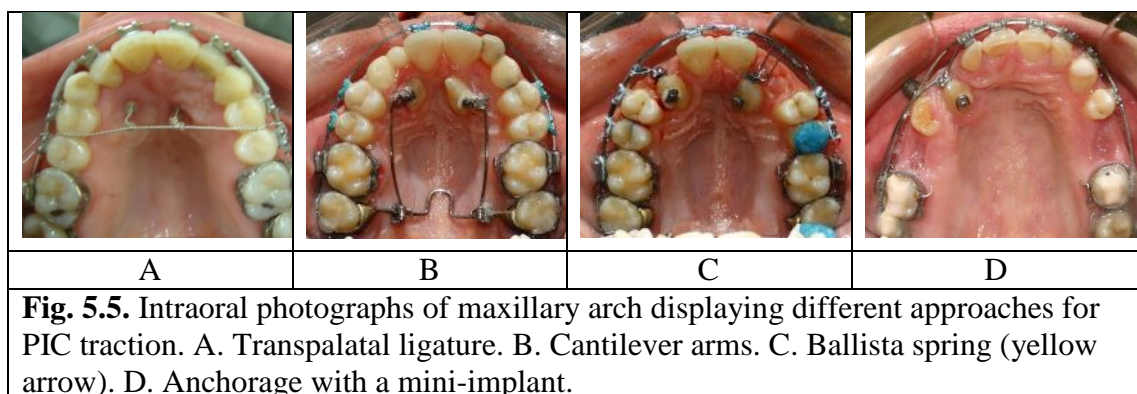


Fig. 5.5. Intraoral photographs of maxillary arch displaying different approaches for PIC traction. A. Transpalatal ligature. B. Cantilever arms. C. Ballista spring (yellow arrow). D. Anchorage with a mini-implant.

Such methods would include pull from the main bucco-labial archwire or from the buccal side (e.g. ballista spring). Whenever possible, appliances anchored on the posterior molars or palatal implants would be less harmful, particularly in instances when the pull on the canine would be sustained for a long period of time (an arbitrary cut-off to be investigated would be 6-8 months).

5.5. Research considerations

5.5.1. *Strengths*

Orthodontic mechanotherapy is based on physical and engineering principles. In prior studies, researchers have used FEA to reconstitute jaws and teeth in fragmented representations and not reconstructed the jaws in their entirety, thus provided fractioned and by and large data and conclusions non-applicable in the clinical setting. Such applications were nearly absent regarding the palatally impacted canine.

Accordingly, the strengths of this study are reflected in its novel approaches to this field of investigation:

1. We developed a unique model of evaluating the individual variation in impaction angulations.
2. Incorporating the individual variation in a finite element analysis study allowed direct evaluation of a spectrum of situations of varying impaction severities, and endowed it with a wider range of clinical credibility and potential applications.
3. FEA proved to be a practical and precise tool to investigate mechanical responses nearly impossible to gauge directly in the mouth in a non-invasive manner. The concordance of routine clinical observations with the study outcome measures, such as the presumed higher stress on the adjacent lateral incisor, supports this

application and future research tying the FEA modeling to parallel clinical investigation.

4. The incorporation of true anatomy of the entire maxilla in finite element analysis, while introduced in this study of palatally impacted canines, and rarely performed in other FEA studies, indicated the importance of incorporating the total anatomic environment in this research field, and should be adopted as the standard FEA application. With a remarkable amount of improvement needed, our results are closer to reality and provide the basis for recommendations in future research.
5. The inclusion of commonly used appliances to gauge responses on adjacent teeth provided a closer link of the FEA potential to direct clinical application with the aim to develop more individual or customized treatment plans.

5.5.2. Limitations

The construction of a finite element model is based on assumptions that are close to but may not reflect the specific data of an individual subject. The complex structure of the periodontal ligament in all FEA studies makes it difficult to simulate because the behavior of the periodontal ligament is still not clearly defined. The segmentation of the bone into cortical and trabecular component would improve the approximation toward true anatomy. Yet, it could also complicate the FEA solution.

The present study, with all the demanding efforts and time consumed, was limited to evaluating the initial response to a force. A deeper understanding of how the impacted canine behaves under different loads would require the application of a dynamic time dependent finite element analysis.

The use of different forces has not been investigated in this study. However, the outcome of linear material properties would have been similar regardless of the amount of force because the response to the force would have been proportional. Force variation would make a difference when non-linear material properties are developed.

The remarkably time-consuming process of generating a single FEA model (several dozens of hours per singular task) limited the ability of developing an original replica for each patient, requiring instead the representation of individual variations in canine impaction within the template model, with careful maintenance of the positional coordinates of the canine as on the patient's original CBCT. This operation preserved the true individual anatomy, but did not reflect differences in tooth and arch sizes, which arguably may have affected the outcome in minor but possibly significant ways. Distances to prosthion or to occlusal plane might have been affected, but the general trend of results is expected to hold. In contrast, one advantage of not varying those measures was factoring them out of the basic pertinent variations regarding the impacted tooth proper.

5.5.3. Future Tracks and Recommendations

This research lays the basic ground for future research in which time dependent displacement will bring the science closer to predicting mechanotherapy applied in individual patients. The combination of improved 3D imaging, clinical research that gauges tooth movement in various individual situations mimicked in FEA models, and knowledge of potential corresponding side effects, all represent necessary ingredients for the prediction of personalized treatment.

This study underscores the fact that FEA is an important tool to simulate a particular clinical situation for which direct research on patients is impossible. However, for FEA to be helpful in reproducing tooth movement, we should reconstitute more knowledge of the biologic system and subject it to further experiments that may not be carried on in the mouth.

Future research should include the application of motion analysis methods through FEA to determine specific movements of the impacted canine with differing severity. Such analysis would be generated by developing viscoelastic materials model to mimic the process of bone resorption which results in tooth movement. Accordingly, planned tooth movement would be forecast with precision commensurate with treatment objectives, with the additional advantage of avoiding side effects of tooth movement.

At a more basic level, the FEA technology should be developed in a parallel way to allow for less time-consuming rendition of the anatomic model and its processing. Such a development is necessary to allow for efficient analyses aimed at the generation of personalized orthodontic mechanotherapy.

CHAPTER 6

CONCLUSIONS

1. A novel measurement of PIC inclination to its simulated virtual aligned position reflects an effective measure of impaction severity. This practical approach describes the problem in reference to the needed treatment outcome, by reflecting the distance needed to align the impacted canine and therefore severity of impaction.
2. The findings indicate that the most severe or obtuse PIC is inclined to the midsagittal plane with canine tip more medial and farther away from the crest, and increased angulation to midline and palatal plane on coronal and sagittal views.
3. The delineation of 30° cutoff for severity seems more realistic than higher cutoff angulations. Newer schemes of severity scoring are contemplated, whereby treatment duration time is a factor in projecting treatment difficulty. Research should explore such association.
4. The inclusion of individual variations is a unique addition to FEA modeling of orthodontic treatment that helped determine trends of responses to force application, and the implementation of personalized rather than generic approaches to the treatment of palatally impacted canines.
5. A differential stress distribution was found with different force directions, the distal force yielding the highest stress values.
6. Stresses were also distributed differentially at the various levels of the canine root. Stresses at the mid-root level with the vertical force direction correlated with PIC/VAC ($r=-0.73$) and most positional measures.

7. Stresses on adjacent teeth were highest with appliances engaging all the teeth in the arch, particularly on the adjacent lateral incisor and first premolar. When the active appliance was anchored on the posterior molar teeth, the side effects decreased or were absent. Thus, supplementary anchorage through different appliances is recommended during PIC traction.
8. Clinical implications include the preference of distal and vertical direction of forces over buccal forces in the initial stages of canine traction, particularly with higher or more inclined canines. The application of a vertical force reduces the stresses at the apex of the canine and its inclusion with the other force directions (distal or buccal) would be recommended.
9. Future research in dynamic time dependent FEA should better elucidate the mechanism of traction of PIC, its association with severity of impaction and force directions, and more personalized treatment planning and execution.

REFERENCES

- Aktan, A. M., Kara, S., Akgünlü, F., & Malkoç, S. (2010). The incidence of canine transmigration and tooth impaction in a Turkish subpopulation. *The European Journal of Orthodontics*, cjp151.
- Al-Nimri, K. S., & Bsoul, E. (2011). Maxillary palatal canine impaction displacement in subjects with congenitally missing maxillary lateral incisors. *American Journal of Orthodontics and Dentofacial Orthopedics*, 140(1), 81-86.
- Alqerban, A., Jacobs, R., Fieuws, S., & Willems, G. (2015). Radiographic predictors for maxillary canine impaction. *American Journal of Orthodontics and Dentofacial Orthopedics*, 147(3), 345-354.
- Aydin, U., Yilmaz, H., & Yildirim, D. (2014). Incidence of canine impaction and transmigration in a patient population. *Dentomaxillofacial Radiology*.
- Baccetti, T. (1998). A controlled study of associated dental anomalies. *The Angle Orthodontist*, 68(3), 267-274.
- Bass, T. (1967). Observations on the misplaced upper canine tooth. *The Dental Practitioner And Dental Record*, 18(1), 25-33.
- Becker, A. (2012). *Orthodontic treatment of impacted teeth*: John Wiley & Sons.
- Becker, A., & Chaushu, S. (2013). Palatally impacted canines: the case for closed surgical exposure and immediate orthodontic traction. *American Journal of Orthodontics and Dentofacial Orthopedics*, 143(4), 451.
- Becker, A., & Chaushu, S. (2015). Etiology of maxillary canine impaction: A review. *American Journal of Orthodontics and Dentofacial Orthopedics*, 148(4), 557-567.
- Blake, M., Woodside, D., & Pharoah, M. (1995). A radiographic comparison of apical root resorption after orthodontic treatment with the edgewise and Speed appliances. *American Journal of Orthodontics and Dentofacial Orthopedics*, 108(1), 76-84.
- Bookstein, F. L. (1987). Describing a craniofacial anomaly: finite elements and the biometrics of landmark locations. *American Journal of Physical Anthropology*, 74(4), 495-509.
- Bourauel, C., Freudenreich, D., Vollmer, D., Kobe, D., Drescher, D., & Jäger, A. (1999). Simulation of orthodontic tooth movements. *Journal of Orofacial Orthopedics/Fortschritte der Kieferorthopädie*, 60(2), 136-151.

- Crescini, A., Nieri, M., Buti, J., Baccetti, T., & Pini Prato, G. P. (2007). Orthodontic and periodontal outcomes of treated impacted maxillary canines: an appraisal of prognostic factors. *The Angle Orthodontist*, 77(4), 571-577.
- Dachi, S. F., & Howell, F. V. (1961). A survey of 3,874 routine full-mouth radiographs: II. A study of impacted teeth. *Oral Surgery, Oral Medicine, Oral Pathology*, 14(10), 1165-1169.
- Dallessandri, D., Migliorati, M., Visconti, L., Contardo, L., Kau, C. H., & Martin, C. (2014). KPG index versus OPG measurements: a comparison between 3D and 2D methods in predicting treatment duration and difficulty level for patients with impacted maxillary canines. *Biomed Research International*, 2014.
- Ericson, S., & Kurol, J. (1986a). Longitudinal study and analysis of clinical supervision of maxillary canine eruption. *Community Dentistry And Oral Epidemiology*, 14(3), 172-176.
- Ericson, S., & Kurol, J. (1986b). Radiographic assessment of maxillary canine eruption in children with clinical signs of eruption disturbance. *The European Journal of Orthodontics*, 8(3), 133-140.
- Ericson, S., & Kurol, J. (1988). Early treatment of palatally erupting maxillary canines by extraction of the primary canines. *The European Journal of Orthodontics*, 10(4), 283-295.
- Ericson, S., & Kurol, J. (2000). Resorption of incisors after ectopic eruption of maxillary canines: a CT study. *The Angle Orthodontist*, 70(6), 415-423.
- Farah, J., Craig, R. G., & Sikarskie, D. L. (1973). Photoelastic and finite element stress analysis of a restored axisymmetric first molar. *Journal of Biomechanics*, 6(5), 511IN9515-514520.
- Fardi, A., Kondylidou-Sidira, A., Bachour, Z., Parisi, N., & Tsirlis, A. (2011). Incidence of impacted and supernumerary teeth-a radiographic study in a North Greek population. *Med Oral Patol Oral Cir Bucal*, 16(1), e56-61.
- Field, C., Ichim, I., Swain, M. V., Chan, E., Darendeliler, M. A., Li, W., & Li, Q. (2009). Mechanical responses to orthodontic loading: a 3-dimensional finite element multi-tooth model. *American Journal of Orthodontics and Dentofacial Orthopedics*, 135(2), 174-181.
- Grover, P. S., & Lorton, L. (1985). The incidence of unerupted permanent teeth and related clinical cases. *Oral Surg Oral Med Oral Pathol*, 59(4), 420-425.
- Haney, E., Gansky, S. A., Lee, J. S., Johnson, E., Maki, K., Miller, A. J., & Huang, J. C. (2010). Comparative analysis of traditional radiographs and cone-beam computed tomography volumetric images in the diagnosis and treatment planning of maxillary impacted canines. *American Journal of Orthodontics and Dentofacial Orthopedics*, 137(5), 590-597.

- Ichim, I., Schmidlin, P., Li, Q., Kieser, J., & Swain, M. (2007). Restoration of non-carious cervical lesions: Part II. Restorative material selection to minimise fracture. *Dental Materials*, 23(12), 1562-1569.
- Jacobs, S. G. (1999). Radiographic localization of unerupted maxillary anterior teeth using the vertical tube shift technique: the history and application of the method with some case reports. *American Journal of Orthodontics and Dentofacial Orthopedics*, 116(4), 415-423.
- Jacoby, H. (1983). The etiology of maxillary canine impactions. *American Journal Of Orthodontics*, 84(2), 125-132.
- Jones, M., Hickman, J., Middleton, J., Knox, J., & Volp, C. (2001). A validated finite element method study of orthodontic tooth movement in the human subject. *Journal of Orthodontics*, 28(1), 29-38.
- Kang, S., Lee, S.-J., Ahn, S.-J., Heo, M.-S., & Kim, T.-W. (2007). Bone thickness of the palate for orthodontic mini-implant anchorage in adults. *American Journal of Orthodontics and Dentofacial Orthopedics*, 131(4), S74-S81.
- Kau, C. H., Pan, P., Gallerano, R. L., & English, J. D. (2009). A novel 3D classification system for canine impactions—the KPG index. *The International Journal of Medical Robotics and Computer Assisted Surgery*, 5(3), 291-296.
- Kokich, V. G. (2004). Surgical and orthodontic management of impacted maxillary canines. *American Journal of Orthodontics and Dentofacial Orthopedics*, 126(3), 278-283.
- Korioth, T., & Versluis, A. (1997). Modeling the mechanical behavior of the jaws and their related structures by finite element (FE) analysis. *Critical Reviews in Oral Biology & Medicine*, 8(1), 90-104.
- Korioth, T. W. P. (1993). *Finite Element Modelling Of Human Mandibular Biomechanics*: University of British Columbia.
- Kramer, R. M., & Williams, A. C. (1970). The incidence of impacted teeth: a survey at Harlem Hospital. *Oral Surgery, Oral Medicine, Oral Pathology*, 29(2), 237-241.
- Levander, E., & Malmgren, O. (1988). Evaluation of the risk of root resorption during orthodontic treatment: a study of upper incisors. *The European Journal of Orthodontics*, 10(1), 30-38.
- Levander, E., & Malmgren, O. (2000). Long-term follow-up of maxillary incisors with sever apical root resorption. *The European Journal of Orthodontics*, 22(1), 85-92.
- Liang, W., Rong, Q., Lin, J., & Xu, B. (2009). Torque control of the maxillary incisors in lingual and labial orthodontics: a 3-dimensional finite element analysis. *American Journal of Orthodontics and Dentofacial Orthopedics*, 135(3), 316-322.

- Litsas, G., & Acar, A. (2011). A review of early displaced maxillary canines: etiology, diagnosis and interceptive treatment. *The Open Dentistry Journal*, 5(1).
- Matsuyama, Y., Motoyoshi, M., Tsurumachi, N., & Shimizu, N. (2014). Effects of palate depth, modified arm shape, and anchor screw on rapid maxillary expansion: a finite element analysis. *The European Journal of Orthodontics*, cju033.
- Mavreas, D., & Athanasiou, A. E. (2008). Factors affecting the duration of orthodontic treatment: a systematic review. *The European Journal of Orthodontics*, 30(4), 386-395.
- Miller, B. (1963). The influence of congenitally missing teeth on the eruption of the upper canine. *Dent Pract Dent Rec*, 13, 497-504.
- More, S. T., & Bindu, R. (2015). Effect of Mesh Size on Finite Element Analysis of Plate Structure. *Int J Eng Sci Innov Technol*, 4(3), 181-185.
- Mosby, S. (2009). Medical dictionary: Elsevier, St Louis.
- Moss, M. L., Skalak, R., Patel, H., Sen, K., Moss-Salentijn, L., Shinozuka, M., & Vilmann, H. (1985). Finite element method modeling of craniofacial growth. *American Journal Of Orthodontics*, 87(6), 453-472.
- NLY, O., & ORM, F. (2001). Generation of 3-D finite element models of restored human teeth using micro-CT techniques. *The International Journal Of Prosthodontics*, 14(4), 311.
- Peck, S., Peck, L., & Kataja, M. (1994). The palatally displaced canine as a dental anomaly of genetic origin. *The Angle Orthodontist*, 64(4), 250-256.
- Peters, M., Poort, H., Farah, J., & Craig, R. (1983). Stress analysis of a tooth restored with a post and core. *Journal of Dental Research*, 62(6), 760-763.
- Phulari, B. (2013). *An Atlas On Cephalometric Landmarks*: JP Medical Ltd.
- Pirinen, S., Arte, S., & Apajalahti, S. (1996). Palatal displacement of canine is genetic and related to congenital absence of teeth. *Journal of Dental Research*, 75(10), 1742-1746.
- Pitt, S., Hamdan, A., & Rock, P. (2006). A treatment difficulty index for unerupted maxillary canines. *The European Journal of Orthodontics*, 28(2), 141-144.
- Power, S. M., & Short, M. (1993). An investigation into the response of palatally displaced canines to the removal of deciduous canines and an assessment of factors contributing to favourable eruption. *British Journal of Orthodontics*, 20(3), 215-223.
- Proffit, W. R., Fields Jr, H. W., & Sarver, D. M. (2014). *Contemporary Orthodontics*: Elsevier Health Sciences.

- Qian, Y., Fan, Y., Liu, Z., & Zhang, M. (2008). Numerical simulation of tooth movement in a therapy period. *Clinical Biomechanics*, 23, S48-S52.
- Singh, G., McNamara Jr, J., & Lozanoff, S. (1998). Mandibular morphology in subjects with Class III malocclusions: finite-element morphometry. *The Angle Orthodontist*, 68(5), 409-418.
- Smith, R. J., & Burstone, C. J. (1984). Mechanics of tooth movement. *American Journal Of Orthodontics*, 85(4), 294-307.
- Stellzig, A., Basdra, E., & Komposch, G. (1994). [The etiology of canine tooth impaction--a space analysis]. *Fortschritte der Kieferorthopadie*, 55(3), 97-103.
- Stewart, J. A., Heo, G., Glover, K. E., Williamson, P. C., Lam, E. W., & Major, P. W. (2001). Factors that relate to treatment duration for patients with palatally impacted maxillary canines. *American Journal of Orthodontics and Dentofacial Orthopedics*, 119(3), 216-225.
- Sung, E.H., Kim, S.J., Chun, Y.S., Park, Y.C., Yu, H.S., & Lee, K.J. (2015). Distalization pattern of whole maxillary dentition according to force application points. *The Korean Journal of Orthodontics*, 45(1), 20-28.
- Sung, S. J., Baik, H. S., Moon, Y. S., Yu, H. S., & Cho, Y. S. (2003). A comparative evaluation of different compensating curves in the lingual and labial techniques using 3D FEM. *American Journal of Orthodontics and Dentofacial Orthopedics*, 123(4), 441-450.
- Takahama, Y., & Aiyama, Y. (1982). Maxillary canine impaction as a possible microform of cleft lip and palate. *The European Journal of Orthodontics*, 4(4), 275-277.
- Tanne, K., Matsubara, S., & Sakuda, M. (1995). Location of the centre of resistance for the nasomaxillary complex studied in a three-dimensional finite element model. *British Journal Of Orthodontics*, 22(3), 227-232.
- Tanne, K., Sakuda, M., & Burstone, C. J. (1987). Three-dimensional finite element analysis for stress in the periodontal tissue by orthodontic forces. *American Journal of Orthodontics and Dentofacial Orthopedics*, 92(6), 499-505.
- Thilander, B., & Myrberg, N. (1973). The prevalence of malocclusion in Swedish schoolchildren. *European Journal of Oral Sciences*, 81(1), 12-20.
- Woloshyn, H., Årtun, J., Kennedy, D. B., & Joondeph, D. R. (1994). Pulpal and periodontal reactions to orthodontic alignment of palatally impacted canines. *The Angle Orthodontist*, 64(4), 257-264.
- Yadav, R., & Shrestha, B. K. (2013). Maxillary Impacted Canines: A Clinical Review. *Orthodontic Journal of Nepal*, 3(1), 63-68.

- Zahrani, A. (1993). Impacted cuspids in a Saudi population: prevalence, etiology and complications. *Egyptian Dental Journal*, 39(1), 367-374.
- Zhang, J., Wang, X. X., Ma, S. L., Ru, J., & Ren, X. S. (2008). [3-dimensional finite element analysis of periodontal stress distribution when impacted teeth are tracted]. *Hua Xi Kou Qiang Yi Xue Za Zhi*, 26(1), 19-22.
- Zienkiewicz, O., & Kelly, D. (1982). Finite elements—a unified problem solving and information transfer method. *Finite Elements in Biomechanics*. New York, John Wiley & Sons, 9-22.
- Zuccati, G., Ghobadlu, J., Nieri, M., & Clauser, C. (2006). Factors associated with the duration of forced eruption of impacted maxillary canines: a retrospective study. *Am J Orthod Dentofacial Orthop*, 130(3), 349-356.
doi:10.1016/j.ajodo.2004.12.028

Appendix 1:

Canine Reposition Script

A mathematical computation to position individual canines in prototype model.
(Simpleware, Exeter, UK)

First a standard import of some headers and a definition of the cross produce

```
from scancad_api import *  
  
from math import acos, pi
```

```
def cross(a, b):  
    c = [a[1]*b[2] - a[2]*b[1],  
         a[2]*b[0] - a[0]*b[2],  
         a[0]*b[1] - a[1]*b[0]]  
    return c
```

These two vectors are the final two vectors from the excel measurements

```
an = [0.522565501, 0.483126595, 0.702505509]  
bn = [0.312602265, 0.201678881, 0.928227048]
```

Find a vector that we can rotate the start tooth around to get the second tooth,
and the angle. Construct the matrix that represents this transformation.

```
v = cross(an, bn) # definitely v^hat
```

```
costheta = an[0] * bn[0] + an[1] * bn[1] + an[2] * bn[2]  
theta = acos(costheta)*(180.0/pi)  
matrix = Matrix.FromAngleAndAxis(theta, v[0], v[1], v[2])
```

Apply this transformation (this will also perform a translation that we want to ignore later)

```
# Get the orientation of the tooth in +CAD-space (so we can apply  
these rotations "in place" later)
```

```
m =
```

```
CADApp.GetInstance().GetActiveDocument().GetModels()[0].Duplicate()
```

```
m.SetTransformationMatrix(matrix, CADDoc.Global)
```

```
ori_v = m.GetOrientation(CADDoc.Global)
```

```
CADApp.GetInstance().GetActiveDocument().RemoveModel(m)
```

And copy the new orientation on to a new tooth (in the correct place):

```
# Apply these rotations in place and translate the tooth
```

```
m =
```

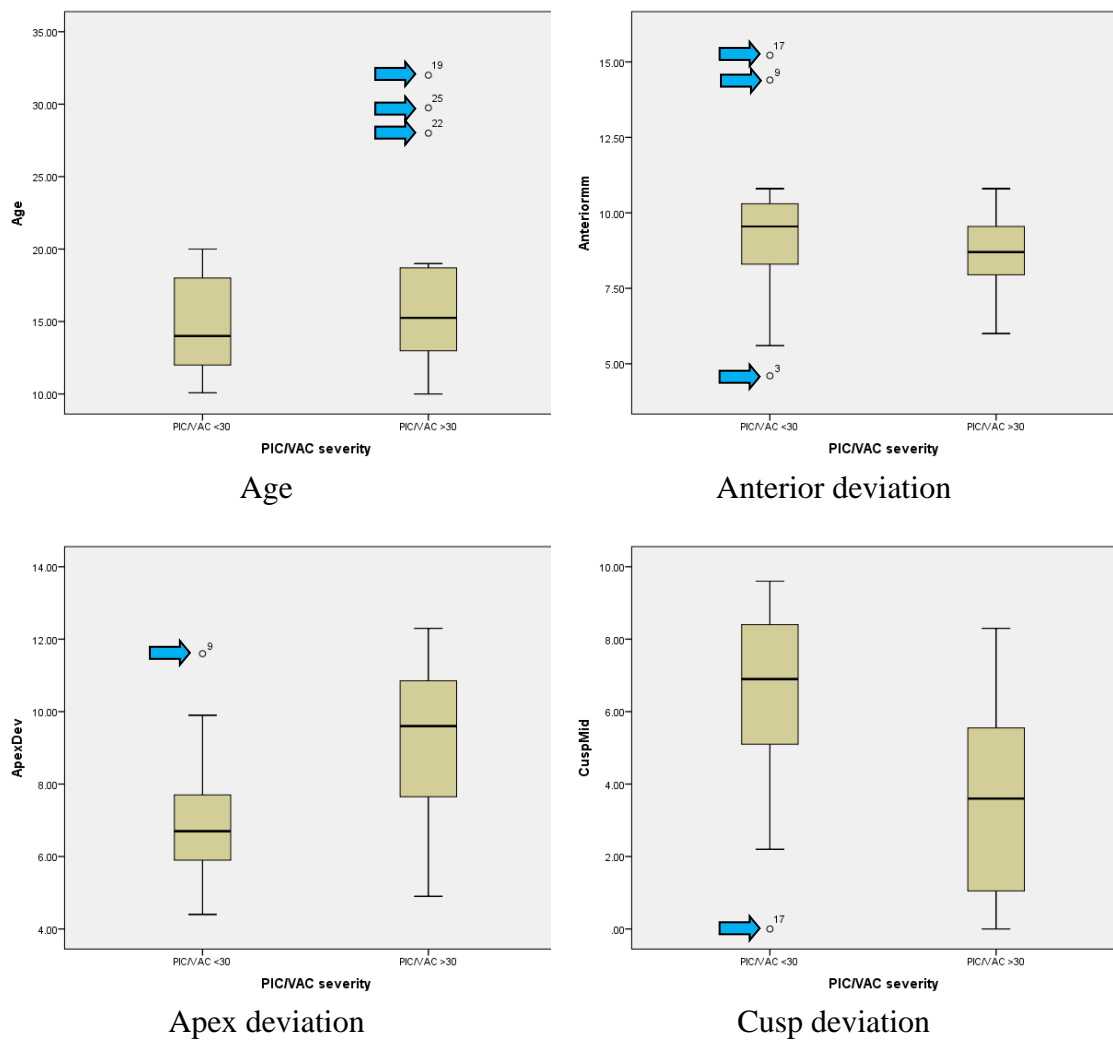
```
CADApp.GetInstance().GetActiveDocument().GetModels()[0].Duplicate()
```

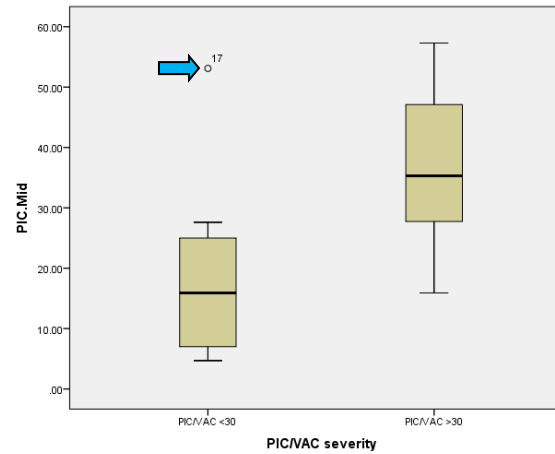
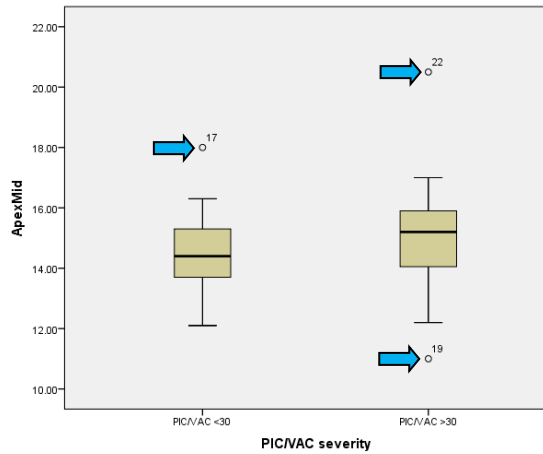
```
m.Rotate(ori_v.GetX(), ori_v.GetY(), ori_v.GetZ(), CADDoc.Redefined)
```

```
m.Translate(-23, -0.9, -9.09, CADDoc.Global)
```

Appendix 2:

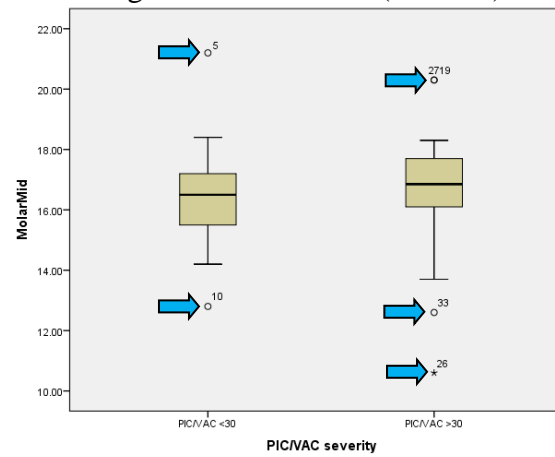
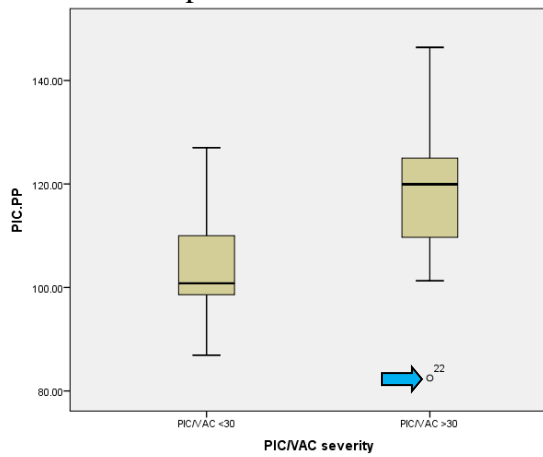
Whisker plots/box plots of the low severity subgroup (PIC/VAC<30, N: 18) vs. the higher severity subgroup (PIC/VAC>30, N: 20) palatally impacted canine*





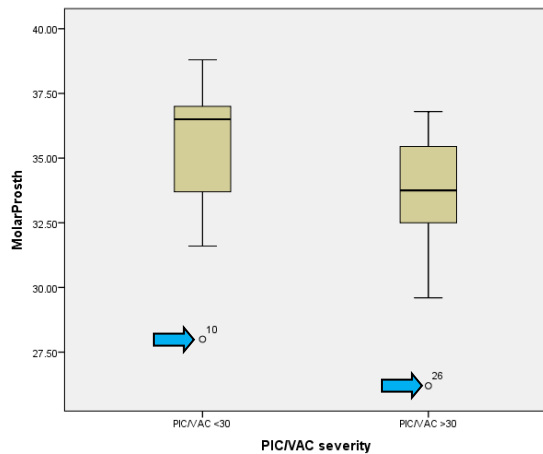
Apex to midline

PIC angulation to midline (Coronal)



PIC angulation to palatal plane (Sagittal)

Molar to midline



Molar to prosthion

* Note the presence of outliers (indicated by blue arrows), indicating the importance of considering individual variation.